

University Hospital Würzburg
Medical Clinics II



Identification of new predictive markers for an early diagnosis of an
imminent acute Graft-versus-Host Disease

Bestimmung neuer prädiktiver Marker zur Früherkennung einer
drohenden akuten Graft-versus-Host Disease

Doctoral thesis for a doctoral degree
at the Graduate School of Life Sciences,
Julius-Maximilians-Universität Würzburg,
Section of Immunology

submitted by

Carina Bäuerlein

from Sommerach

Würzburg, December 2012

Submitted on:
Office stamp

Members of the *Promotionskomitee*:

Chairperson: Prof. Dr. Thomas Hünig

Primary Supervisor: Dr. Andreas Beilhack

Supervisor (Second): Prof. Dr. Hermann Einsele

Supervisor (Third): Prof. Dr. Harald Wajant

Supervisor (Fourth): Prof. Dr. Tor B. Stuge

Date of Public Defense:

Date of receipt of Certificates:

Für meine Eltern

Der Wert davon, dass man zeitweilig eine *strenge Wissenschaft* streng betrieben hat, beruht nicht gerade auf deren Ergebnissen: denn diese werden, im Verhältnis zum Meere des Wissenswerten, ein verschwindend kleiner Tropfen sein. Aber es ergibt einen Zuwachs an Energie, an Schlussvermögen, an Zähigkeit der Ausdauer; man hat gelernt, einen *Zweck zweckmäßig* zu erreichen. Insofern ist es sehr schätzbar, in Hinsicht auf Alles, was man später treibt, einmal ein wissenschaftlicher Mensch gewesen zu sein

– *Friedrich Nietzsche*

Table of Content

TABLE OF CONTENT	I
LIST OF ABBREVIATIONS	V
1. ABSTRACT	1
2. INTRODUCTION	2
2.1 ALLOGENEIC HEMATOPOIETIC STEM CELL TRANSPLANTATION (ALLO-HCT).....	2
2.2 ACUTE GRAFT-VERSUS-HOST DISEASE (AGVHD)	3
2.2.1 <i>aGvHD pathophysiology</i>	3
2.2.2 <i>Predictive markers for aGvHD</i>	6
2.2.3 <i>aGvHD diagnosis</i>	7
2.2.4 <i>aGvHD prophylaxis and treatment</i>	8
2.3 T CELL MIGRATION AND HOMING	9
3. SPECIFIC AIMS	13
4. MATERIAL AND METHODS	14
4.1 MICE	14
4.2 CELL ISOLATION FROM MOUSE ORGANS	14
4.2.1 <i>Bone Marrow</i>	14
4.2.2 <i>Spleen</i>	15
4.2.2.1 T cell enrichment of splenocytes	15
4.2.2.2 T cell depletion of splenocytes	16
4.2.3 <i>Lymph nodes</i>	16
4.2.4 <i>Peripheral Blood Mononuclear Cell (PBMC) collection</i>	16

Table of Content

4.3	ALLOGENEIC AND SYNGENEIC HCT	17
4.4	IMMUNOSUPPRESSIVE TREATMENTS	17
4.5	CLINICAL GVHD SCORING	18
4.6	IN VIVO AND EX VIVO BIOLUMINESCENCE IMAGING.....	18
4.7	BUFFERS AND ANESTHETIC	18
4.8	FLOW CYTOMETRY.....	19
4.8.1	<i>Antibodies and Titration</i>	19
4.8.2	<i>Compensation</i>	21
4.8.3	<i>Fluorescence minus one</i>	22
4.8.4	<i>Surface Phenotyping</i>	23
4.8.5	<i>Intracellular Staining</i>	23
4.9	CD107 DEGRANULATION ASSAY	24
4.10	IMMUNOFLUORESCENCE STAINING AND IMMUNOHISTOCHEMISTRY	25
4.11	HISTOLOGIC EVALUATION	25
4.12	STATISTICAL ANALYSES	26
5.	RESULTS	27
5.1	DYNAMICS OF AGVHD PATHOPHYSIOLOGY	27
5.1.1	<i>Physiological changes caused by aGvHD</i>	27
5.1.2	<i>Donor T cells accumulate in target organs</i>	29
5.1.3	<i>Tracking of donor T cell migration after HCT</i>	32
5.1.4	<i>Early detection of donor T cells in the peripheral blood</i>	36
5.1.5	<i>CD107 surface mobilization of peripheral blood T cells proves alloreactivity</i>	38
5.1.6	<i>Localization of donor T cells in target organs</i>	39

Table of Content

5.2	CHARACTERIZATION OF MIGRATING DONOR T CELL EXPRESSION PROFILES.....	44
5.2.1	<i>α4β7 integrin is highly up-regulated on donor T cells.....</i>	45
5.2.2	<i>Alloreactive donor T cells up-regulate selectin ligands</i>	47
5.2.3	<i>Chemokine receptors do not define alloreactive donor T cells.....</i>	50
5.2.4	<i>Alloreactive donor T cells are highly activated</i>	52
5.3	THERAPEUTIC INTERVENTION DURING DIAGNOSTIC WINDOW	54
5.3.1	<i>Prednisolone treatment.....</i>	54
5.3.2	<i>Pentostatin treatment.....</i>	57
5.3.3	<i>Rapamycin treatment.....</i>	59
5.3.3.1	10 days of rapamycin treatment prolong survival	59
5.3.3.2	Rapamycin treatment influences regulatory T cell expansion	61
5.3.3.3	Single shots of rapamycin insufficient for survival benefit	62
6.	DISCUSSION.....	65
6.1	AGVHD PATHOPHYSIOLOGY AFTER MIHAG MISMATCH ALLO-HCT	65
6.2	DONOR T CELL RECEPTOR PROFILE AFTER MIHAG MISMATCH ALLO-HCT	68
6.2.1	<i>α4β7 integrin is highly up-regulated on donor T cells.....</i>	68
6.2.2	<i>Alloreactive donor T cells up-regulate selectin ligands</i>	70
6.2.3	<i>Chemokine receptors do not define alloreactive donor T cells.....</i>	71
6.2.4	<i>Alloreactive donor T cells are highly activated</i>	73
6.3	DIRECTED PREEMPTIVE TREATMENT WITH RAPAMYCIN SIGNIFICANTLY PROLONGS SURVIVAL	75
7.	ZUSAMMENFASSUNG.....	79
8.	REFERENCE LIST	81
9.	APPENDIX.....	97

Table of Content

9.1	LIST OF FIGURES.....	97
9.2	LIST OF TABLES.....	98
9.3	ACKNOWLEDGEMENT	99
9.4	CURRICULUM VITAE	100
9.5	AVIDAVIT (EIDESSTÄTTLICHE ERKLÄRUNG)	104

List of Abbreviations

aGvHD	Acute Graft-versus-Host Disease
AICD	Activation-induced cell death
Allo-HCT	Allogeneic hematopoietic cell transplantation
APC	Antigen presenting cell
APC	Allophycocyanine
BM	Bone marrow
BSA	Bovine serum albumin
BW	Body weight
CCR	Chemokine receptor
CD	Cluster of differentiation
CFDA-SE	carboxyfluorescein diacetate succinimidyl ester
CFSE	Carboxyfluorescein succinimidyl ester
cLN	Cervical lymph node
CTL	Cytotoxic T lymphocyte
Cy	Cytochrome
DAPI	4',6-Diamidin-2-phenylindol
DC	Dendritic cell
DNA	Deoxyribonucleic acid
EDTA	Ethylenediaminetetraacidic acid
FACS	Fluorescence associated cell sorting
FC	Flow cytometry
FCS	Fetal calf serum
FITC	Fluorescein isothiocyanate
FMO	Fluorescence minus one

List of Abbreviations

FoxP3	Forkhead box P3
g	Gram
GIT	Gastrointestinal tract
GSC	Glucksberg-Seattle criteria
GvHD	Graft-versus-Host Disease
GvL	Graft-versus-Leukemia
GvTE	Graft-versus-Tumor Effect
Gy	Gray
HCT	Hematopoietic cell transplantation
HEV	High endothelial venule
HGF	Hepatic growth factor
HLA	Human leukocyte antigen
HSC	Hematopoietic stem cells
HPF	High Power Field
IDO	Indoleamine 2,3-dioxygenase
IFM	Immunofluorescence microscopy
IFN- γ	Interferon gamma
IgG	Immunoglobulin G
IL	Interleukin
iLN	Inguinal lymph node
IL-2R α	Interleukin-2 receptor alpha
IU	International unit
kg	Kilogram
LN	Lymph node
LPAM-1	Lymphocyte Peyer's patch adhesion molecule-1

List of Abbreviations

LPS	Lipopolysaccharide
MadCAM-1	mucosal addressin cell adhesion molecule-1
MDSC	Myeloid-derived suppressor cell
mg	Milligram
MALT	Mucosa-associated lymphatic tissue
miHA _g	Minor histocompatibility antigen
min	Minute
MHC	Major histocompatibility complex
ml	Milliliter
mLN	Mesenteric lymph node
mM	Millimolar
mTOR	Mammalian target of rapamycin
μg	Microgram
ng	Nanogram
NRS	Normal rat serum
OT-1	OVA specific TCR transgenic MHC Class I-restricted
OVA	Ovalbumin
PB	Pacific blue
PB	Peripheral blood
PBMC	Peripheral blood mononuclear cell
PBS	Phosphate buffered saline
PE	Phycoerythrin
PerCP	Peridinin chlorophyll
PFA	Paraformaldehyde
PI	Propidium iodide

List of Abbreviations

pLN	Peripheral lymph node
PP	Peyer's patch
PSGL-1	P-selectin glycoprotein ligand-1
RBC	Red blood count
REG3 α	Regenerating islet-derived 3-alpha
rhIL-2	Recombinant human IL-2
RT	Room temperature
SD	Standard deviation
SEM	Standard error of the mean
sIL-2R α	Soluble IL-2 receptor alpha
SLO	Secondary lymphoid organ
TCR	T cell receptor
TNF- α	Tumor necrosis factor alpha
TNFR1	Tumor necrosis factor receptor 1
UCB	Umbilical cord blood
WBC	White blood count
WT	Wild type

1. Abstract

Acute graft-versus-host disease (aGvHD) is an immune syndrome associated with allogeneic hematopoietic cell transplantation (allo-HCT) that is mediated by alloreactive donor T cells attacking the gastrointestinal tract, liver, and skin of the host. Early diagnosis remains problematic and to date mainly relies on clinical symptoms and histopathology. Previously, different groups demonstrated that in order to cause aGvHD, alloreactive T cells require the expression of appropriate homing receptors to efficiently migrate from their priming sites to their target tissues. Therefore, the development of a predictive test based on the homing receptor expression profile of peripheral blood T cells seems attractive to identify patients at risk before the onset of aGvHD.

The aim of this study was to analyze migrating alloreactive donor T cell kinetics in the peripheral blood early after allo-HCT in a murine model across minor histocompatibility antigens (miHA_g) followed by a precise characterization of the homing receptor expression profile of migrating donor lymphocytes in order to identify suitable predictive markers. Combining daily bioluminescence imaging (BLI) and flow cytometry (FC) allowed defining two weeks of massive alloreactive donor T cell migration before clinical aGvHD symptoms became apparent. Peripheral blood donor T lymphocytes highly up-regulated the homing markers $\alpha 4\beta 7$ integrin, and P- and E-selectin-ligand at peak time points of cell migration. The combination with the activation markers CD25 and CD69 and low expression levels of L-selectin allowed alloreactive donor T cell definition. Based on this migration phase we postulated a potential diagnostic window to precisely identify alloreactive donor T cells upon their homing receptor expression profile. Consequently, targeted pre-emptive treatment with rapamycin starting at the earliest detection time point of alloreactive donor T cells in the peripheral blood (day+6) significantly prolonged survival of treated mice. Based on this data, we propose a potential diagnostic window for alloreactive cell detection based on their homing receptor expression profile for a timely and effective therapeutic intervention before the clinical manifestation of aGvHD.

2. Introduction

2.1 Allogeneic Hematopoietic Stem Cell Transplantation (allo-HCT)

Hematopoietic cell transplantation (HCT) is a successful therapy for life-threatening malignant and non-malignant diseases of the hematopoietic system such as leukemia and lymphomas.¹ The principle behind this curative strategy is to destroy the hosts' malignant or leukemic cells by irradiation and/or chemotherapy, replacing them with stem cells from a closely related donor (allogeneic HCT). Immunocompetent donor cells transferred with or arisen from the stem cell graft reconstitute a functional immune system in the host which is able to attack residual tumor cells. This desired immune response, known as graft-versus-tumor effect (GvTE), works independently of toxic side effects caused by high-dose irradiation or chemotherapy.² Barnes and colleagues first described this phenomenon in 1956, showing the successful treatment of leukemic mice by injection of allogeneic but not syngeneic marrow transplants after irradiation.³ Already in 1952, the discovery that the injection of bone marrow (BM) significantly increases the survival rates in mice and guinea-pigs after lethal irradiation⁴ opened the doors for applications in patients with the first successful allo-HCTs in humans performed in 1968. Three children suffering from congenital immune deficiency diseases completely recovered after allo-HCT and immunological capacities could be fully reconstituted.⁵⁻⁷ Since then, more than 800.000 patients have received a stem cell graft, and the number of allo-HCT recipients has steadily increased with more than 55.000 per year worldwide.¹

Unlike pluripotent embryonic stem cells that can develop into any kind of cell type of an organism, hematopoietic stem cells (HSCs) are multipotent and lineage specific. They can be isolated from various fetal and adult tissues.⁸ Until the 1990s, BM was the only source for HSCs due to its rich stem cell supply. In recent years, the development of alternative techniques allows for alternatively deriving HSCs from peripheral blood (PB) or umbilical cord blood (UCB). Such methods are less time-consuming and stressful for the donor. Thus, HCT has evolved in a way that BM, PB, and UCB can each be used as HSC source, yet they all appear to have significant biological differences affecting the outcome.⁹

UCB presents a good source of immunologically naïve HSCs, and the rapid availability without donor searching, screening and typing is advantageous. Wagner and colleagues published the first report of the successful use of UCB as stem cell source in allogeneic sibling HCTs in children with malignant and non-malignant diseases.¹⁰ Since then, UCB effectively serves as HSC source in more than 55 % of HCTs in children under the age of 10.¹ However, for many years a limiting factor for the broader use of UCB stem cells in adults was the relatively small amount of cells in the graft, therefore confining its use for children.⁹ In 2005, the combined use of two UCB units to increase the graft cell dose succeeded, paving the way for the extended use of UCB as a source of HSCs also for adults.¹¹ However, the delayed immune reconstitution compared to other HSC sources remains a significant barrier.⁹

In 1995, several groups established cytokine based mobilization protocols for hematopoietic precursors into the PB, enabling its use as HSC source.¹² PB is the source of choice for donor cells in the majority of HCTs today since it is relatively easy to obtain by leukapheresis (in 70 % of related donor and 60 % of unrelated donor HCTs).¹ A faster neutrophil and platelet recovery due to a higher cell number together with more T cells that exert the beneficial GvTE⁹ has led to the PB as the first choice in HSC source decisions.

However, in many cases the immunocompetent cells of the graft – independent of the graft source – also recognize antigens on the recipient's cell surfaces and mount an immune response against them. This immune syndrome is commonly known as graft-versus-host disease (GvHD) and represents the major complication after allo-HCT.¹³

2.2 Acute Graft-versus-Host Disease (aGvHD)

2.2.1 aGvHD pathophysiology

GvHD limits the broader use of allo-HCT as a promising therapy.^{9,14} 50 years ago, Billingham postulated 3 requirements for the development of this immune syndrome: the stem cell graft must contain immunocompetent cells, the recipient must be incapable of mounting an immune response to eliminate the foreign cells and the recipient must express tissue antigens not present in the donor transplant.¹⁵ Today we know that the immunocompetent cells are T lymphocytes that react against tissue

antigens of the host. These tissue antigens are highly polymorphic molecules expressed on the cell surfaces and determine the compatibility of the donor with organ or cell grafts.¹⁶ Since patients receiving HCT are typically immunosuppressed by chemotherapy and/or radiation, they cannot eliminate those activated T cells which eventually cause GvHD.¹⁷

There are basically two different forms of GvHD: an acute and a chronic form. Chronic GvHD shows symptoms of autoimmune and other immunological disorders, but the pathophysiology of this syndrome is insufficiently understood.¹⁸ For many years, the acute form was simply distinguished from the chronic form by the time of disease onset (before or after day+100 of the HCT, respectively). In 2005, the National Institute of Health Consensus Conference suggested to distinguish between the two categories in more detail, considering a persistent, recurrent or late form of GvHD beyond day+100 as acute whereas chronic GvHD can also comprise an overlap syndrome in which features of both forms occur.¹⁹

Two recent studies report that aGvHD can be divided into different phases in murine allo-HCT models across major MHC barriers. *In vivo* imaging techniques defined a spatiotemporal distinct initiation phase in secondary lymphoid organs (SLOs) and a subsequent effector phase in peripheral target tissues.^{20,21}

After allo-HCT, donor T cells first migrate to SLOs including the spleen, lymph nodes (LNs), Peyer's patches (PPs) and other mucosa-associated lymphatic tissues (MALT). Here, they encounter host antigen presenting cells (APCs) and, similarly to other adaptive immune responses, start to proliferate and differentiate into alloreactive effector T cells.²²⁻²⁴ After three days, they leave the SLOs and migrate via the peripheral blood towards their respective target organs, which are mainly the gastrointestinal tract (GIT), liver and skin.²⁵ Inflammation induced by the conditioning regimen plays a pivotal role in the migratory process of alloreactive donor T cells towards their target tissues. An inflammatory cascade supports the recruitment of further alloreactive lymphocytes to these sites.²⁶ The irradiation-induced differential up-regulation of distinct adhesion and costimulatory molecules on epithelial tissues helps donor T cells to enter their respective target tissues.^{27,28} Organ destruction leads to aGvHD manifestation, accompanied by severe clinical symptoms such as diarrhea, skin rash, and liver failure.¹⁴

In summary, aGvHD initiation and development proceeds in three subsequent steps (as shown in Figure 1): host APCs are activated by the conditioning regimen (1),

followed by donor T cell activation, proliferation, and migration (2), which eventually cause target tissue damage (3) in combination with inflammatory effects initiated by the conditioning.

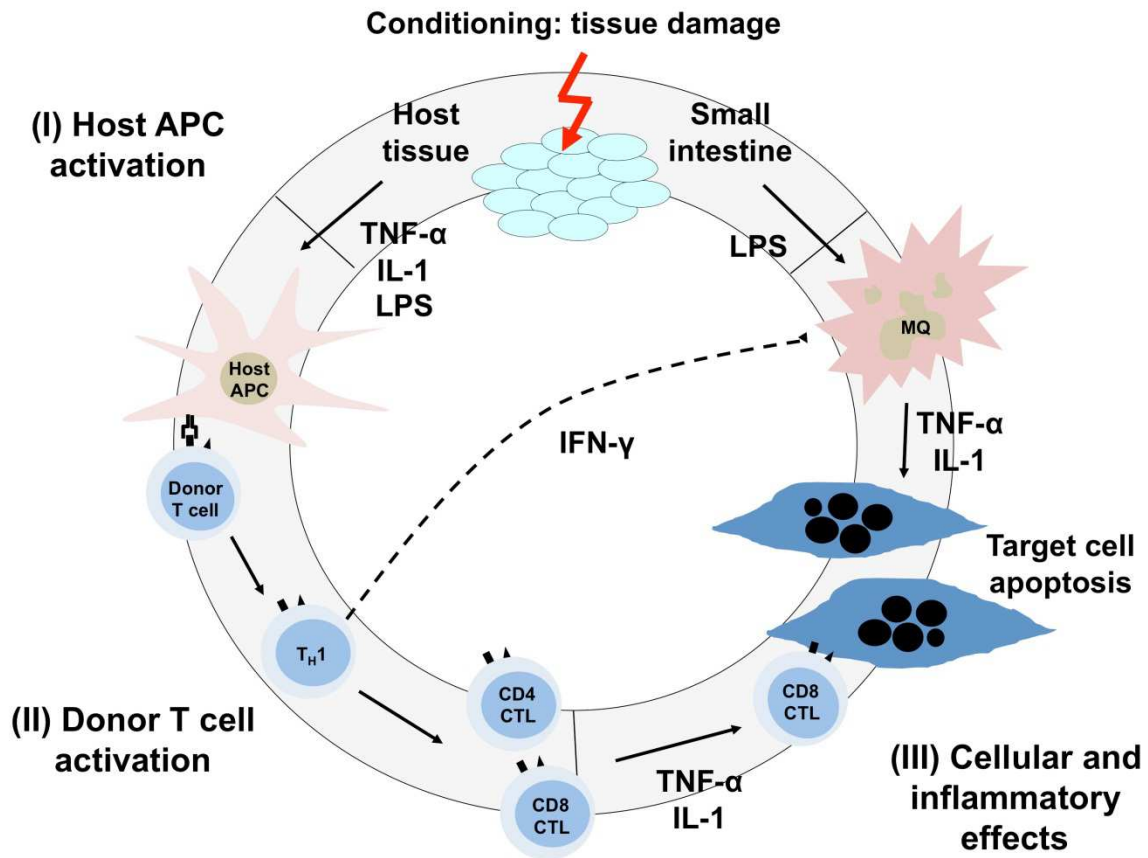


Figure 1: Pathophysiology of aGvHD

Three subsequent steps summarize aGvHD progression: (1) activation of recipients' APCs, (2) activation, proliferation, differentiation, and migration of donor T lymphocytes, and (3) destruction of recipients' tissues. Figure adapted from Ferrara et al.¹⁴

Research intensively focused on the antigens recognized on recipients' tissues which led to the discovery of so-called human leukocyte antigens (HLA) in 1958 by Jean Dausset.²⁹ The HLA system which is the human analogue of the major histocompatibility complex (MHC) in mice is a collection of genes that encode for highly polymorphic molecules expressed on the cell surface and determine the biological identity of an individual's cells and tissues. MHC molecules on the cell surfaces present peptides to circulating T cells and are the main players in T cell activation. This mechanism allows the immune system to distinguish between self and non-self.^{2,16} In the context of GvHD, there are two forms of alloantigen

recognition by T cells depending on whether the presenting MHC molecules are matched or mismatched between donor and recipient.³⁰ Differences in MHC molecules themselves are referred to as major antigen mismatch leading to a severe, hyperacute form of GvHD.³¹ In contrast, if MHC molecules between donor and recipient are matched, donor T cells only recognize foreign MHC-bound peptides – a so-called minor histocompatibility antigen (miHAg) mismatch – leading to a slower development of a less severe form of aGvHD in patients as well as in miHAg mismatched mouse models.³²

2.2.2 Predictive markers for aGvHD

Early aGvHD diagnosis remains problematic and is currently assessed mainly by clinical symptoms and histopathology. The search for reliable predictive markers to identify patients at risk before aGvHD onset has become the focus of attention in recent years. The perfect biomarker would be predictive of both disease onset and prognosis, inexpensive, easily available and consistently usable across different laboratories. Furthermore, a simple and fast read out would be advantageous allowing a timely intervention for clinicians.

Recently, several groups identified a broad range of different aGvHD-associated molecules and thoroughly investigated their use as potential predictive markers. The soluble part of the IL-2 receptor alpha chain (sIL-2R α) presents one well investigated candidate. Several studies found elevated serum levels of sIL-2R α in patients that developed aGvHD compared to patients that did not.^{33,34} However, also patients suffering from other diseases showed higher serum sIL-2R α levels lowering its value as a reliable marker for aGvHD prediction.³⁵ The test for sIL-2R α in combination with different pro- and anti-inflammatory cytokines did not identify a cytokine expression pattern specific for aGvHD despite the known important role of cytokines in aGvHD pathophysiology.^{36,37} A correlation of elevated serum levels of some other molecules such as cytokeratin-18, a filament protein of epithelial tissues and a marker for apoptosis, or syndecan-1, an adhesion molecule on epithelial cells, with aGvHD was also possible but they lack specificity as single predictive marker.^{38,39}

More recently, using proteomic discovery and validation strategies, the Ferrara group tested a panel of four previously identified plasma biomarkers. They could show the

combination of TNFR1, IL-2R α , IL-8, and hepatocyte growth factor (HGF) to effectively discriminate between patients with and without aGvHD.⁴⁰ The same group also identified aGvHD target organ specific plasma biomarkers: the overexpression of the elastase inhibitor elafin in skin biopsies as well as significantly higher plasma elafin levels correlated with skin aGvHD in patients.⁴¹ Furthermore, the antimicrobial protein, regenerating islet-derived 3-alpha (REG3 α), expressed in Paneth cells of the small intestine correlated with lower gastrointestinal GvHD. The REG3 α plasma concentration measured at aGvHD onset predicted the treatment response and non-relapse mortality of the patients.⁴² Based on these results, they tested two different panels of previously identified biomarkers: IL-2R α , TNFR1, HGF, IL-8, elafin, REG3 α ⁴³ and REG3 α , HGF, cytokeratin-18⁴⁴, respectively, and successfully predicted both treatment response and survival of patients. These results may be promising, however, both studies concentrated on an early identification of patients' treatment responsiveness rather than aGvHD prediction.

The use of mass spectrometry-based proteomic approaches for the diagnosis of aGvHD led to the identification of two indicative polypeptides of the leukotriene A4 hydrolase and of serum albumin in the urine of patients.⁴⁵ Using these markers allowed the discrimination between patients with and without aGvHD with 82 % specificity and 100 % sensitivity. However, this study only included 40 patients and a validation of the data with a bigger sample size is necessary.

Although these results look promising, a reliable predictive marker panel to identify patients at risk for aGvHD before symptoms occur rather than at clinical disease onset has not been found yet.

2.2.3 aGvHD diagnosis

aGvHD diagnosis is usually based on diarrhea, serum bilirubin, and skin rash and confirmed by biopsies of the GvHD target organs gastrointestinal tract, liver, and skin. A standardized system grades clinical aGvHD severity from I (mild) to IV (life-threatening). The overall grade is defined as the sum of the individual grades of each target organ. The most commonly used grading system was introduced almost 40 years ago, known as the classical Glucksberg-Seattle criteria (GSC)⁴⁶ and was revised by Przepiorka and colleagues in 1994⁴⁷ and the International Bone Marrow Transplant Registry (IBMTR) in 1997.⁴⁸

2.2.4 aGvHD prophylaxis and treatment

For aGvHD prevention, patients undergoing allo-HCT are commonly treated with a combination of a calcineurin inhibitor and a cytostatic drug to avoid T cell proliferation.⁴⁹ Calcineurin inhibitors specifically inhibit intracellular signalling required for T cell activation by forming complexes with the protein phosphatase calcineurin in the cell plasma.⁵⁰ Despite these prophylactic agents, many patients still develop aGvHD. The initial treatment at the onset of the syndrome usually consists of systemic glucocorticosteroids which have lympholytic effects and anti-inflammatory properties. A complete response to this first-line therapy is rather low (20 – 50 %) and patients often suffer from toxic side effects and opportunistic infections or develop resistances to steroids.^{51,52} If the primary therapy fails, multiple different agents have been tested alone or in combination as second-line therapy to treat corticosteroid-refractory aGvHD. These substances include anti-lymphocyte antibodies⁵³⁻⁵⁵, antibodies against various surface molecules of activated T cells⁵⁶⁻⁵⁹ or against tumor necrosis factor alpha (TNF- α)^{60,61}, immunotoxin-based⁶² or pharmacological agents⁶³⁻⁶⁶ or extracorporeal photopheresis^{67,68}.

In many cases, pilot studies showed some promising results but the success rate in improving long term patient survival with second-line therapy is low, often due to toxic side effects of the substances and occurring opportunistic infections.⁶⁹ The perfect therapy would effectively eliminate alloreactive donor T cells while maintaining beneficial Graft-versus-Leukemia (GvL) effects and support a rapid immune recovery. Until today, the drug combination for aGvHD prophylaxis and treatment is far from ideal and many patients still die from this immune syndrome and its associated complications.

In the context of this study, the treatment of mice after miHA_g mismatch allo-HCT consisted of three different reagents given separately and affecting different cellular components:

Prednisolone, a glucocorticoid hormone, exerts anti-proliferative effects on lymphocytes and shows immunosuppressive properties. It binds to cytoplasmic glucocorticoid receptors and translocates them to the nucleus transactivating a wide range of genes.^{70,71} Prednisolone or its derivatives have been used as one of the main corticosteroids for systemic aGVHD treatment for more than 30 years.⁷² Data from a

mouse model also shows the protective effect of Prednisolone when starting the treatment shortly after aGvHD onset.⁷³

Pentostatin or 2'-deoxycoformycin, a purine analogue isolated from the bacteria *Streptomyces antibioticus*, tightly binds to and inhibits the enzyme adenosine desaminase and thereby interferes with DNA processing in the cells.^{74,75} Lymphocytes are especially sensitive to this cytotoxic drug which induces apoptosis. In a murine model, pretreatment of the transferred cells with pentostatin protected from aGvHD.⁷⁶ However, data from animal aGvHD models are limited. In 2005, a pilot study reported the successful use of pentostatin in steroid refractory aGvHD in patients⁶⁶ followed by some small clinical studies with promising response rates.^{77,78}

Rapamycin, an antifungal drug produced by the bacteria *Streptomyces hygroscopicus* with immunosuppressive properties was first described in the 1970s.⁷⁹⁻⁸¹ It belongs to the family of macrolide lactones and blocks cell cycle progression in the G1 phase.⁸² It specifically binds to and inhibits the protein kinase activity of the mammalian target of rapamycin (mTOR), a characteristic component of conventional T cell activation.^{83,84} Rapamycin exerts a protective activity in aGvHD prevention in different mouse models across MHC major mismatch barriers⁸⁵ as well as in human aGvHD prevention^{86,87} and therapy^{88,89}.

2.3 T cell migration and homing

Coordinated leukocyte migration and homing are essential for the development of systemic immune responses. Multistep sequential engagement of adhesion molecules and signalling receptors determine these processes.⁹⁰ Different groups precisely characterized the migration of circulating lymphocytes into SLOs via high endothelial venules (HEVs).⁹¹⁻⁹³ This multistep process is mediated by L-selectin constitutively expressed on naïve lymphocytes and its carbohydrate ligands on HEVs for migration into peripheral lymph nodes (pLNs). Upon activation, the cells down-regulate L-selectin.^{94,95} To enter mucosa-associated lymphoid tissues (MALT) and especially the PPs interactions between $\alpha 4\beta 7$ integrin on lymphocytes and mucosal addressin cell adhesion molecule-1 (MadCAM-1) on mucosal tissues and on PPs, HEVs are pivotal.⁹¹ However, other signals are required to define which leukocyte population homes into a lymph node. SLOs constitutively express certain

chemoattractant molecules – so-called chemokines – such as CCL19, CCL21, CXCL12 and CXCL13 to induce the chemotactic migration of T and B lymphocytes towards these organs. With the help of the respective chemokine receptors (CCRs; CCR7 on T cells for CCL19 and CCL21, and CXCR4 on B cells for CXCL12 and CXCL13) the lymphocyte populations migrate towards and into SLOs. Moreover, the precise positioning of the different cell populations within SLOs is controlled by overlapping chemokine gradients expressed in separate areas.⁹⁶

Nevertheless, it still remains elusive how lymphocytes migrate into parenchymal tissues during inflammation. The molecular interactions of effector cells during this migration process in aGvHD and the endothelial molecules involved are a focus of investigations as these interactions represent potential therapeutic targets. Host APC – donor T cell interactions in SLOs not only activate donor cells to become alloreactive but also lead to the up-regulation of certain homing receptors which are essential for migrating to and entering into peripheral target organs.^{25,27} In general, molecules involved in T cell homing can be categorized into three different groups: integrins, CCRs and selectins. Integrins – heterodimeric molecules consisting of an α and a β subunit – are important mediators of interactions between leukocytes and APCs as well as epithelial cell surface receptors with differing specificity.⁹⁷ Integrins containing the β_7 subunit enable lymphocytes to home into the intestinal mucosa and are involved in aGvHD initiation in the gut by interacting with MadCAM-1 and E-cadherin expressed on the intestinal epithelium.^{98,99} Inflamed tissues also produce chemokines which mainly function as chemoattractants for leukocytes to sites of infection. Activated lymphocytes express CCRs on their surfaces to be able to respond to the chemokine gradients.^{100,101} In contrast to L-selectin on lymphocytes which is down-regulated upon activation, endothelial tissues up-regulate different members of the selectin family including P- and E-selectin, in response to inflammation. In order to enter these tissues activated T cells express ligands for a specific interaction with these molecules.¹⁰²

Several murine studies investigated the involvement of specific homing receptor expression on donor T cells in aGvHD development. Previously, our group showed the importance of SLO access for donor T cells in aGvHD initiation after MHC major mismatch allo-HCT in mice.¹⁰³ Donor T cells isolated from mesenteric LNs (mLNs) and PPs highly up-regulated the integrins $\alpha 4\beta 7$ ¹⁰⁴ and $\alpha E\beta 7$ ¹⁰⁵ as well as CCR9¹⁰⁶ which are involved in the homing to MALT. Figure 2 schematically summarizes the

potential role of these receptors in T cell homing to the intestinal lamina propria. CCR9⁺ α4β7⁺ T cells in the blood stream initially interact with CCL25 constitutively produced by the epithelium. Upon this interaction, α4β7 integrin is activated and its avidity for its ligand MadCAM-1, expressed by small intestinal endothelial surfaces, is increased. The transmigration of the cell through the endothelium follows this interaction. In the lamina propria the cells migrate towards a CCL25 gradient to the epithelium, down-regulate α4β7 expression and up-regulate αEβ7 integrin to interact with E-cadherin for intraepithelial lymphocyte adhesion.¹⁰⁷

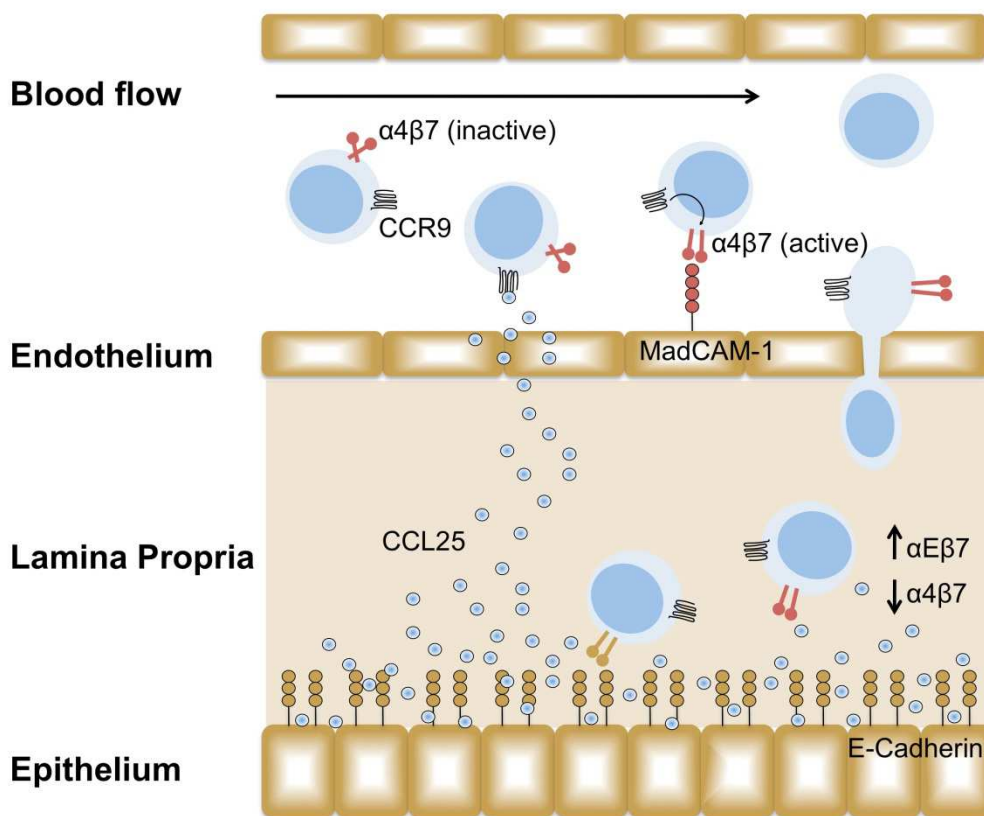


Figure 2: T cell homing to the lamina propria

Potential role of α4β7 integrin and CCR9 in the T cell homing process to the lamina propria. Figure adapted from Agace et al.¹⁰⁷

Recipients of α4β7 integrin negative donor T cells developed significantly less intestinal and liver aGvHD compared to recipients of wild type (WT) T cells in well-defined MHC matched and mismatched murine allo-HCT models indicating the importance of this molecule for the invasion of alloreactive cells into the gut and subsequent aGvHD morbidity and mortality.¹⁰⁸ Donor cells derived from pLNs preferentially expressed E- and P-selectin ligand, molecules involved in skin

homing.^{103,104,109} Interactions between the activation marker CD44 and its ligand hyaluronate are also required for T cell rolling and firm adhesion to endothelial surfaces.^{109,110} CD44 and to a lesser extent also P-selectin-ligand are expressed on donor cells from all SLOs implicating their general role in effector lymphocyte trafficking to inflamed tissues.¹⁰³ Lu and colleagues showed the importance of P-selectin expression on endothelial tissues and its interactions with P-selectin-ligands on T cells for donor cell trafficking into aGvHD target organs as P-selectin knock out mice developed less aGvHD compared to WT recipients.¹¹¹

Many groups investigated the role of different chemokine receptors in aGvHD initiation and development. For example, recipients of CCR2 knock out CD8⁺ T cells developed less overall aGvHD morbidity and mortality in comparison to recipients of WT cells.¹¹² Similar to some other chemokine receptors, CCR2 controls leukocyte migration during inflammation¹¹³ and T cells lacking CCR2 showed an intrinsic migratory defect to gut and liver. Furthermore, another group reported that CCR5 is important for liver infiltration of donor T cells.¹¹⁴ CCR5 is expressed on effector T lymphocytes in various inflammatory conditions¹¹⁵ and the administration of an anti-CCR5 antibody protected against liver damage in aGvHD. An anti-MIP1 α antibody which is the main ligand for CCR5 led to similar effects in this study. Coghill and colleagues investigated the separation of aGvHD from GvL by targeting CCR7¹¹⁶ which plays an important role in trafficking of lymphocytes into SLOs.¹¹⁷ They showed that CCR7 knock out cells caused attenuated aGvHD responses compared to mice receiving WT T cells. However, the GvL effect was preserved by cells lacking CCR7. Another group described CXCR3 as an important molecule for the migration of CD8⁺ donor T cells to aGvHD target organs.¹¹⁸ CXCR3 represents a general inflammation marker¹¹⁵ and recipients of CXCR3 knock out CD8⁺ T cells developed less gut and liver damage and showed an improved overall survival.

Based on these studies and others dealing with single homing receptors and their involvement in aGvHD development, a thorough investigation of the homing receptor expression profile consisting of a combination of surface molecules which specifically characterizes alloreactive donor T cells appears attractive.

3. Specific aims

Since aGvHD still poses a major complication after allo-HCT and early diagnosis is limited to patients with established disease manifestation, the development of predictive assays for the early identification of patients at risk for aGvHD and for an improved disease prevention is of high importance.

The principal aim of this doctoral thesis was to establish a clinical relevant mouse model of aGvHD across miHAg mismatch barriers in order to identify suitable homing receptors expressed on peripheral blood T lymphocytes which allow an alloreactive cell detection early after allo-HCT.

This study addressed the following questions:

1. Is it possible to detect alloreactive donor T cells early after HCT in the peripheral blood before clinical aGvHD symptoms become apparent?
2. Which time points early after allo-HCT are suitable for a precise phenotypical analysis of alloreactive donor T cells in the peripheral blood?
3. Can mice at risk for aGvHD development be identified according to the homing receptor expression profile of alloreactive peripheral blood T cells?
4. Does a timely immunosuppressive intervention prevent aGvHD and prolong survival of identified animals?

To answer these questions we employed bioluminescence imaging (BLI) and multicolor flow cytometry (FC) for a precise characterization of donor T cell migration kinetics after allo-HCT followed by a detailed analysis of the homing receptor expression profile of donor T cells in the peripheral blood.

Thus, the long term goal of my thesis project was to set the basis for developing a simple, predictive blood test for early identification of patients at risk to develop aGvHD.

4. Material and Methods

4.1 Mice

The following mice were obtained from Charles River (Sulzfeld, Germany): Balb/C (H-2^d, Thy1.2), C57Bl/6 (B6, H-2^b, Thy1.2) and OT-I (C57Bl/6-tg(tcra/tcrb)425Cbn/Crl). OT-I CD8⁺ T cells recognize the chicken ovalbumin peptide OVA₂₅₇₋₂₆₄ (SIINFEKL) associated with H-2k^b. Balb/B (H-2^b, Thy1.2), congenic C57Bl/6 (B6, H-2^b, CD45.1), C57Bl/6J-Tyrc-2J/J (B6 albino, H-2^b, Thy1.2) and C57Bl/6-tg(βA-OVA) (βA-OVA, H-2^b, Thy1.2) were purchased from Jackson Laboratories (Bar Harbor, ME). βA-OVA mice express chicken ovalbumin under the β-actin promoter. A luciferase-expressing (*luc*⁺) transgenic FVB/N line was generated as previously described¹¹⁹. Female heterozygous *luc*⁺ offspring of the transgenic founder line FVB-L2G85 were backcrossed for more than 12 generations onto C57Bl/6 (H-2^b, Thy1.1) and OT-I (H-2^b, Thy1.1) backgrounds. All mice were housed in a specified pathogen-free animal facility at the Center for Experimental Molecular Medicine (ZEMM), Würzburg. All animal experiments were approved by local authorities (Regierung von Unterfranken) and complied with German animal protection law.

4.2 Cell isolation from mouse organs

Mice were sacrificed by cervical dislocation and single cell suspensions from different organs were prepared. All single cell suspensions were washed and resuspended in 1 x PBS (Phosphate Buffered Saline without calcium and magnesium, PAN Biotech, Aidenbach, Germany) before injections into the mice.

4.2.1 Bone Marrow

BM from WT B6 donor mice was flushed from femur and tibia bones with PBS using a 1 ml syringe and passed through a 70 μl cell strainer (Becton Dickinson, BD, Heidelberg, Germany) to obtain a single cell suspension. The total yield from two hind leg bones usually was around 1.5 x 10⁸ cells.

4.2.2 Spleen

After removal of the spleen it was carefully mashed through a 70 μ l cell strainer and flushed with lysis buffer (see 4.7) for red blood cell (RBC) depletion via hypertonic lysis from the cell suspension. After 2 minutes (min) of incubation, cells were washed with 1 x PBS, filtered again through a cell strainer and counted in a Neubauer chamber using trypan blue (1:10 dilution; AppliChem, Darmstadt, Germany). The total yield from a spleen usually was 1×10^8 splenocytes.

4.2.2.1 T cell enrichment of splenocytes

Splenic CD3⁺ single cell suspensions were enriched using the Dynal Mouse T cell Negative Isolation Kit (Invitrogen, Darmstadt, Germany) according to the manufacturer's protocol. Briefly, after blocking of unspecific binding sites with fetal calf serum (FCS, Invitrogen) the provided antibody mix was added for 20 min at 4°C. Cells were washed and resuspended in Dynal Buffer (see 4.7) before the addition of Depletion Dynabeads for 15 min at room temperature (RT). After resuspending the suspension carefully the tube was placed into a magnet for 2 min. The removed supernatant contained untouched CD3⁺ T cells. Post enrichment fluorescence-associated cell sorting (FACS) analysis confirmed cell purity (> 90 %) as shown in Figure 3.

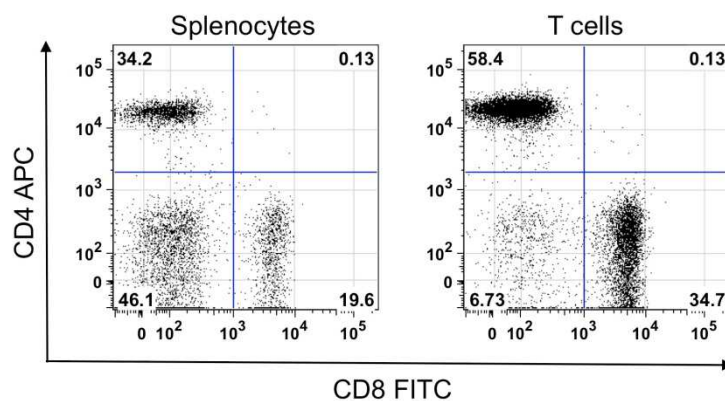


Figure 3: Prior and post enrichment FACS analysis

FACS analysis of splenocytes before (Splenocytes) and after (T cells) T cell negative isolation. PI staining excluded dead cells. Dot blots show different T cell subpopulations stained for the surface markers CD4 and CD8. Quadrants show percentages of all living cells.

4.2.2.2 T cell depletion of splenocytes

Splenocytes were T cell-depleted using the Dynal Mouse CD4⁺ and CD8⁺ T cell Kit (Invitrogen) according to the manufacturer's protocol. Briefly, cells were resuspended in Dynal Buffer (see 4.7) and anti-CD4 and/or anti-CD8 antibodies were added for 10 min at 4°C. After washing cells with ice cold buffer resuspended Dynabeads were added and incubated for 15 min at 4°C. The tube was placed in the magnet for 1 min and the removed supernatant contained all splenocytes except CD4⁺ and/or CD8⁺ T cells. Post depletion FACS analysis confirmed cell purity (< 5 % T cells left) as shown in Figure 4.

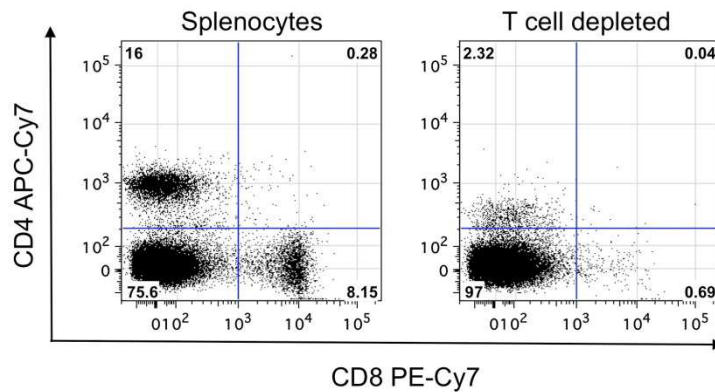


Figure 4: Prior and post depletion FACS analysis

FACS analysis of splenocytes before (Splenocytes) and after T cell depletion. PI staining excluded dead cells. Dot plots show different T cell subpopulations stained for the surface markers CD4 and CD8. Quadrants show percentages of all living cells.

4.2.3 Lymph nodes

Cervical, inguinal and mesenteric lymph nodes (cLNs, iLNs, mLNs) were removed and carefully squeezed through a cell strainer. Single cell suspensions were washed with 1 x PBS before FACS analysis.

4.2.4 Peripheral Blood Mononuclear Cell (PBMC) collection

Peripheral whole blood samples of mice were taken from the tail vein and collected in lysis buffer (see 4.7) for RBC depletion via hypotonic lysis in preparation for FACS analysis. In addition, 25 µl of peripheral whole blood samples from mice of interest were added to 100 µl PBS / EDTA (1 mM; Roth, Karlsruhe, Germany) for white blood

cell counts using a Sysmex XT-2000i (Horgen, Switzerland). In some experiments, cardiac puncture of deeply anesthetized animals was performed and the blood samples were used for FACS analysis and total white blood counts.

4.3 Allogeneic and syngeneic HCT

Prior to HCT, 8- to 12-week-old female recipient mice were myeloablatively irradiated (Balb/C, Balb/B 8 Gy, B6 9 Gy) with an electron linear accelerator (Mevatron Primus, Siemens, Germany). For hematopoietic reconstitution, animals were injected with 5×10^6 B6 WT BM cells intravenously. To induce aGvHD, Balb/C recipients (MHC major mismatch model) received 1.2×10^6 , Balb/B recipients (miHAg mismatch model) 5×10^6 splenic *luc+* B6 T cells within 3 hours after irradiation. Syngeneic B6 control mice received 1.2×10^6 T cells. Thy1.1 (CD90.1) or Ly5.2 (CD45.1) served as congenic markers to distinguish between donor and host (CD90.2, CD45.2) T cells. Transplanted mice were monitored daily for survival, weight change and symptoms of clinical GvHD. Drinking water was supplemented with an antibiotic (Baytril, Bayer, Leverkusen, Germany) for one week starting on the day of HCT to prevent infections following myeloablative irradiation.

4.4 Immunosuppressive treatments

For *in vivo* studies, prednisolone (Merck, Darmstadt, Germany) was dissolved in distilled water according to manufacturer's instructions. Intraperitoneal injections (5 mg / kg body weight, BW) were given daily, starting on day+0 or day+6 after allo-HCT, until the end of the experiments. Pentostatin (Hospira, Munich, Germany) was dissolved in distilled water. Five intraperitoneal injections of 0.75 mg / kg BW each were given on days+6, +11, +15, +18, +21 after allo-HCT. Rapamycin (Wyeth, Bergshire, UK) was dissolved in carboxymethylcellulose sodium salt (C-5013, Sigma-Aldrich, Munich, Germany) and polysorbate 80 (P-8074, Sigma-Aldrich) to a final concentration of 1.5 mg / kg BW as previously described.¹²⁰ Intraperitoneal injections were given daily from day+6 to day+15. Dosages were adjusted to the BW every other day.

4.5 Clinical GvHD Scoring

Five different parameters (weight loss, posture, activity, fur texture, diarrhea) were monitored daily and graded 0 to 3 depending on severity and a total score per mouse was calculated.

4.6 In vivo and ex vivo bioluminescence imaging

For *in vivo* BLI, mice were anesthetized and D-luciferin (Biosynth AG, Staad, Switzerland) was administered at a dose of 150 μg / g BW intraperitoneally. 10 min after injection, images were acquired as previously described^{20,119} using an IVIS Spectrum charge-coupled device (CCD) imaging system (Caliper-Xenogen, Alameda, CA). For *ex vivo* imaging, mice were injected with an additional dose of luciferin after *in vivo* imaging, sacrificed 10 min later and images were taken from organs of interest. Imaging data was analyzed and quantified with Living Image Software 3.1 (Caliper-Xenogen).

4.7 Buffers and Anesthetic

- 10 x Lysis Buffer: 89.9 g NH_4Cl
10 g KHCO_3
0.37 g EDTA in 1000 ml aqua dest.
- 10 x PBS: 80 g NaCl
14.2 g $\text{Na}_2\text{HPO}_4 \cdot 2 \text{H}_2\text{O}$
2 g KCl
2 g KH_2PO_4 in 1000 ml aqua dest.
pH: 6.8
- Dynal Buffer: 0.5 g BSA
0.2 ml EDTA (0.5 M) in 500 ml 1 x PBS

- PFA: 4 g PFA in 100 ml 1 x PBS (4 %)
Dissolve at 65°C
pH: 7.4

All chemicals were purchased from Roth, Karlsruhe, Germany.

- cRPMI 1640 RPMI-1640 medium supplemented with
10 % FCS
Penicillin (100 U / ml)
Streptomycin (100 µg / ml)
L-glutamine (2 mM)
2-mercaptoethanol (50 µM)

All purchased from Invitrogen, Darmstadt, Germany

- Anesthetic: 8 ml Ketanest (25 mg / ml), Pfizer Pharma, Berlin, Germany
2 ml Rompun (2 %) Xylazin, CP-Pharma, Burgdorf, Germany
15 ml 1 x PBS

4.8 Flow Cytometry

Flow cytometric (FC) analyses were performed in 96-well plates using the plate reader system of a BD LSR II or BD FACSCanto II (BD). Cytometer Setup and Tracking Beads (CS&T, BD) were run daily before measurements for cytometer setup. Application settings associated with the cytometer configuration in FACSDiva software were updated automatically. FACS data was analyzed with FlowJo Software version 8 (Treestar, Ashland, OR).

4.8.1 Antibodies and Titration

All antibodies used were titrated for optimal dilutions to avoid overstainings and false positive signals. Titrations were performed using isolated splenocytes. For some homing receptors and activation markers, stimulation of the cells was necessary to

4 Material and Methods

induce the expression of the desired molecule. Six different dilutions were tested starting with 1:100 as shown in Figure 5. The dilution giving the best separation of positive and negative cell populations without overstaining the negative cell population was chosen for further experiments. In the shown example, a titer of 1:400 was used for further experiments.

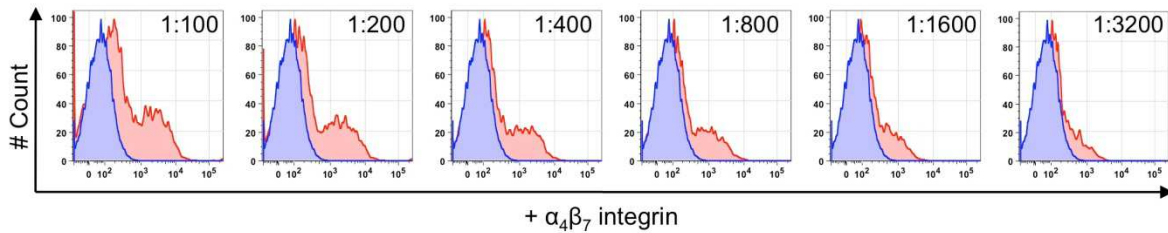


Figure 5: Titration row for an anti- $\alpha_4\beta_7$ integrin antibody

Splenocytes were isolated on day+6 after transplantation and stained with six different dilutions (in PBS) of an anti- $\alpha_4\beta_7$ integrin antibody (red) conjugated to PE. Histograms show the results compared to splenocytes of an untreated WT B6 mouse ($\alpha_4\beta_7$ integrin negative, blue).

Source, specificity, clone, and conjugation of all antibodies, synthetic proteins and secondary reagents used for FC analyses and immunofluorescence microscopy (IFM) are shown in Table 1 to 3.

Table 1: Antibodies used for FC and IFM

Antigen	Clone	Conjugate	Dilution	Usage	Company
CCR2	475301	APC	1:400	FC	R&D
CCR4	2G12	APC	1:200	FC	Biolegend
CCR5	C34-3448	PE	1:200	FC	Biolegend
CCR6	FAB590P	PE	1:200	FC	R&D
CCR7	4B12	APC	1:200	FC	Biolegend
CCR9	242503	FITC	1:100	FC	R&D
CD103 α E	2E7	PB	1:200	FC	Biolegend
CD107a	1D4B	FITC	1:100	FC	Biolegend
CD107b	M3/84	FITC	1:100	FC	Biolegend
CD25	PC61	PB	1:800	FC	Biolegend
CD4	RM 4-5	Biotin	1:100	IFM	Biolegend
CD4	RM 4-5	FITC	1:1600	FC	Biolegend
CD4	RM 4-5	APC	1:800	FC	Biolegend
CD4	RM 4-5	APC-Cy7	1:400	FC	Biolegend
CD44	IM7	PE	1:800	FC	Biolegend
CD45RA	14.8	Biotin	1:1600	FC	BD
CD62L	MEL-14	FITC	1:3200	FC	Biolegend
CD69	H1.2F3	PB	1:800	FC	Biolegend
CD8 α	53-6.7	PE-Cy7	1:1600	FC	Biolegend

4 Material and Methods

CD8 α	53-6.7	Alexa488	1:100	IFM	Biolegend
CD90.1	HIS51	APC-eF750	1:1600	FC	eBioscience
CD90.1	HIS51	APC	1:100	IFM	eBioscience
CXCR3	CXCR3-173	APC	1:1600	FC	Biolegend
FoxP3	FJK-16s	Purified	1:50	IFM	eBioscience
IFN γ	XMG1.2	PE	1:400	FC	Biolegend
IFN γ	XMG1.2	PerCP-Cy5.5	1:1600	FC	Biolegend
TNF α	MP6-XT22	PE	1:1600	FC	Biolegend
V α 2	B20.1	Biotin	1:800	FC	BD
α 4 β 7	DATK32	PE	1:400	FC	Biolegend

Table 2: Synthetic proteins

Antigen	Description	Dilution	Company
P-selectin ligand	Purified Mouse P-Selectin-IgG Fusion Protein	1:800	BD
E-selectin ligand	Recombinant Mouse E-Selectin/CD62E Fc Chimera	1:800	R&D Systems

Table 3: Secondary reagents

Reagent	Binds to	Conjugate	Dilution	Company
Streptavidin	Biotin	Alexa750	1:800	Invitrogen
Streptavidin	Biotin	eFluor450	1:800	Invitrogen
AffiniPure goat anti-human IgG, FC γ Fragment specific	Purified Mouse P-Selectin-IgG Fusion Protein	FITC, PE	1:800	Jackson Immunoresearch
AffiniPure donkey anti-rat IgG	Purified rat anti-mouse Ab	Cy3	1:400	Jackson Immunoresearch

4.8.2 Compensation

Since the emission spectra of different fluorochromes overlap it is necessary to compensate the measured data to avoid false positive signals in different channels.¹²¹ By creating a compensation matrix before analyzing the data flowjo software calculates the percentage of overlaps of the different fluorochromes used and subtracts them from each other. By applying this matrix to the samples of interest, the data is corrected and false positive signals from other fluorochromes

than the one measured in that given channel can be excluded. Either mouse splenocytes or polystyrene micro particles (CompBeads, BD) were used for compensation controls. CompBeads bind to the κ -chain of any antibody used. The addition of negative control beads which cannot bind to κ -chains results in distinct positive and negative stained populations for each fluorophore independently of the antibody specificity. This method is especially useful for the compensation of homing receptors or activation markers which are not expressed on untreated splenocytes as well as for the use of tandem-dyes which may have different spectral characteristics for each conjugate. Figure 6 shows a compensation row with CompBeads. One antibody per well per color was added.

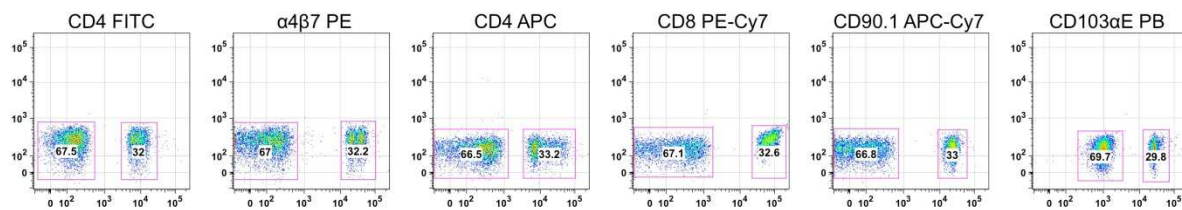


Figure 6: Compensation row for a 6 color FACS analysis using CompBeads

Dot blots showing the positive and negative populations of CompBeads stained with an antibody for each color separately. x-axis: fluorophore of interest, y-axis: any other unstained channel.

4.8.3 Fluorescence minus one

For analyzing the FACS data the fluorescence minus one-gating strategy according to Tang et al. was used.¹²² To define the positivity in a given channel, fluorescence minus one (FMO) controls were performed for each individual flow cytometric analysis. In a FMO control sample all reagents of a multicolor staining were included except for the one the threshold had to be defined to assess background and nonspecific staining within the given channel. Figure 7 shows representative FMO controls for CD8 α and CD90.1 stainings. After definition of the double positive population the comparison of one sample with (red) and one without (blue) the PE-conjugated anti- $\alpha_4\beta_7$ antibody allowed to define the $\alpha_4\beta_7$ integrin expressing subset.

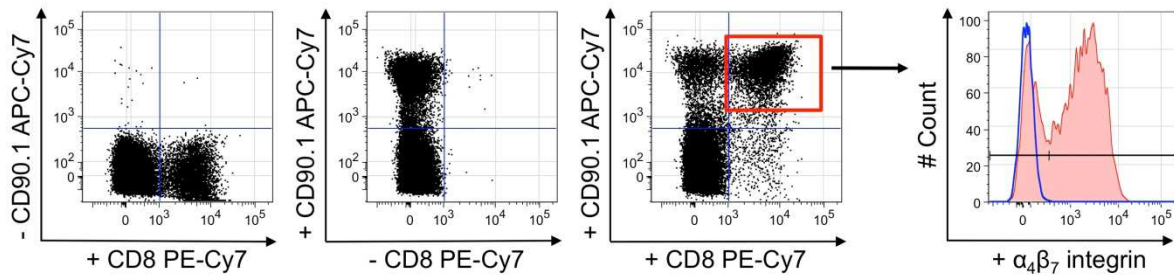


Figure 7: FMO gating example

Dot blots of splenocytes stained (from left) only with an anti-CD8 antibody, only with an anti-CD90.1 antibody and with both to define the double positive population. The histogram shows the portion of $\alpha_4\beta_7$ expressing cells (red) from the previously defined $CD8^+ CD90.1^+$ double positive cells compared to $\alpha_4\beta_7$ negative cells (blue line).

4.8.4 Surface Phenotyping

Surface phenotyping was performed in 96-well round bottom plates in a total volume of 200 μ l PBS per well. First, unspecific binding sites were blocked with 100 μ l normal rat serum (NRS, Invitrogen) diluted 1:20 in PBS for 5 min on ice. The antibody cocktail was added and the plate was incubated at 4°C for 30 min in the dark. After washing, the pellet was resuspended in 100 μ l PBS and 100 μ l of secondary antibody dilution was added, if necessary. After another 30 min incubation time, cells were washed again and resuspended in 200 μ l PBS for analysis. Dead cells were excluded by adding 4',6-Diamidin-2-phenylindol (DAPI, Invitrogen) or propidium iodide (PI, Invitrogen) shortly before measurement. Figure 8 shows a gating example for $\alpha_4\beta_7$ integrin expression on $CD90.1^+$ donor T cells.

4.8.5 Intracellular Staining

Intracellular cytokine stainings were performed using the intracellular staining kit (BD) according to the manufacturer's instructions. For fixation and permeabilization, cells were resuspended in 100 μ l BD Cytfix / Cytosperm and incubated for 20 min at 4°C. After washing twice with 1 x BD Perm / Wash Buffer the antibody cocktail was added in a total volume of 200 μ l BD Perm / Wash Buffer and incubated for 30 min at 4° in the dark. Prior to cytometric analysis cells were washed again and resuspended in 200 μ l staining buffer.

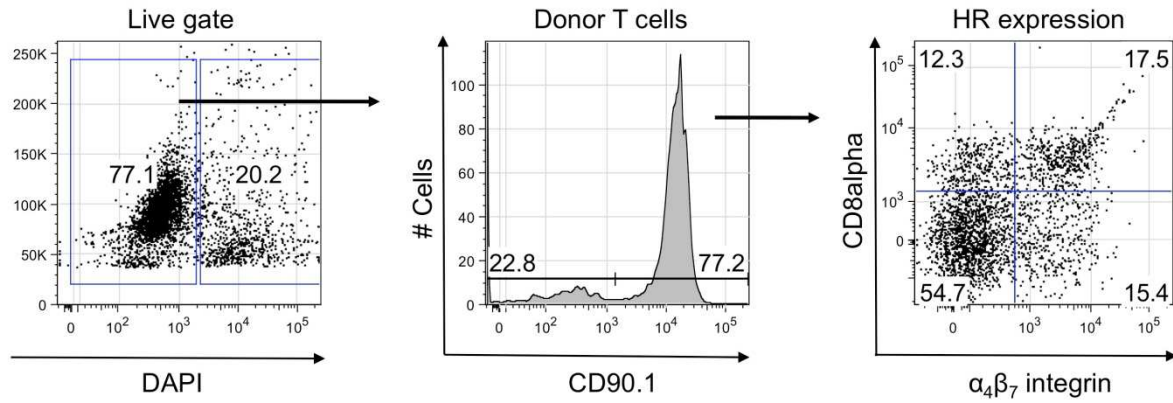


Figure 8: Phenotyping gating example

A life gate separates the living (DAPI negative) from the dead cells (DAPI positive), shown as dot blot on the left. The CD90.1 staining defines the donor cells among all living cells (shown in the Histogram). Gated on all donor cells the $\alpha_4\beta_7$ expressing populations among the donor T cells can be defined (dot blot on the right): CD8⁺ $\alpha_4\beta_7$ ⁺ (upper right quadrant) or CD8⁻ $\alpha_4\beta_7$ ⁺ (these cells most likely are CD4⁺ T cells; lower right quadrant).

4.9 CD107 degranulation assay

The CD107 degranulation assay was performed as previously described.^{123,124} Briefly, to test an antigen specific T cell response, *in vitro* stimulated TCR transgenic OT-I CD8⁺ T cells were mixed with SIINFEKEL expressing target cells from B6-OVA donors or SIINFEKL negative WT cells, respectively.

For stimulation, 50 ng / ml purified anti-CD3 monoclonal antibody and 300 IU / ml rhIL-2 (Biolegend) were added to a tissue culture flask. After 24 hours and every 2 to 3 days thereafter, cells were divided into flasks with new media supplemented with rhIL-2 (300 IU / ml) but not restimulated with anti-CD3. Highly activated CD8⁺ T cells for 7 to 10 days in culture were used to establish the CD107 degranulation assay and as positive controls for *in vivo* experiments.

An effector : target ratio of 1:8 was found to be optimal for the assay. T cell depleted splenocytes were used as target cells. Cultures were set up in 96-well round bottom plates in cRPMI medium (see 4.7). FITC-conjugated anti-CD107a and -CD107b antibodies were added to the cells prior to incubation. As a negative control for spontaneous degranulation and cytokine expression, no target cells were added. After incubation for 5 hours at 37°C and 5 % CO₂ in the presence of the secretion

inhibitors monensin and/or brefeldin A (BD Pharmingen) cells were washed twice with PBS and prepared for surface and intracellular FACS stainings.

For *in vivo* experiments, the degranulation assay was performed on day+5 after HCT using PBMCs from transplanted mice and the degranulation rate of alloreactive T cells was measured against allogeneic and syngeneic T cell depleted splenocytes, respectively.

4.10 Immunofluorescence staining and immunohistochemistry

Organs were embedded in O.C.T. (Sakura, Zoeterwoude, Netherlands) and cut into 5 μm thick sections. Slides were kept at -20°C until staining. After air drying and acetone fixation (10 min RT), sections were incubated with blocking solution (15 min in PBS + 1 % FCS) prior to the antibody staining for 1 hour. After washing with PBS a secondary antibody was added for an additional 30 min where needed. Nuclei were stained with Hoechst (diluted 1:1000 in 1 x PBS) or DAPI (diluted 1:3000 in 1 x PBS) for 3 min. Washing steps after antibody incubation and Hoechst / DAPI staining were performed in 1 x PBS (3 times, 2 min each). Fluorescence microscopic evaluation was performed on a Carl Zeiss AxioImager Z1. Alternatively, for immunohistochemistry, air dried slides were incubated with 1 % H_2O_2 for 10 min before blocking with avidin-biotin (Avidin / Biotin Blocking Kit, Vector, Linaris GmbH, Wertheim, Germany) for 15 min each, followed by a 15-minute block with 1 % FCS. CD90.1-biotin antibody conjugate was used for donor T cell staining for 1 hour followed by the ABC method (Vector) based on an immunoperoxidase reaction according to the manufacturer's protocol.

4.11 Histologic evaluation

For histological analysis, organs were fixed in PBS containing 4 % paraformaldehyde (PFA; Roth). Representative PFA fixed samples of GIT, liver, and skin of each group were embedded in paraffin, cut into 3 μm thick sections, and stained with hematoxylin and eosin. GvHD scoring was performed according to Lerner et al.¹²⁵ based on tissue damage. The scoring system categorized 0 as normal, 1 for mild, 2

for moderate, and 3 for severe tissue damage caused by donor T cells. All slides were examined by a blinded pathologist.

4.12 Statistical analyses

Survival times among groups were compared using the log-rank test with GraphPad Prism Version 5 (GraphPad Software, USA). Differences of groups in light emission of BLI and homing receptor expression of peripheral blood CD4⁺ and CD8⁺ T cells were analyzed by ANOVA or Student's t test where appropriate. Group comparisons were performed with Dunnett's multiple comparison test. Differences in GvHD scores were analyzed by the Kruskal-Wallis test as Singly Ordered R x C tables with StatXact 8 (Cytel Inc., USA). P values <0.05 were considered statistically significant.

5. Results

5.1 Dynamics of aGvHD pathophysiology

To develop a reliable predictive test for aGvHD it is of high importance to precisely know the disease development and progression at early stages after allo-HCT. Therefore, we closely monitored the dynamics of aGvHD pathophysiology and donor T cell migration kinetics early after allo-HCT in order to identify suitable time points for early aGvHD prediction which should facilitate a timely therapeutic intervention.

5.1.1 Physiological changes caused by aGvHD

To establish a miHAg mismatched mouse model (B6 → Balb/B) for non-invasive imaging of aGvHD survival, weight change, and clinical aGvHD scoring after HCT were compared to the well-defined major mismatched aGvHD model (B6 → Balb/C).²⁰ To induce aGvHD across miHAg mismatch barriers myeloablatively conditioned Balb/B mice (H-2^b) received 5×10^6 B6 (H-2^b) *luc*+ splenic T cells plus 5×10^6 WT B6 BM cells intravenously. Initially, all miHAg mismatched recipients lost and regained weight similar to syngeneic control mice (Figure 9B) and did not display any clinical signs of aGvHD within the first 2 weeks after allo-HCT (Figure 9C). By day+15 miHAg mismatched Balb/B recipients started to lose weight again and by day+21 mice developed aGvHD. They presented first signs of diarrhea followed by ruffled fur and hunched posture leading to an increase in the clinical aGvHD score. Yet, most animals survived until the end of the experiments at day+30 (Figure 9A). The transfer of 1.2×10^6 B6 *luc*+ splenic T plus BM cells into myeloablatively conditioned major mismatched Balb/C recipients (H-2^d) led to aGvHD induction. All mice developed signs of a hyperacute form of GvHD (weight loss, ruffled fur, diarrhea, hunched posture, and lethargy) within 6 to 10 days after HCT and succumbed to the disease soon thereafter, mostly between days+6 and +14 (Figure 9A – C, left panels). Transfer of BM cells alone rescued all recipients from myeloablative irradiation except for one BM control mouse that likely did not engraft (Figure 9A). Syngeneic albino B6 recipients (H-2^b) transplanted with 1.2×10^6 B6 *luc*+ splenic T plus BM cells did not develop any signs of aGvHD (Figure 9C), regained their body

5 Results

weight and survived until the end of the experiments (Figure 9A, B). One syngeneic mouse died during the imaging procedure.

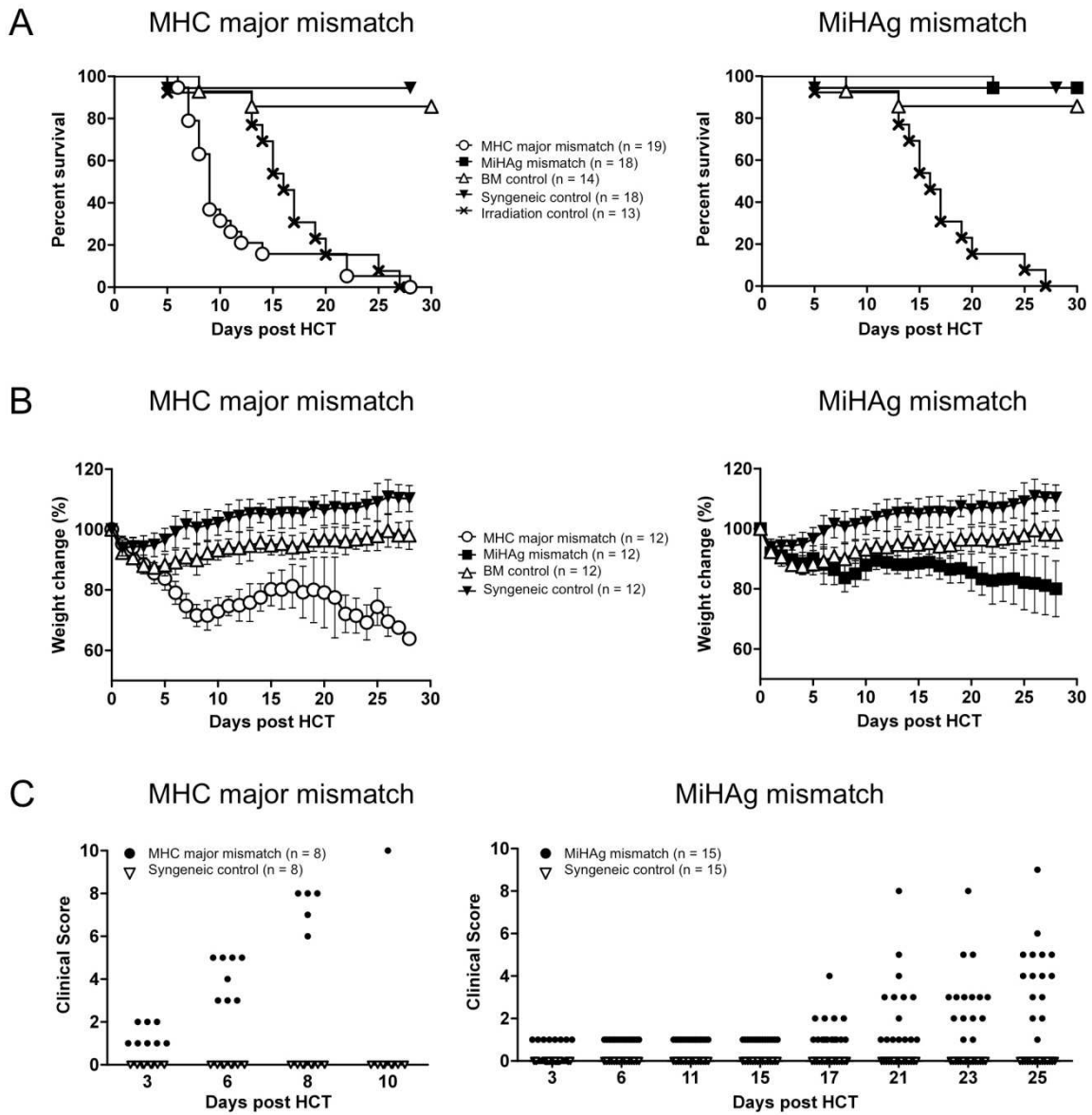


Figure 9: Survival, weight change and clinical aGvHD scoring of representative experiments

(A) Survival of MHC major mismatched Balb/C (left panel) or miHAg mismatched Balb/B (right panel) mice after allo-HCT with the accordant control groups included. Graphs show summary of two independent experiments. (B) Weight change displayed relative to day 0 of HCT for Balb/C (left panel) and Balb/B (right panel) recipients, respectively. Error bars show mean plus or minus SD. One representative experiment out of three is shown. (C) Clinical aGvHD score of one representative experiment. Each dot represents one out of 8 (MHC major mismatch, left panel) or 15 (miHAg mismatch, right panel) animals.

These experiments proved differences in disease onset and survival between the miHAg mismatched model of aGvHD and the MHC fully mismatched hyperacute GvHD model. MiHAg mismatched allo-HCT recipients showed a delayed disease onset and prolonged survival rates.

5.1.2 Donor T cells accumulate in target organs

Histopathological analyses of target organs according to Lerner et al.¹²⁵ at day+6 and day+21 after HCT confirmed aGvHD in allogeneic recipients (Figure 10). MHC major mismatched allo-HCT recipients showed massive target organ destruction already on day+6 with the small and large bowel being most severely affected (up to grade 3). Mice transplanted across miHAg mismatch barriers displayed only mild histopathological signs of aGvHD on day+6 not exceeding grade 2 in the gastrointestinal tract and even less tissue damage in liver and skin. In contrast, by day+21 when first clinical aGvHD symptoms appeared (Figure 9), especially the large bowel and the liver showed most severe tissue damage (grade 2 to 3 in all mice) followed by the skin. Syngeneic control mice did not show any organ damage.

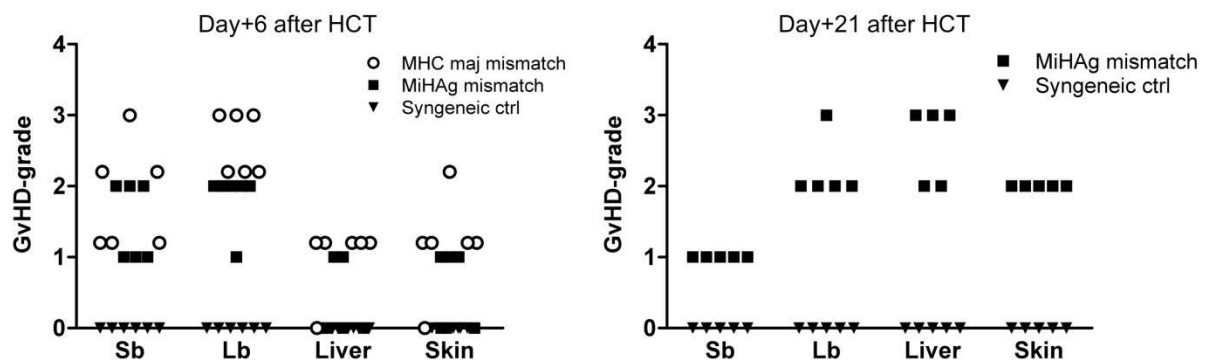


Figure 10: aGvHD scoring on days+6 and +21 after HCT

Histopathological aGvHD scoring of target organs according to Lerner et al.¹²⁵ on days+6 and +21 after HCT. Summary of two independent experiments (n = 6 on day+6, n = 5 on day+21). Sb = small bowel, Lb = large bowel

Immunohistochemical stainings at indicated time points confirmed a massive infiltration of target organs by donor T cells which led to a severe destruction of recipients' tissues. Figure 11 and Figure 12 (upper panels) show representative pictures of CD90.1⁺ donor T cell infiltrates of the small and large bowel, respectively. In MHC major mismatched allo-HCT recipients large numbers of donor T cells

already accumulated in the gastrointestinal tract by day+6 which led to the massive tissue destruction of the small and large bowel. In contrast, in miHA_g mismatched allo-HCT recipients only some donor T cells appeared in the gastrointestinal tract at this early time point compared to huge infiltrates especially of the large bowel on day+21 in this group (Figure 12, middle panel). In syngeneic control tissues only few single cells stained positive for CD90.1.

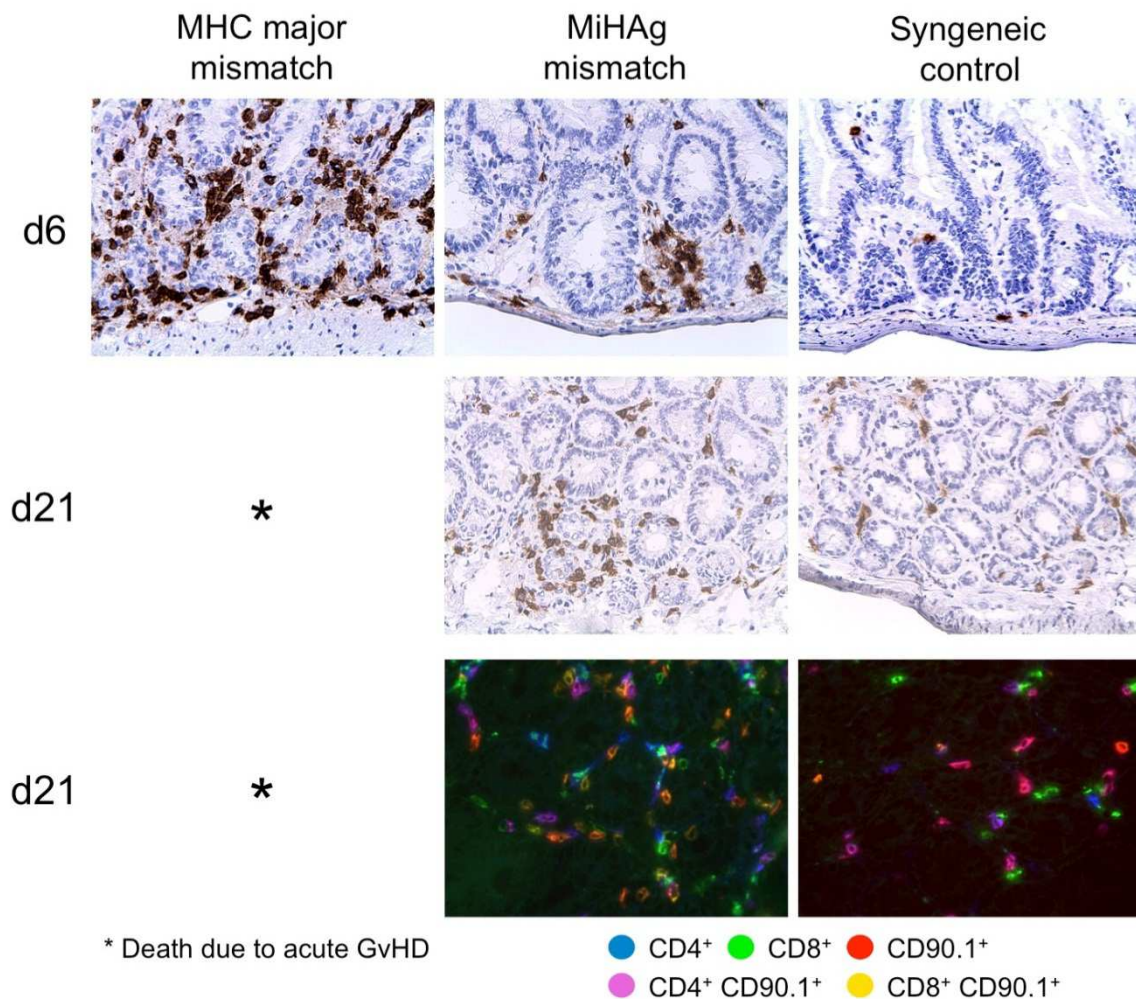


Figure 11: Donor T cell infiltration of the small bowel

Histopathological stainings show CD90.1⁺ donor T cell infiltrates of the small bowel in the three different models on days+6 and +21 after HCT (upper and middle panel). Immunofluorescence microscopy shows distribution of different T cell subsets in the miHA_g and syngeneic settings on day+21 (lower panel). 40x magnification

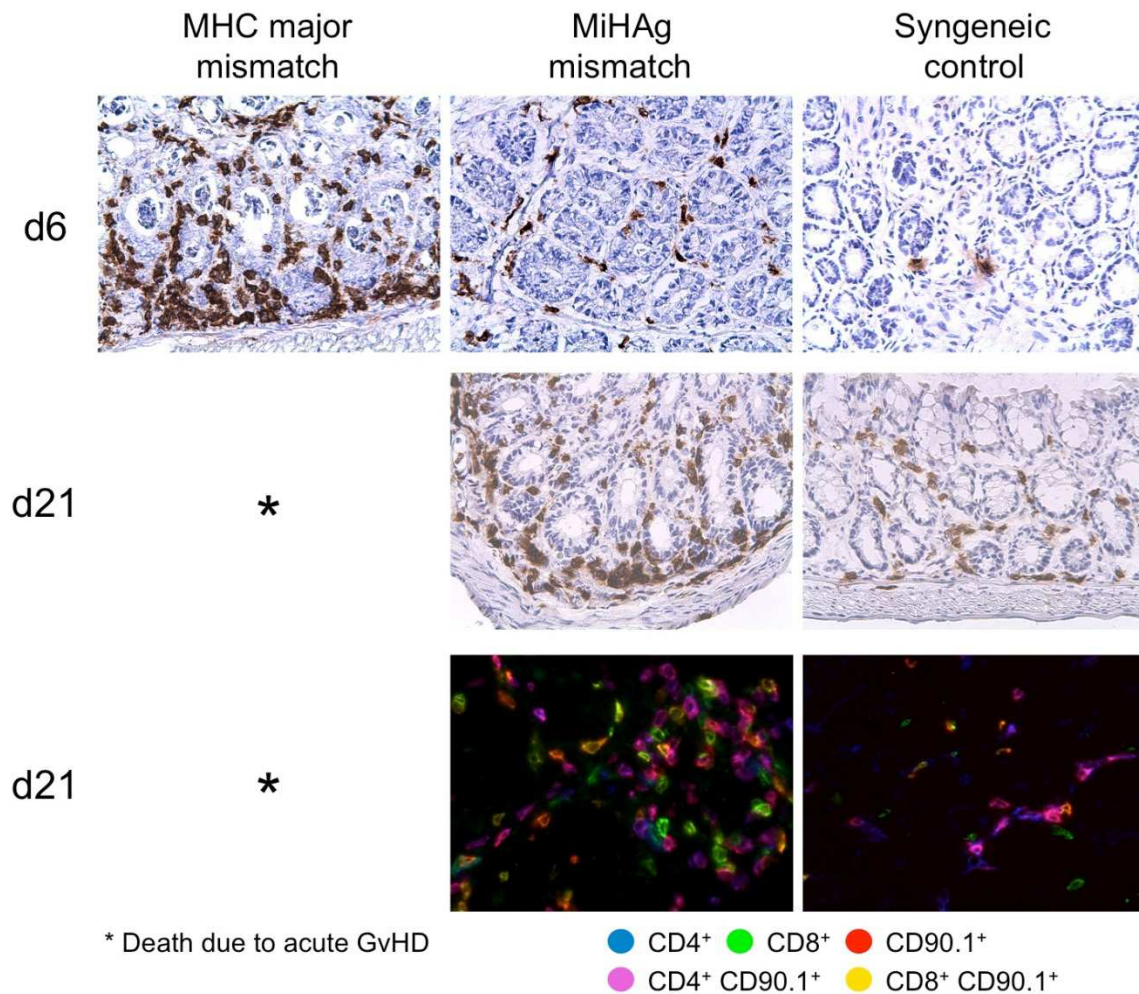


Figure 12: Donor T cell infiltration of the large bowel

Histopathological stainings show CD90.1⁺ donor T cell infiltrates of the large bowel in the three different models on days+6 and +21 after HCT (upper and middle panel). Immunofluorescence microscopy shows distribution of different T cell subsets in the miHA_g and syngeneic settings on day+21 (lower panel). 40x magnification

Immunofluorescence stainings of representative samples on day+21 showed the distribution of donor T cell subsets in the miHA_g and syngeneic settings (Figure 11 and Figure 12, lower panels). Donor T cell infiltrates consisted of CD4⁺ as well as CD8⁺ CD90.1⁺ double positive donor T cells. The few cells single positive for CD4 or CD8 most likely were either recipient T cells that survived irradiation or other cell populations that also express these markers.

The quantification of cells infiltrating the different target organs confirmed a strong accumulation of cells in all target tissues in the MHC major mismatch model already by day+6 with especially high numbers found in the gastrointestinal tract (Figure 13,

left panel). By day+21, allogeneic CD4⁺ CD90.1⁺ and CD8⁺ CD90.1⁺ donor T lymphocytes massively infiltrated target organs after miHAg mismatched allo-HCT with a more than 3-fold increase in cell numbers in both small and large bowel compared to day+6. Also skin and liver were strongly infiltrated (Figure 13, right panel). Number of detected donor T cells in organs of syngeneic HCT recipients stayed constantly low.

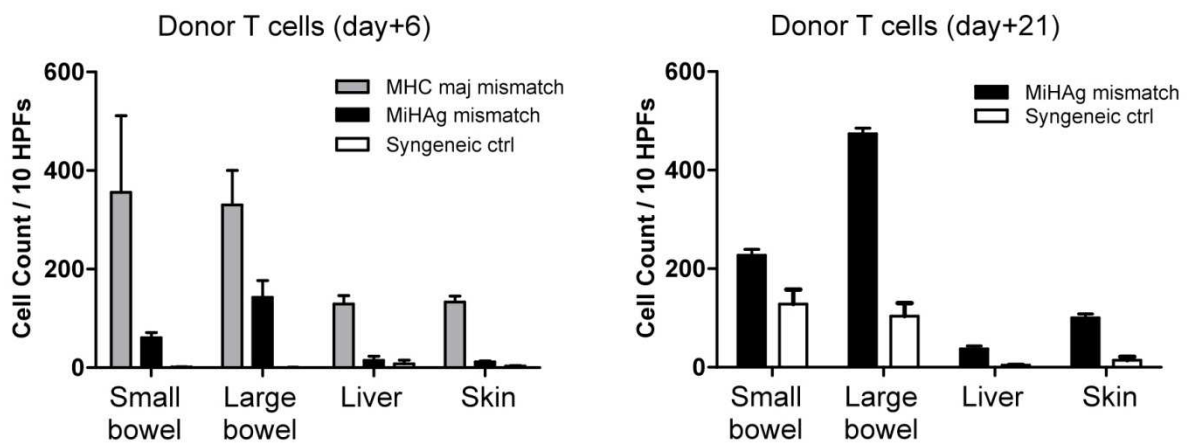


Figure 13: Quantification of target organ infiltrating donor T cells

Quantification of infiltrating donor T cells in the different target tissues. Shown is one out of two independent experiments ($n = 3$). Error bars display plus or minus SEM. HPF = High Power Field

These experiments confirmed that target organs are already strongly infiltrated by donor T cells at disease onset (day+6 after MHC major mismatched and day+21 after miHAg mismatched allo-HCT) leading to the observed severe tissue damage in both models.

5.1.3 Tracking of donor T cell migration after HCT

Non-invasive bioluminescence imaging (BLI) allows following *luc+* donor T cell migration patterns after HCT (Figure 14). Following both miHAg mismatched and MHC major mismatched allo-HCT, donor T cells initially homed to and proliferated in SLOs denoting the aGvHD initiation phase (until day+3)^{20,21}. Similar to the previously published FVB/N (H-2^q) → Balb/C (H-2^d) MHC major mismatch aGvHD model, BLI revealed signals from abdominal areas, spleen, and cervical LNs within two days after allo-HCT.²⁰ After MHC major mismatched allo-HCT (Figure 14A, B upper panels), the intestinal signal rapidly increased after day+3 accompanied by a strong

splenic signal increase indicating the shift from initiation to effector phase with skin infiltration starting at day+6 before mice succumbed to aGvHD.

After miHA_g mismatched allo-HCT (Figure 14A, B, middle panels), donor T cells initially proliferated less intensely in SLOs than after MHC major mismatched allo-HCT. First signals appeared in cervical LNs and spleen (day+2) followed by the abdomen (day+3). Similar to the MHC major mismatch model, donor T cells started to leave SLOs between days+4 and +5 after allo-HCT and infiltrated target organs leading to a whole body signal increase. This defines the shift from the aGvHD initiation to effector phase. Skin infiltration started after day+5 with lower intensity than in the MHC major mismatch model, first with a weak tail infiltration followed by signals from ears and paws few days later. From day+8 on, whole body signal intensity increased strongly.

To distinguish homeostatic T cell proliferation from aGvHD we used syngeneic albino B6 mice transplanted with *luc+* donor T cells plus B6 WT bone marrow cells (Figure 14A, B, lower panels) as controls. In contrast to allogeneic recipients, BLI of syngeneic transplanted mice revealed donor T cell homing to the BM compartment early after HCT (after day+3). Between days+3 and +15 signal intensity projecting to the femur increased 33-fold in one representative mouse of this group. Additionally, from day+5 on distinct thymic signals developed. However, thymic *ex vivo* imaging (Figure 19B) revealed that the overall signal intensity was much lower compared to allo-HCT recipients (23-fold to Balb/C and 56-fold to Balb/B on day+6, respectively). Syngeneic donor T cells also homed to and weakly proliferated in LNs early after HCT (day+2) followed by a weak BLI signal from the spleen. Between days+8 and +10 mice showed the first signs of skin infiltration. Over time thymus, BM, and the spleen turned out to be the main locations of donor T cell accumulation and proliferation in syngeneic recipients leading to a moderate whole body signal increase compared to allo-HCT recipients.

Quantification of dynamic total body and single organ BLI signal changes showed a dramatic increase in signal intensity in mice with aGvHD in both allo-HCT groups compared to a modest increase in syngeneic transplanted mice (Figure 14C). Ventral whole-body images revealed a 12-fold increase in signal intensity in mice after miHA_g mismatched allo-HCT between day+3 and +6 compared to a more than 40-fold increase after MHC major mismatched allo-HCT. Between days+3 and +11 signal intensity increased 80-fold in both models. The strongest signal increase due

to cell proliferation occurred between days+7 and +11 after miHAg mismatched allo-HCT. Single organ BLI measurements demonstrated the same spatio-temporal pattern of donor T cell migration in both models with a more moderate increase in signal intensity of the spleen as well as of the GIT and the cLNs after miHAg mismatched allo-HCT (Figure 14C). Syngeneic recipients showed a more moderate donor T cell proliferation leading to a low whole body ($p < 0,0001$ on days+6, +11, +15, +21) as well as single organ (skin: $p < 0,0001$; spleen: $p < 0,0001$; GIT: $p = 0,0002$; cLN: $p < 0,0001$ on day+11) signal increase compared to miHAg mismatched allo-HCT recipients.

5 Results

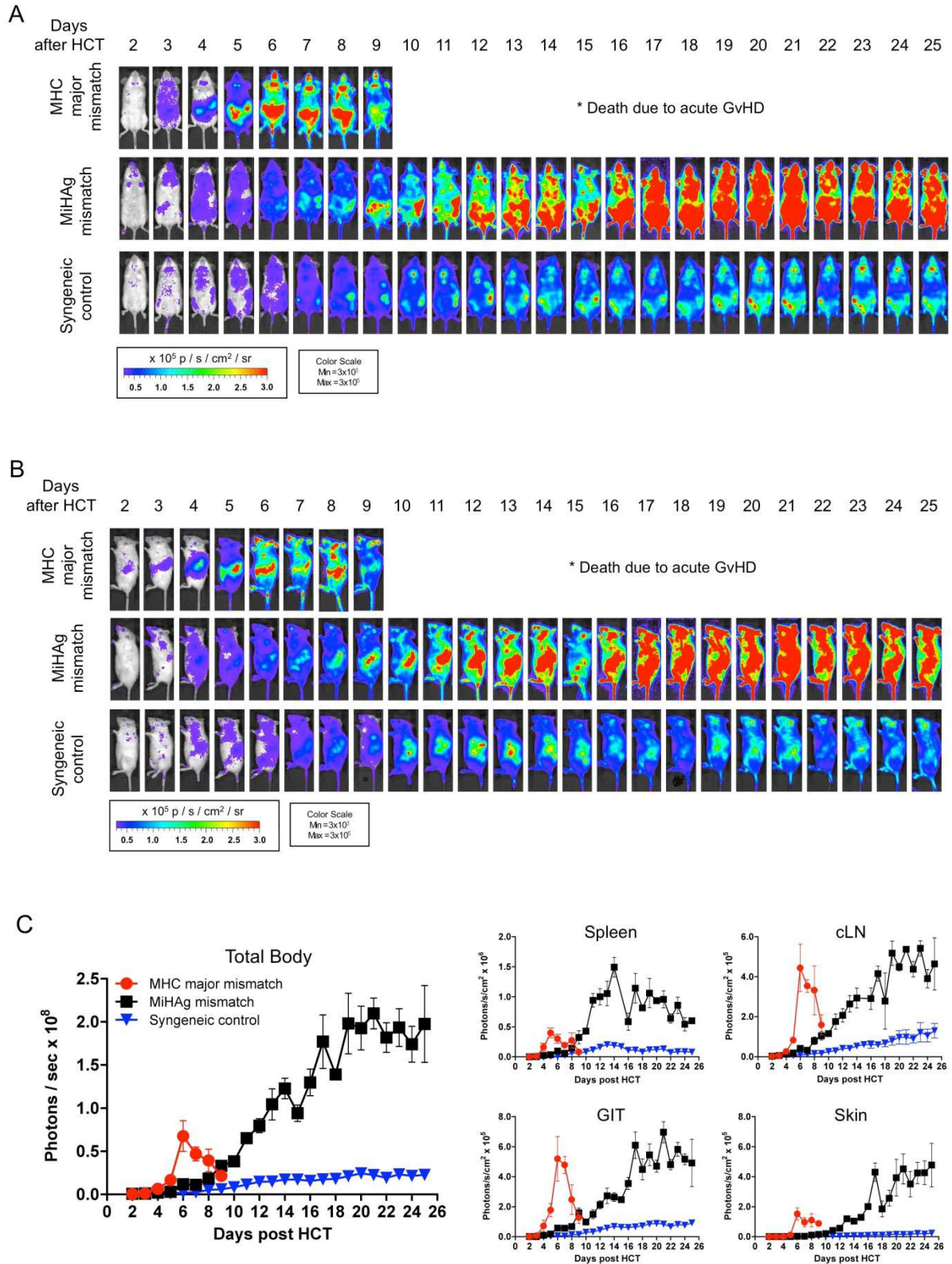


Figure 14: Daily in vivo BLI

(A) ventral and (B) lateral view of one representative mouse per group ($n = 6$) imaged daily after HCT. (C) Quantification of total body and single organ signal changes over time. Photon emissions per second per whole animal and average photon radiation for representative SLOs (spleen and cLN) and for target organs (GIT and skin) are displayed. Error bars show means plus or minus SEM.

5 Results

To resolve the predominant organ distribution despite the strong signal increase an adjustment of the threshold settings on days+11 and +21 was required. Figure 15 shows one representative mouse per group at selected time points with adjusted thresholds.

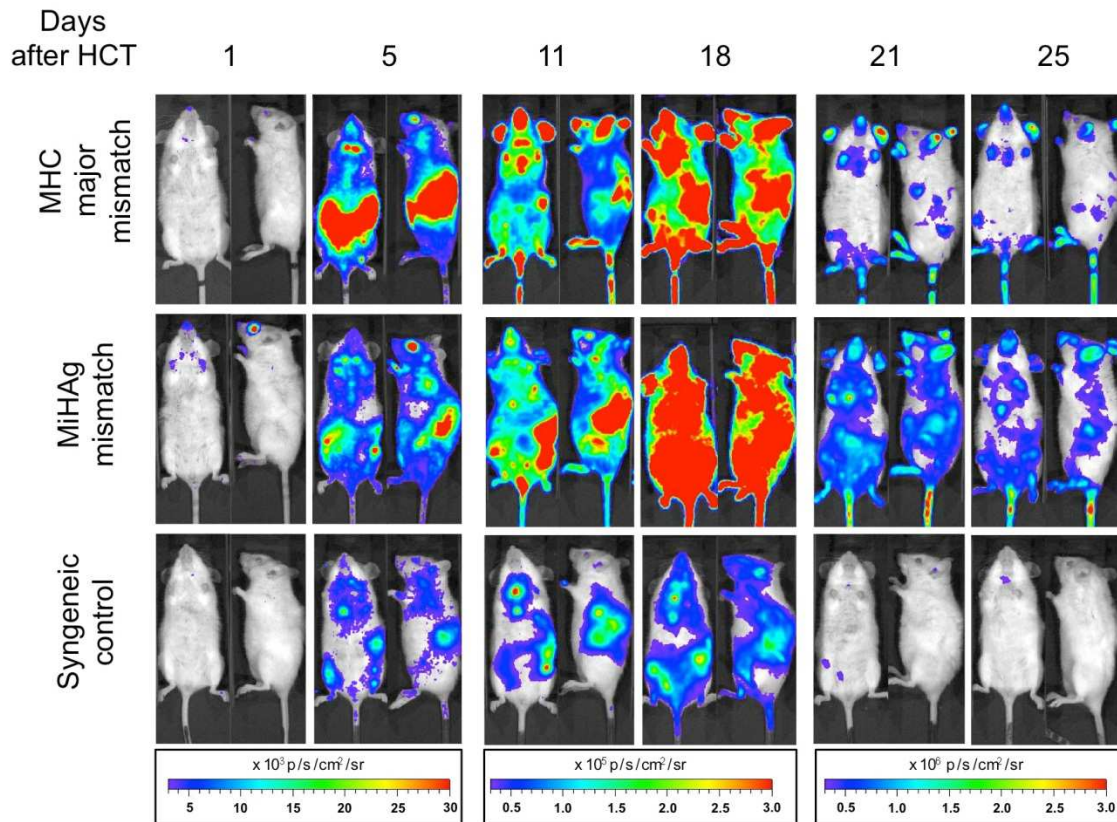


Figure 15: Ventral and lateral views of representative mice

One representative mouse is shown at selected time points ($n = 6$). To resolve organ distribution threshold settings were changed at days+11 and +21. The respective color bars are displayed underneath the pictures.

Daily *in vivo* BLI revealed a similar spatio-temporal allogeneic T cell migration pattern but diverging signal increases in the miHAg mismatched versus the MHC major mismatched allo-HCT model.

5.1.4 Early detection of donor T cells in the peripheral blood

To better understand the kinetics of donor T cell migration we daily analyzed peripheral blood samples of transplanted mice by multiparameter flow cytometry. After miHAg mismatched allo-HCT, we found a phase of approximately 2 weeks

(between days+5 and +20) of massive donor T cell migration with differing amounts of detectable cells at different time points (Figure 16A). Donor T cells started to leave SLOs and migrated via the PB to target tissues by day+4 after allo-HCT. CD4⁺ donor T lymphocytes mobilized to the blood stream shortly before CD8⁺ T cells peaking on day+7 before CD8⁺ T cell numbers also increased. By day+10, numbers of donor CD8⁺ T cells equaled or slightly exceeded CD4⁺ T cells. Migration of both subpopulations peaked between days+10 and +11 followed by a slight decrease of detectable cells. Number of CD8⁺ T cells now exceeded CD4⁺ cells. After another slight increase in cell numbers of both lymphocyte populations on day+15 absolute donor cell numbers declined shortly before clinical symptoms became apparent (around day+21 after HCT, see Figure 9C).

Comparable to miHA_g allo-HCT, on day+4 after MHC major mismatched allo-HCT the first detectable donor T cells appeared in the PB and rapidly increased in numbers. Donor CD4⁺ and CD8⁺ T cell migration peaked between days+6 and +8. After day+8, migrating donor CD8⁺ T cells slightly dominated over CD4⁺ T cells. Similar to miHA_g allo-HCT, after the migration peak donor T cells decreased slowly in numbers in the PB. However, in this model of MHC major mismatch allo-HCT mice died of a hyperacute form of GvHD very rapidly after one phase of massive donor T cell migration (Figure 16B, left graph).

In syngeneic recipients donor T cell numbers slowly but constantly increased suggesting a homeostatic T cell reconstitution of the immune system. In the beginning, CD4⁺ and CD8⁺ T cell migration did not differ. From day+11 on CD8⁺ donor T cell numbers slightly exceeded CD4⁺ T cells (Figure 16B, right graph).

These experiments indicate that it is possible to detect donor T cells in the PB early after HCT in both allogeneic models. MHC major mismatched allo-HCT recipients die very rapidly of hyperacute GvHD after one massive donor T cell migration phase. In contrast, after miHA_g mismatch allo-HCT, daily PB analyses revealed a donor T cell migration phase of approximately two weeks before clinical symptoms become apparent. Accordingly, when maxima of donor T cells appeared in the PB, we defined these time points on days+6, +11 and +15 as critical for alloreactive donor T cell detection.

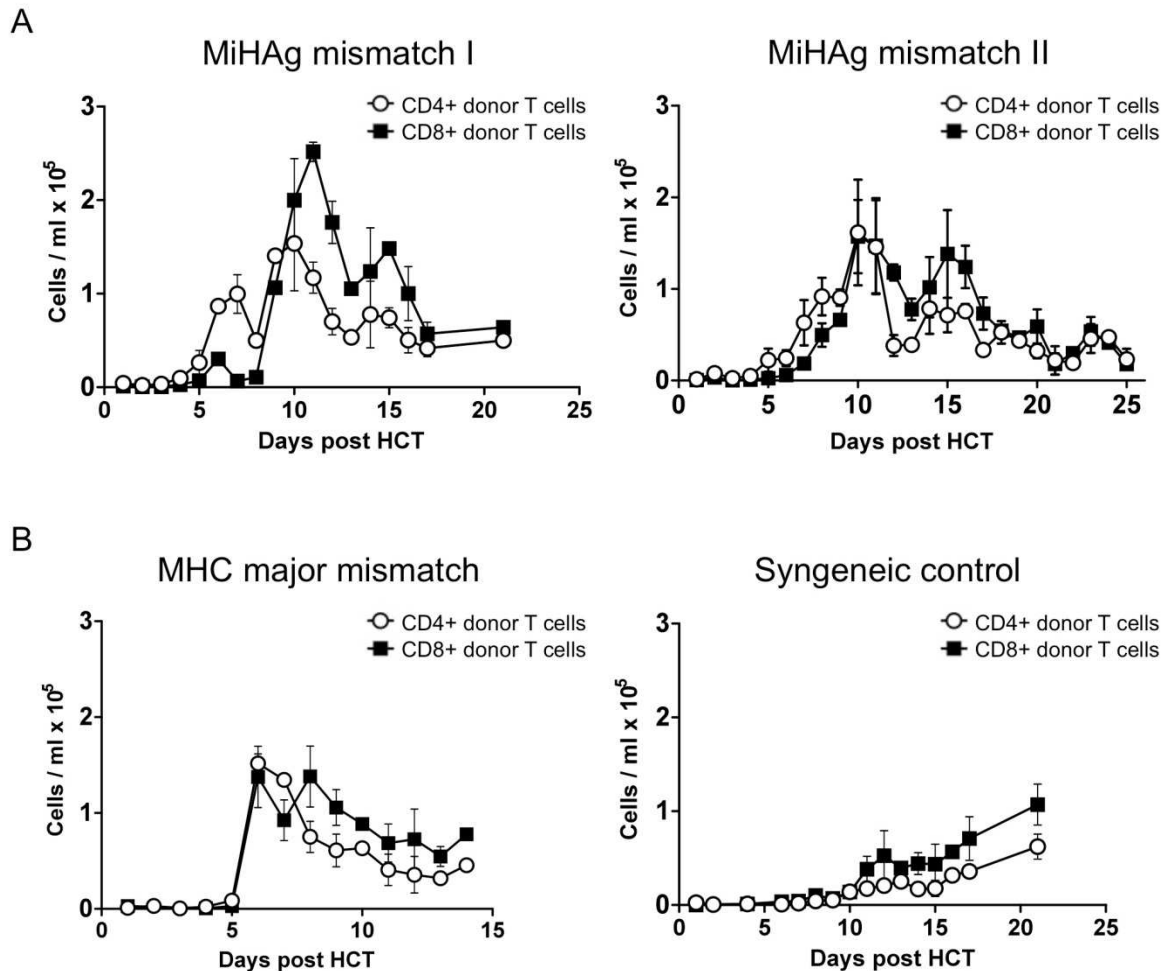


Figure 16: Daily measurement of donor T cells in the PB.

PB of 3 mice per group per day was analyzed ($n = 15$) and three independent experiments performed. (A) displays the results of two independent miHAg mismatch allo-HCT experiments compared to the MHC major mismatch allo-HCT model and a syngeneic control group (B). Error bars show means plus or minus SEM.

5.1.5 CD107 surface mobilization of peripheral blood T cells proves alloreactivity

To proof the alloreactive nature of the detected PB cells we analyzed the degranulation rate of donor T cells upon exposure to allogeneic and syngeneic targets by labeling the transiently exposed lysosomal-associated membrane proteins (LAMP)-1 and -2 (CD107a and b) as described in chapter 4.9. To establish the CD107 degranulation assay, we measured the degranulation rate of an antigen specific T cell response of *in vitro* stimulated OT-1 CD8⁺ T cells against SIINFEKL peptide expressing target cells (β A-OVA) and against B6 WT targets by FC. The degranulation rate of OT-1 CD8⁺ T cells against SIINFEKL expressing targets (T cell

depleted β A-OVA splenocytes) was significantly higher than against B6 WT targets (T cell depleted B6 splenocytes). Without any targets the spontaneous degranulation rate was similarly low (Figure 17B). CD107 detection correlated with intracellular IFN- γ production. In addition, degranulating cells highly up-regulated the activation marker CD25 (Figure 17B).

In vivo stimulated PB T cells isolated on day+5 after MHC major mismatch allo-HCT degranulated against allogeneic targets (T cell depleted Balb/C splenocytes) and also against syngeneic targets (T cell depleted B6 splenocytes). A small amount of cells degranulated spontaneously without contact to target cells indicating the high reactivity of these cytotoxic T cells (Figure 17C). Reactive donor T cells isolated from syngeneic controls were negligible (< 1000 cells / ml). Adoptively transferred antigen specific PB CD8⁺ T cells from antigen expressing recipients served as positive control. Cells highly degranulated against SIINFEKL expressing targets (T cell depleted β A-OVA splenocytes) in contrast to a low degranulation rate against B6 WT targets. Only few cells degranulated spontaneously (Figure 17D).

5.1.6 Localization of donor T cells in target organs

Due to the dramatic signal increases observed in both allogeneic groups by *in vivo* BLI and due to the high numbers of donor T cells migrating in the PB, we investigated the donor T cell accumulation in lymphoid organs and parenchymal tissues in more detail. Therefore, we performed *ex vivo* imaging analyses of representative animals of each group (Figure 18). Figure 18B gives an overview of the organ distribution on *ex vivo* BLI images. Based on the migration kinetics of donor T cells we chose the following critical time points after HCT for *ex vivo* analyses: d+4, +6, +15, +21 (see results in 5.1.4, Figure 16). Day+4 represents the transition from aGvHD initiation to effector phase when donor T cells start to leave SLOs for peripheral aGvHD target tissues.²⁰ Donor T cell migration peaked on days+6, +11 and +15 (see Figure 16). Day+21 marked the onset of clinical aGvHD symptoms (see Figure 9).

Ex vivo BLI revealed that in both allogeneic groups donor T cells first proliferated in SLOs (day+4) before infiltrating mucosal sites (Figure 18). High BLI signal intensities in mesenteric as well as inguinal and cervical LNs, PPs, and spleen indicate high T cell proliferation in both allo-HCT settings. On day+6, donor T cells infiltrated the

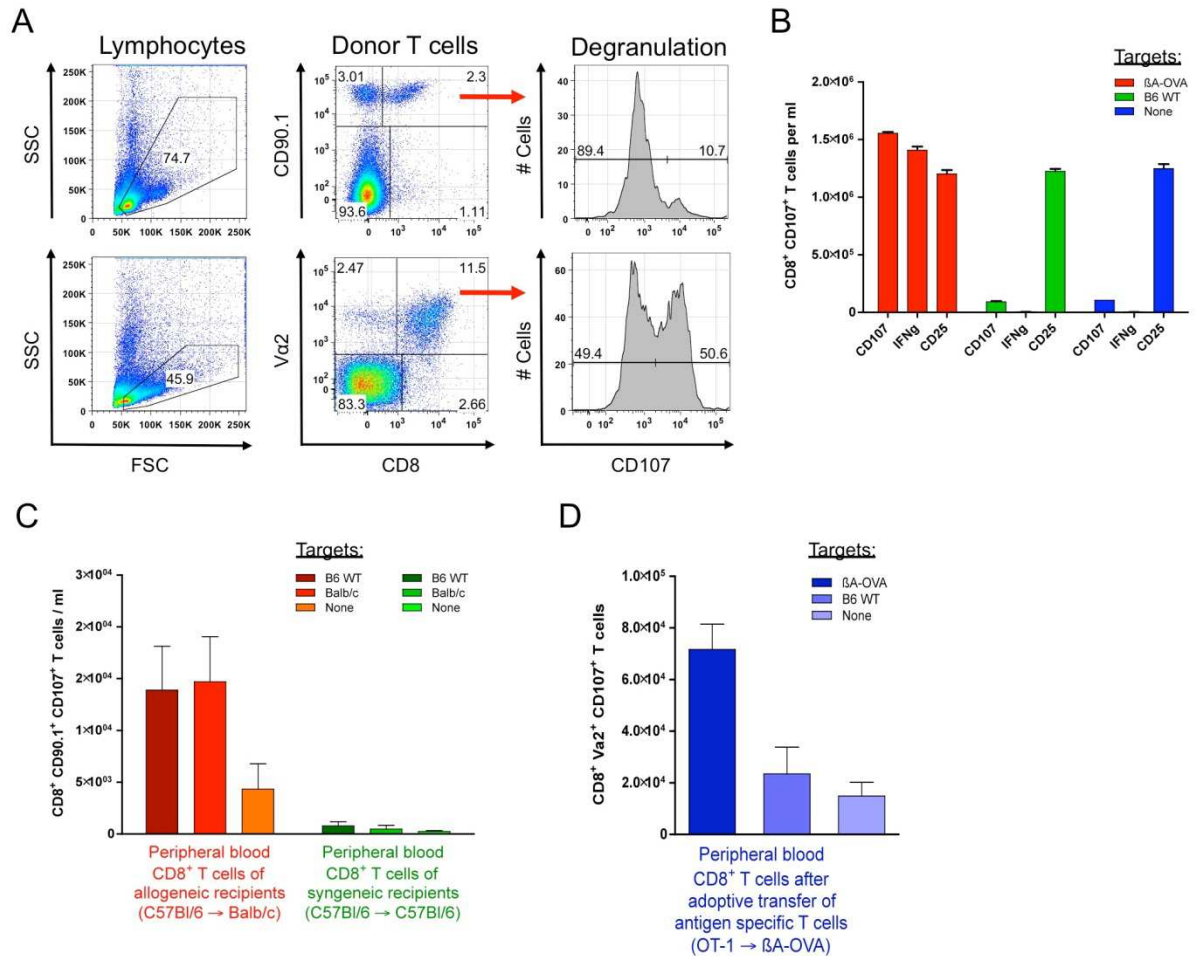


Figure 17: CD107 degranulation assay to proof alloreactivity of PB donor T cells

(A) Gating example of PBMCs of an allogeneic transplanted mouse against allogeneic targets (upper row) and of antigen specific T cells adoptively transferred into antigen expressing recipients (lower row). Degranulation was measured after 5 hours incubation with antigen expressing targets. PBMCs were isolated on day+5 after HCT. (B) Quantification of degranulation rate, cytokine expression and activation status of *in vitro* stimulated antigen specific OT-1 T cells incubated with antigen expressing targets (β-OVA), with WT targets (B6) and without targets, respectively. (C) Quantification of the degranulation rate of *in vivo* stimulated PBMCs on day+5 after HCT. Graph shows degranulating CD8⁺ PB donor T cells of allogeneic or syngeneic recipients against allogeneic, syngeneic or no target cells. (D) CD107 expression of antigen specific donor T cells against indicated targets served as positive control. One out of 3 experiments is shown (n = 3). Standard deviations display plus or minus SEM.

lungs and the thymus in both allo-HCT models and BLI signal intensity increased in both organs until day+11. After MHC major mismatched allo-HCT, BLI signal also projected to small and large intestine as well as the stomach revealing a high target organ infiltration of donor T cells. Splenic signals slightly declined until day+11 in the latter model before mice died of hyperacute GvHD. In contrast, after miHAg mismatch allo-HCT, SLOs remained the sites of predominant cell proliferation on day+6 and BLI signal intensity of target tissues remained rather weak. The initial

discrete GIT infiltration involved stomach, cecum, small and large intestines by day+11 and continued to strongly increase until day+21. First liver signals occurred on day+11 and peaked by day+15. Splenic BLI signals peaked at day+15 after HCT, when the enlarged spleen displayed macroscopically visible proliferation nodules indicating high cell turnover.

In contrast to the allogeneic models, syngeneic T cells predominantly remained within SLOs (initially spleen, later also PPs, LNs), proliferated less and the weak splenic signal increase after day+11 suggested homeostatic T cell expansion. From day+11 on, donor T cells also slightly infiltrated the lungs and the thymus. On days+15 and +21 weak signals of some areas of the small and large intestine indicated discrete infiltration of these tissues. Overall BLI signals of syngeneic recipients remained weak throughout all time points.

Quantification of BLI signals confirmed high donor T cell proliferation in SLOs early after HCT: Splenic signals increased in all three models until day+15 (between day+6 and day+15 17-fold after miHA_g mismatch allo-HCT; 11-fold after syngeneic HCT, Figure 19A). Cervical and mesenteric LNs as well as PPs of allogeneic recipients already showed increased signals compared to syngeneic controls on day+6 after HCT. After MHC major mismatch allo-HCT, GIT signal intensity peaked at day+6 and declined thereafter (Figure 19B). In contrast, miHA_g mismatched allo-HCT recipients showed the strongest GIT signal on day+15 after allo-HCT being 20-fold higher than the GIT signal of syngeneic recipients. Other target organs showed similar results: Liver signal after miHA_g mismatch allo-HCT peaked at day+15 followed by a slight decrease on day+21. BLI lung signal intensity reached its peak by day+21. At this time point mice after miHA_g mismatch allo-HCT showed an 11-fold higher lung signal compared to syngeneic controls.

Ex vivo BLI proved donor T cell proliferation in SLO early after allo-HCT in both models and confirmed the same spatio-temporal shift from aGvHD initiation to effector phase already observed by *in vivo* imaging. Furthermore, *ex vivo* BLI located migrated donor T cells in target tissues indicating a migration phase towards these organs.

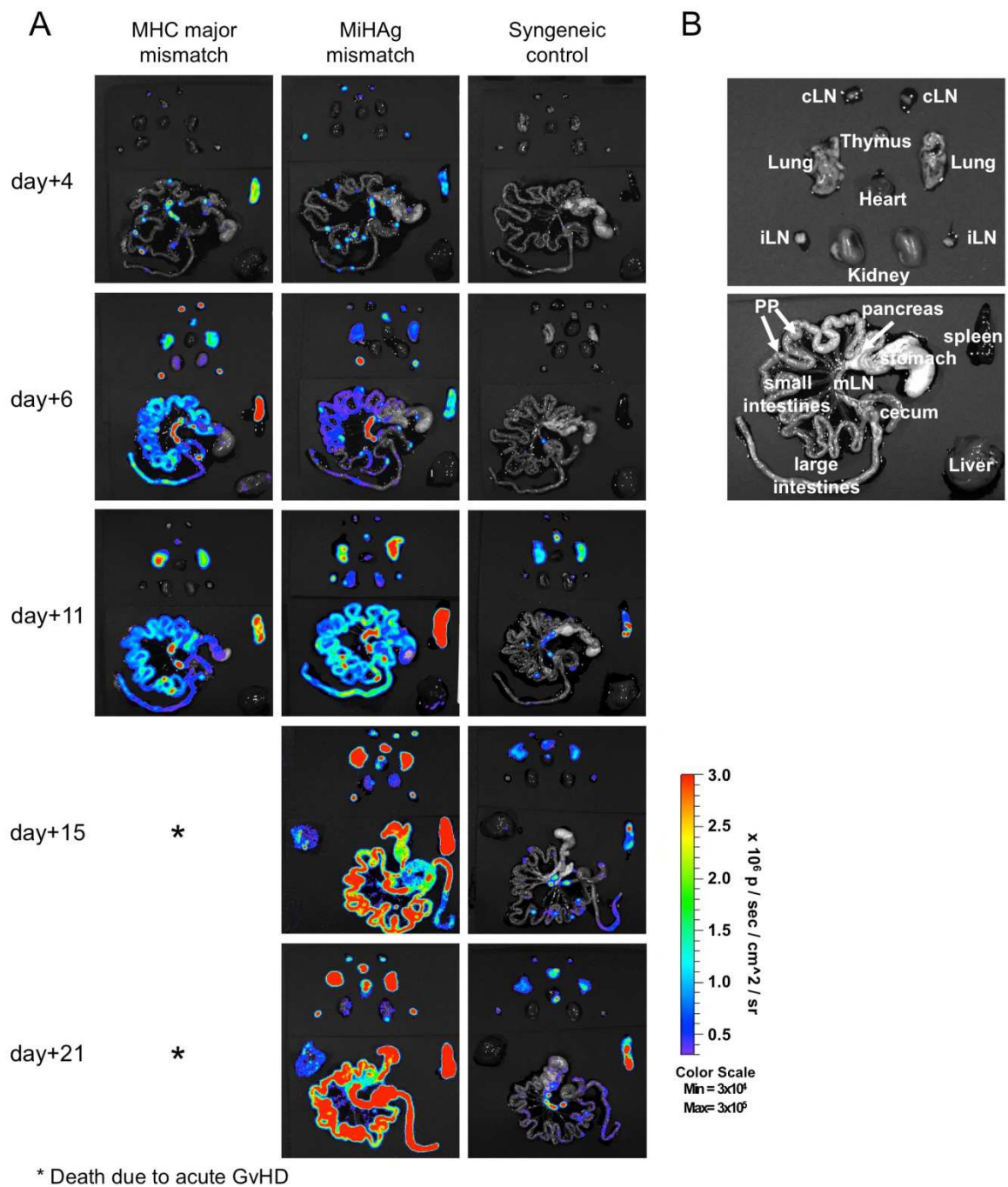
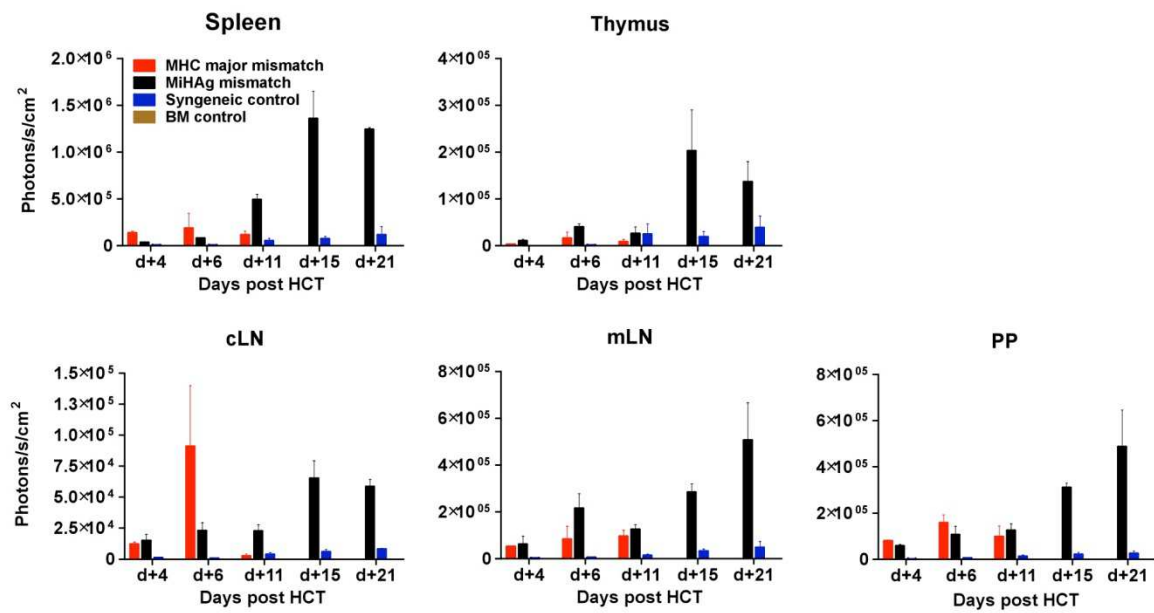


Figure 18: ex vivo BLI of target organs and parenchymal tissues

(A) Donor T cell infiltration of lymphoid organs and parenchymal tissues at indicated time points of one representative mouse per group ($n = 3$) of one out of two independent experiments is shown. (B) Overview of target organ and parenchymal tissue distribution on ex vivo BLI images. cLN = cervical lymph node; iLN = inguinal lymph node; mLN = mesenteric lymph node; PP = peyer's patch

A Lymphoid organs



B Parenchymal tissues

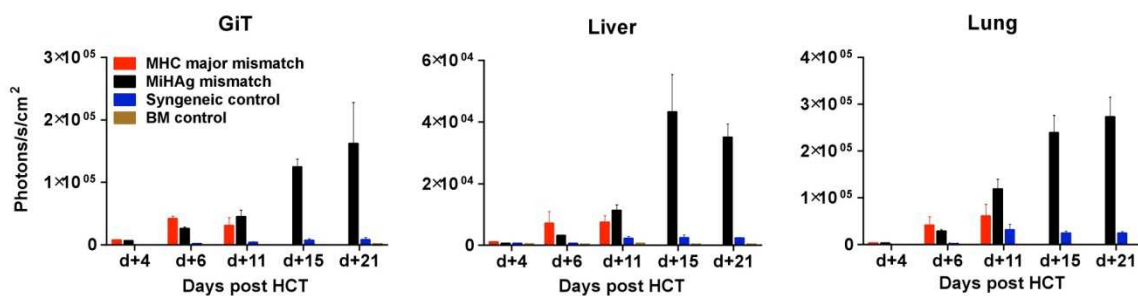


Figure 19: Quantification of ex vivo BLI signals at indicated time points after HCT

Quantification of the average radiance of lymphoid organs (A) and parenchymal tissues (B) after *ex vivo* imaging of different organs at indicated time points. Summary of one out of two independent experiments ($n = 3$). Error bars show plus or minus SEM. cLN = cervical lymph node; mLN = mesenteric lymph node; PP = peyer's patches; GiT = gastrointestinal tract;

Figure 20 summarizes the different stages of donor T cell migration kinetics after miHAg mismatch allo-HCT. First, donor T cells highly proliferate in SLO before starting to migrate via the PB towards their target organs between days+3 and +5. By day+11, target tissues already showed slight histological damage but clinical symptoms did not appear before day+21. Therefore, the close monitoring of donor T cell migration patterns revealed a vulnerable phase of cell migration early after allo-HCT prior to the onset of clinically apparent aGvHD. Based on this data we propose a potential diagnostic window for the identification of alloreactive donor T cells and the application of predictive tests at early time points to identify patients at risk for

aGvHD. Early alloreactive T cell identification in the PB may allow for a timely therapeutic intervention to prevent aGvHD development.

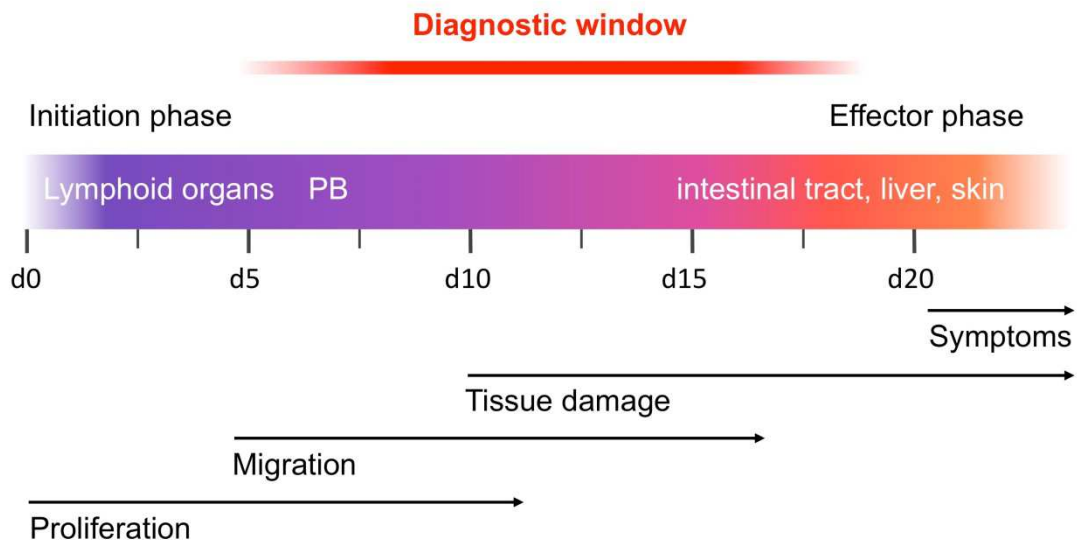


Figure 20: Proposal of a potential diagnostic window based on donor T cell migration kinetics

The timeline shows the different phases of donor T cell migration in days after miHAg mismatch allo-HCT. The time frame of massive donor T cell migration in the PB between aGvHD initiation phase and appearance of first clinical symptoms serves as potential diagnostic window.

5.2 Characterization of migrating donor T cell expression profiles

Since it was feasible to detect migrating donor T cells early after allo-HCT in the PB, we next aimed to precisely analyze the receptor profile of these cells as aGvHD organ infiltration depends on the appropriate homing receptor expression of migrating cells. We tested a panel of 16 different adhesion molecules, chemokine receptors, and activation markers known to be involved in this process by FACS analysis, daily or at identified migration peaks during the proposed diagnostic window.

Figure 21 displays representative FACS blots for the integrin $\alpha 4\beta 7$ and P-selectin ligand, respectively.

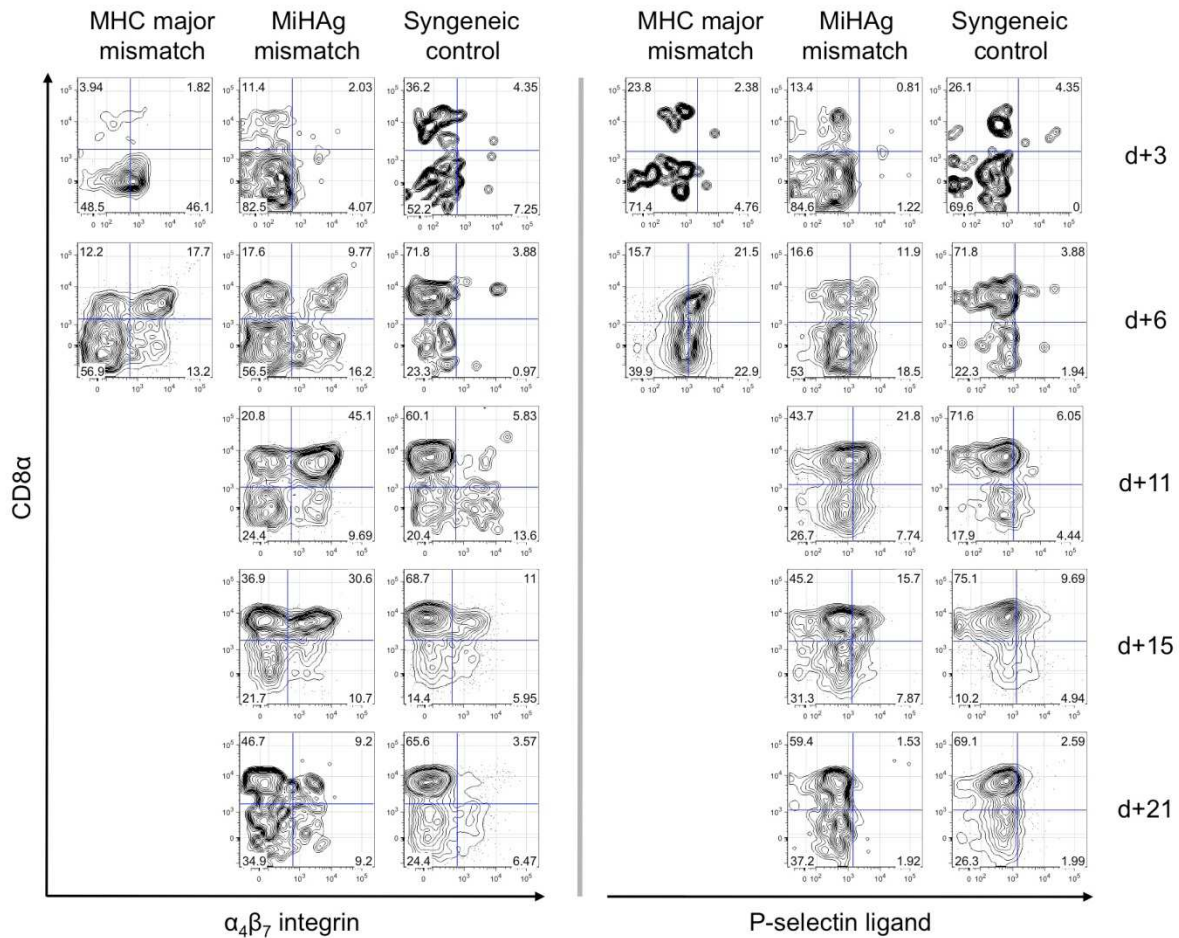


Figure 21: Representative FACS blots of homing receptor analyses at important time points

Representative contour blots of PB samples of one representative mouse per group at indicated time points ($n = 15$, 3 mice per day per group were analyzed). Dead cells were excluded by DAPI staining and the expression of $\alpha 4\beta 7$ integrin (left) or P-selectin ligand (right) on donor T cells was measured. Quadrants show percentages of all CD90.1⁺ donor T cells.

5.2.1 $\alpha 4\beta 7$ integrin is highly up-regulated on donor T cells

Integrins play a pivotal role in T cell homing by selectively interacting with adhesion molecules on the tissue under homeostatic as well as inflamed conditions. Therefore, we analyzed donor T cells for the expression of the integrins $\alpha 4\beta 7$ and $\alpha E\beta 7$ which are important for the homing process to mucosa-associated tissues.

Daily measurements of $\alpha 4\beta 7$ integrin expression on PB donor T cells revealed high expression levels on both CD4⁺ and CD8⁺ lymphocytes between day+4 and day+21 after HCT in both allogeneic groups (Figure 22). After miHAg mismatch allo-HCT, relative as well as absolute amounts of $\alpha 4\beta 7$ integrin expressing cells significantly

exceeded respective cell numbers found after syngeneic HCT from day+4 on at all analyzed time points. Between 20 % and 40 % of the CD4⁺ and between 40 % and 60 % of the CD8⁺ T cell subpopulation highly up-regulated this molecule during the donor T cell migration phase compared to less than 20 % of PB T cells found in syngeneic HCT recipients. As an additional control we monitored T cells from untreated B6 WT mice for relative $\alpha 4\beta 7$ integrin expression levels. Less than 10 % of both lymphocyte subpopulations stained positive for this marker, similar to CD8⁺ $\alpha 4\beta 7$ integrin⁺ T cells in syngeneic HCT recipients. In contrast, a small portion of CD4⁺ T cells slightly up-regulated $\alpha 4\beta 7$ integrin after syngeneic HCT as well compared to the WT controls from day+10 on.

Absolute cell numbers of $\alpha 4\beta 7$ integrin expressing cells in the PB correlated with the identified peaks of cell migration with the highest amount of cells detectable between days+10 and +11 after miHA_g mismatch allo-HCT (Figure 22, lower panels). At most time points, the number of $\alpha 4\beta 7$ ⁺ donor T cells after allo-HCT exceeded those after syngeneic HCT significantly.

The expression level of $\alpha E\beta 7$ integrin on donor T cells varied and did not differ significantly between allogeneic and syngeneic HCT recipients. Compared to untreated WT mice – where approximately 30 % of the CD8⁺ lymphocyte population stained positive for this molecule – allogeneic donor T cells expressed slightly higher levels of $\alpha E\beta 7$ integrin at most time points (data not shown).

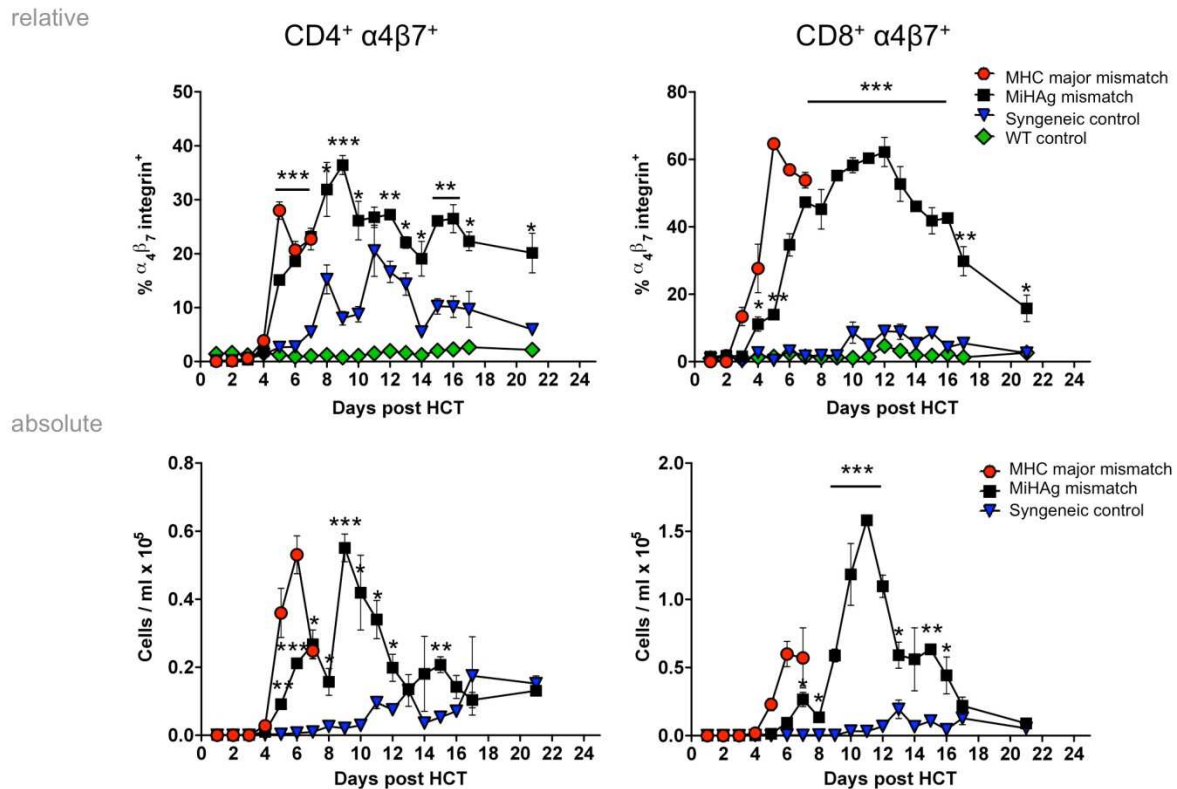


Figure 22: $\alpha 4\beta 7$ integrin expression on PB donor T cells daily after HCT

Change of $\alpha 4\beta 7$ integrin expression measured daily after HCT on PB donor CD4⁺ (left panels) and CD8⁺ (right panels) T cells, respectively. The upper panels show relative expression values of both allo-HCT models in comparison to the syngeneic HCT model and untreated B6 WT control mice. The lower panels show the correlating absolute cell counts after HCT. One representative experiment out of 3 is displayed ($n = 15$, 3 mice per day per group were analyzed). Error bars show plus or minus SEM. * $p < 0.05$; ** $p < 0.01$; *** $p < 0.001$ for miHAg versus syngeneic.

5.2.2 Alloreactive donor T cells up-regulate selectin ligands

Another important group of molecules involved in T cell homing are selectins. Therefore, we analyzed the expression of ligands for P- and E- selectin and of L-selectin (CD62L) on PB donor T cells.

Daily measurements of P-selectin ligand revealed this marker to be highly up-regulated in relative as well as absolute numbers in both allo-HCT models (Figure 23). In miHAg mismatched allo-HCT recipients the expression levels were significantly higher during the early phase of cell migration compared to syngeneic controls. 20 to 40 % of all CD4⁺ and up to 50 % of CD8⁺ donor T lymphocytes found in the PB blood of miHAg mismatch allo-HCT recipients expressed this marker. From day+12 on, the amount of detectable cells that stained positive for P-selectin ligand

5 Results

dropped and almost equaled the expression level after syngeneic HCT which stayed below 20 % at all measured time points. T cells of untreated WT controls barely expressed this marker.

The absolute amount of cells expressing P-selectin ligand in the PB after miHAg mismatch allo-HCT also significantly exceeded the numbers after syngeneic HCT between day+5 and day+12. This held true for both donor T cell subpopulations. Numbers of CD8⁺ P-selectin ligand⁺ T cells almost doubled CD4⁺ P-selectin ligand⁺ T cells around day+11. After syngeneic HCT absolute cell numbers stayed constantly low until day+12 and only slightly increased thereafter.

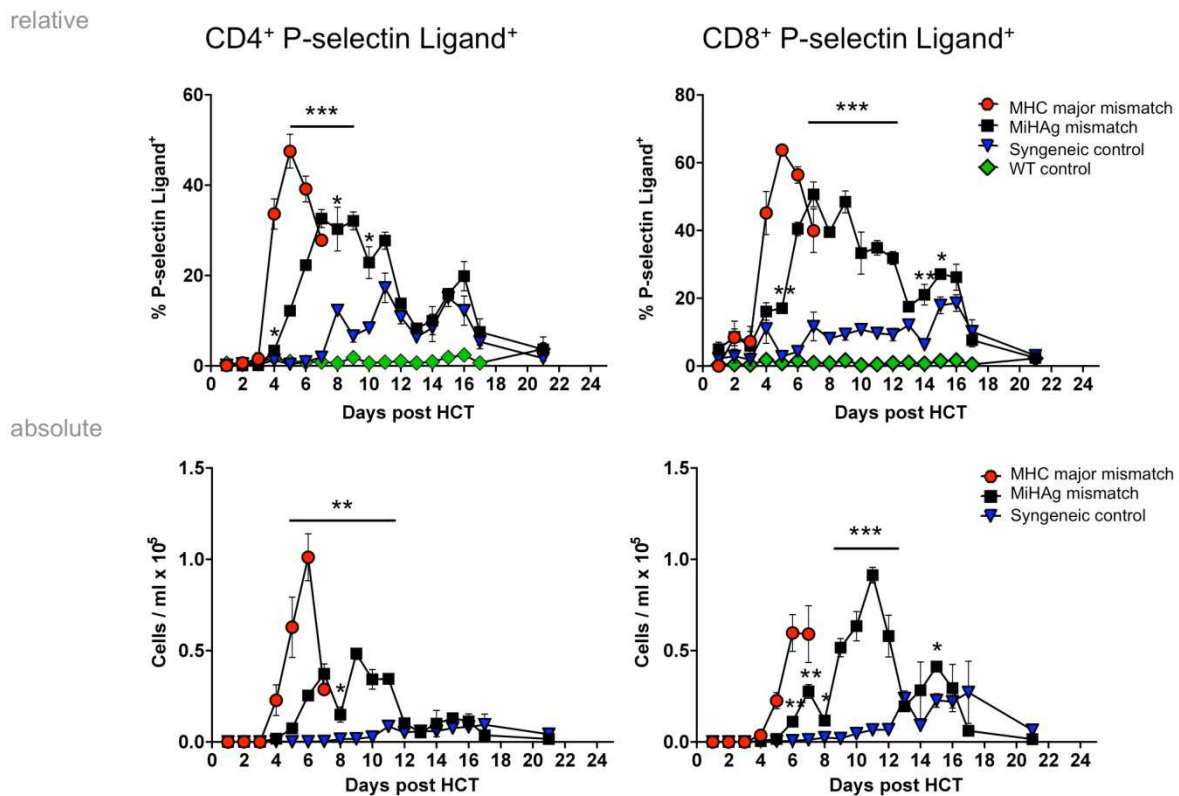


Figure 23: P-selectin ligand expression on PB donor T cells daily after HCT

Change of P-selectin ligand expression measured daily after HCT on PB donor CD4⁺ (left panels) and CD8⁺ (right panels) T cells, respectively. The upper panels show relative expression values of both allo-HCT models in comparison to the syngeneic HCT model and untreated B6 WT control mice. The lower panels show the correlating absolute cell counts after HCT. One representative experiment out of 3 is displayed (n = 15, 3 mice per day per group were analyzed). Error bars show plus or minus SEM. *p<0.05; **p<0.01; ***p<0.001 for miHAg versus syngeneic.

5 Results

For L-selectin and E-selectin ligand expression analysis on PB donor T cells we chose days +6, +11, +15 and +21 after HCT (see 5.1.4). In addition, we also measured the expression of L-selectin on day+4 after HCT to follow the shift from naïve to effector T cell phenotype.

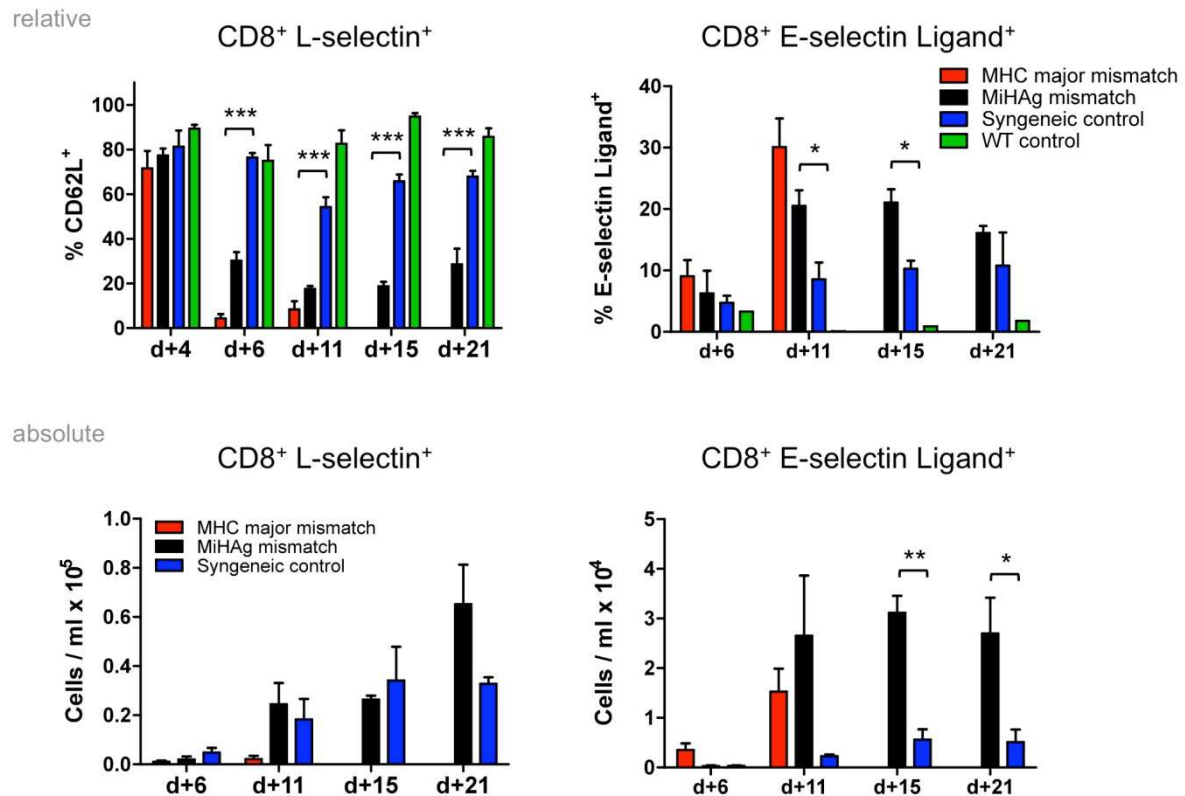


Figure 24: L-selectin and E-selectin ligand expression on PB CD8⁺ T cells

Expression of L-selectin (left panels) and E-selectin ligand (right panels) in relative (upper panels) and absolute (lower panels) values on CD8⁺ donor T cells at indicated time points. Graphs show summary of 2 independent experiments (n = 6). Error bars display plus or minus SEM. *p<0.05; **p<0.01; ***p<0,001 for miHAg versus syngeneic.

On day+4 after HCT, L-selectin expression levels hardly differed between groups. Similar to untreated controls, around 80 % of all PB T cells expressed this marker (Figure 24, left upper panel). In contrast, from day+6 on, L-selectin expression on PB donor T cells was significantly lower after allogeneic than after syngeneic HCT. The frequency of CD8⁺ L-selectin⁺ PB donor T cells in syngeneic HCT recipients was only slightly lower than the percentage of this cell population in untreated WT control mice.

However, absolute numbers did not significantly differ between miHAg mismatched allogeneic and syngeneic HCT recipients (Figure 24, left lower panel).

On day+6, approximately 10 % of all donor T cells expressed E-selectin ligand after allo-HCT, slightly more than after syngeneic HCT (Figure 24, right upper panel). On days+11 and +15 E-selectin ligand expression was further up-regulated in allo-HCT recipients. Significantly more donor CD8⁺ T cells expressed this marker in miHAg mismatch allo-HCT recipients than after syngeneic HCT. However, by day+21 the relative expression levels were almost equal between both groups although absolute cell counts still differed significantly (Figure 24, right lower panel).

5.2.3 Chemokine receptors do not define alloreactive donor T cells

Another important group of molecules involved in T cell homing are chemokine receptors. Thus, we analyzed the expression of a panel of 7 different CCRs on PB donor T cells.

Daily measurements of CXCR3 expression revealed up to 40 % of CD4⁺ and up to 60 % of CD8⁺ PB donor T cells as positive for this marker after miHAg mismatch allo-HCT. However, also after syngeneic HCT donor T cells highly up-regulated CXCR3 (Figure 25, upper panels). After day+3, donor CD4⁺ T cells of both allo-HCT models highly up-regulated CXCR3. Its expression level after miHAg mismatch allo-HCT exceeded that of syngeneic HCT recipients significantly until day+10 before it dropped to a similar level in both models. In miHAg mismatched allo-HCT recipients the expression level increased again significantly until the last measured time points. Less than 10 % of WT CD4⁺ T cells stained positive for CXCR3. However, 20 to 40 % of WT CD8⁺ T cells expressed this marker. The frequency of CD8⁺ CXCR3⁺ donor T cells in all three HCT models raised similarly between days+2 and +6 followed by a decrease after allo-HCT. In contrast, in syngeneic HCT recipients between 60 and 80 % of the detected cells expressed this marker at all measured time points (Figure 25, right upper panel).

Absolute CXCR3⁺ T cell numbers increased for both T cell subpopulations with peaks between days+10 and +11 after miHAg mismatch allo-HCT. However, from day+10 on the amount of CXCR3⁺ T cells in syngeneic HCT recipients also increased and

5 Results

equaled ($CD4^+$) or outnumbered ($CD8^+$) $CXCR3^+$ cells after miHAg mismatch allo-HCT (Figure 25, lower panels).

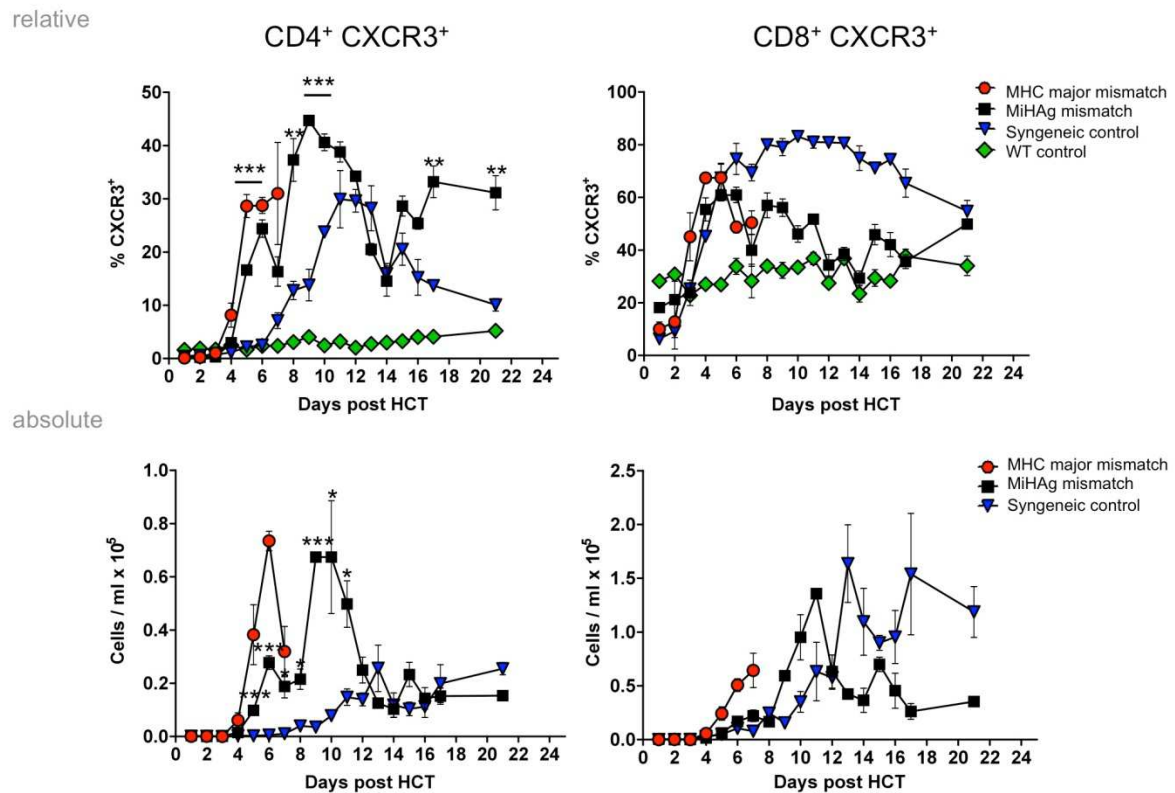


Figure 25: CXCR3 expression on PB donor T cells daily after HCT

Change of CXCR3 expression measured daily after HCT on PB donor $CD4^+$ (left panels) and $CD8^+$ (right panels) T cells, respectively. The upper panels show relative expression values of both allo-HCT models in comparison to the syngeneic HCT model and untreated B6 WT control mice. The lower panels show the correlating absolute cell counts after HCT. One representative experiment out of 3 is displayed ($n = 15$, 3 mice per day per group were analysed). Error bars show plus or minus SEM. * $p < 0.05$; ** $p < 0.01$; *** $p < 0.001$ for miHAg versus syngeneic.

Figure 26 summarizes the results for the expression levels of further CCRs on PB $CD8^+$ donor T cells analyzed at indicated time points. On day+6, MFI of all tested receptors exceeded the expression levels of PB $CD8^+$ T cells of untreated WT controls. Allogeneic and syngeneic HCT recipients did not differ significantly. At later time points (day+11, +15 and +21) MFI of all CCRs decreased compared to day+6 but still slightly differed compared to the MFI of WT T cells. Differences in the expression levels of CCRs in miHAg mismatched allogeneic and syngeneic HCT recipients did not reach statistical significance at any of these time points.

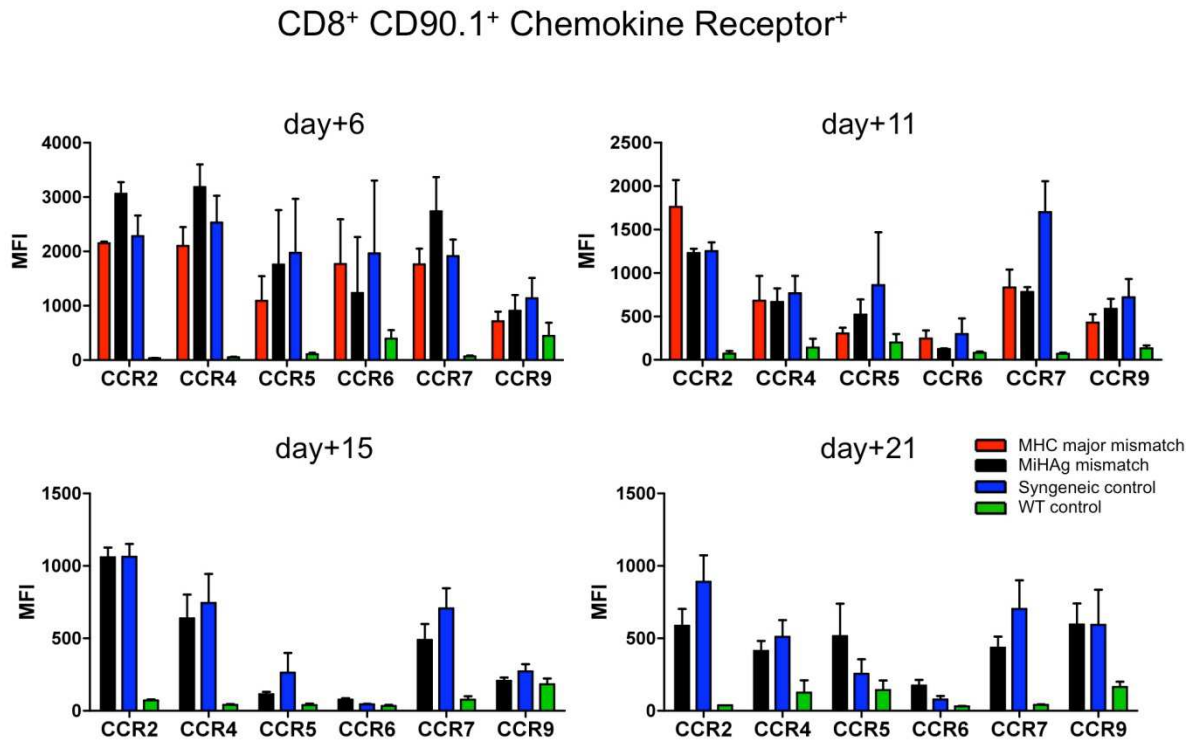


Figure 26: Chemokine receptor expression on PB CD8⁺ donor T cells daily after HCT

Mean fluorescence intensity (MFI) of different chemokine receptors measured at indicated time points. Graphs display summary of two independent experiments ($n = 3-6$). Error bars show plus or minus SEM.

5.2.4 Alloreactive donor T cells are highly activated

In addition to the above mentioned homing receptors, we analyzed CD44, CD69 and CD25 expressions to test the activation status of the detected PB donor T cells at important time points (Figure 27). More than 90 % of the detected PB CD8⁺ T cells expressed the T cell activation marker CD44 at all time points indicating that the cells are highly activated after allogeneic as well as syngeneic HCT. In untreated WT control mice 20 to 40 % of PB CD8⁺ T cells stained positive for CD44. MFI values for this marker also exceeded that of control animals at all time points. CD44 expression levels on CD8⁺ donor T cells did not differ significantly between allogeneic or syngeneic HCT recipients (Figure 27A). On day+4 after HCT, CD8⁺ donor T cells additionally expressed the activation markers CD69 (Figure 27B) and CD25 (Figure 27C). However, at later time points, the frequencies of PB CD8⁺ donor T cells expressing CD69 or CD25 differed between miHAg mismatch and syngeneic HCT

5 Results

recipients reaching statistical significance from day+6 on (CD69) and on days+6, +15, +21 (CD25), respectively. On day+21 after miHA_g mismatch allo-HCT, MFI values of both markers also exceeded the values after syngeneic HCT significantly. Only few PB CD8⁺ T cells from WT control animals expressed these markers.

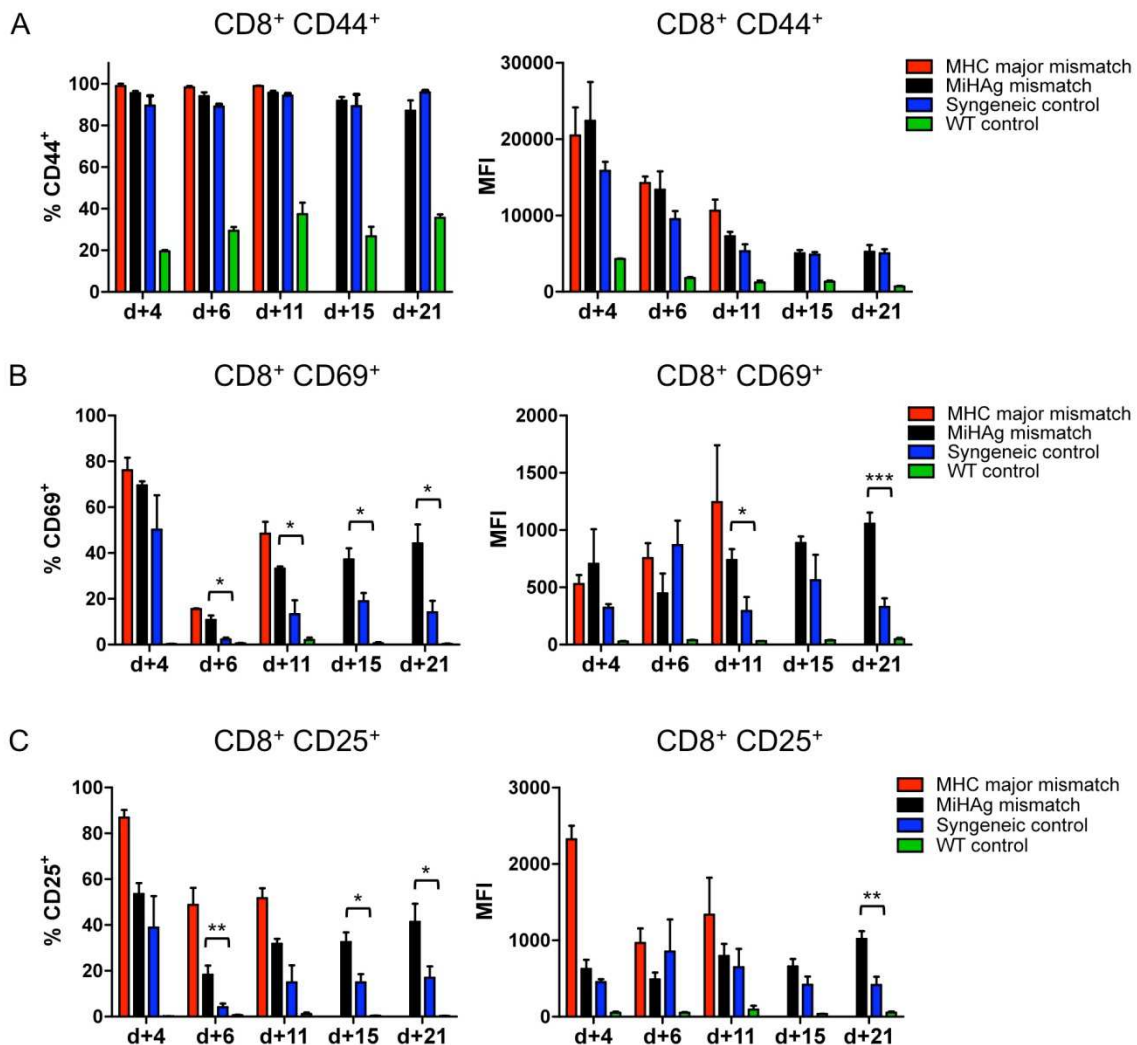


Figure 27: Activation marker expression on PB CD8⁺ donor T cells

Expression of the activation markers CD44 (A), CD69 (B) and CD25 (C) on PB CD8⁺ donor T cells at indicated time points after HCT. Graphs show relative values (left panels) and MFI (right panels). Displayed are the summaries of two independent experiments (n = 3-6). Error bars show plus or minus SEM.

These experiments showed that it is possible to detect alloreactive donor T cells in the peripheral blood early after allo-HCT according to their homing receptor expression. Based on these results, we suggest $\alpha 4\beta 7$ integrin as well as P- and E-selectin ligand and L-selectin in combination with the activation markers CD69 and

CD25 as promising candidates for a precise alloreactive cell definition prior to the onset of aGvHD.

5.3 Therapeutic intervention during diagnostic window

Next, we investigated whether the proposed potential diagnostic window prior to the clinical manifestation of aGvHD onset would allow for a timely therapeutic intervention when alloreactive donor T cells can be detected upon their homing receptor profile early in the PB (day+6). Therefore, we started to treat miHAg mismatch allo-HCT recipients with three different immunosuppressive drugs based on our previous data.

5.3.1 Prednisolone treatment

Since the glucocorticoid prednisolone is one of the standard steroids used as first-line treatment of patients showing signs of aGvHD it was the first choice for treatment of the mice. In a preliminary experiment the lowest dose used in humans (1mg / kg BW) did not show any effects when given daily after miHAg mismatch allo-HCT (data not shown). Consequently, we used a high dose of 5 mg / kg BW for further experiments. The drug was given daily starting at the time point of first alloreactive cell detection (day+6) or on the day of HCT until the end of the experiments (day+28, Figure 28A). BLI revealed that prednisolone treatment did not influence early donor T cell proliferation and overall migration patterns in both treated groups (Figure 28B). Cell distribution throughout the organs did not differ between treated and untreated control mice after allo-HCT (see Figure 14). However, at later time points, prednisolone treated mice showed slightly reduced whole body BLI signals compared to the controls. We detected reduced signals from the abdominal areas as well as from the skin in comparison to vehicle controls. Lateral images revealed a very strong splenic signal. Surprisingly, on day+11, the effect of reduced signal intensity was more pronounced when we started the treatment on day+6 than on the day of HCT. The total ventral body signal of all three groups increased over time but measured average values of prednisolone treated mice stayed 1.5-fold and 1.6-fold below control values on day+15 and day+21, respectively, when starting the treatment on the day of HCT. When giving prednisolone from the time point of first alloreactive cell

detection on (day+6) we already detected a 1.7-fold lower signal on day+11, and a 2.3-fold and 2.8-fold signal reduction on days+15 and +21, respectively. However, signal intensities between the treated group and the aGvHD control group did not differ significantly (Figure 28B).

All mice but one survived until the end of the experiment (day+28, Figure 28C). One treated mouse died during the imaging procedure on day+21 likely due to an injection failure rather than due to aGvHD. Histopathological aGvHD scoring of target organs revealed a slightly reduced but not statistically significant tissue damage of prednisolone treated mice versus untreated controls on day+28 after miHAg mismatch allo-HCT. Weight change over time was similar in all three groups.

5 Results

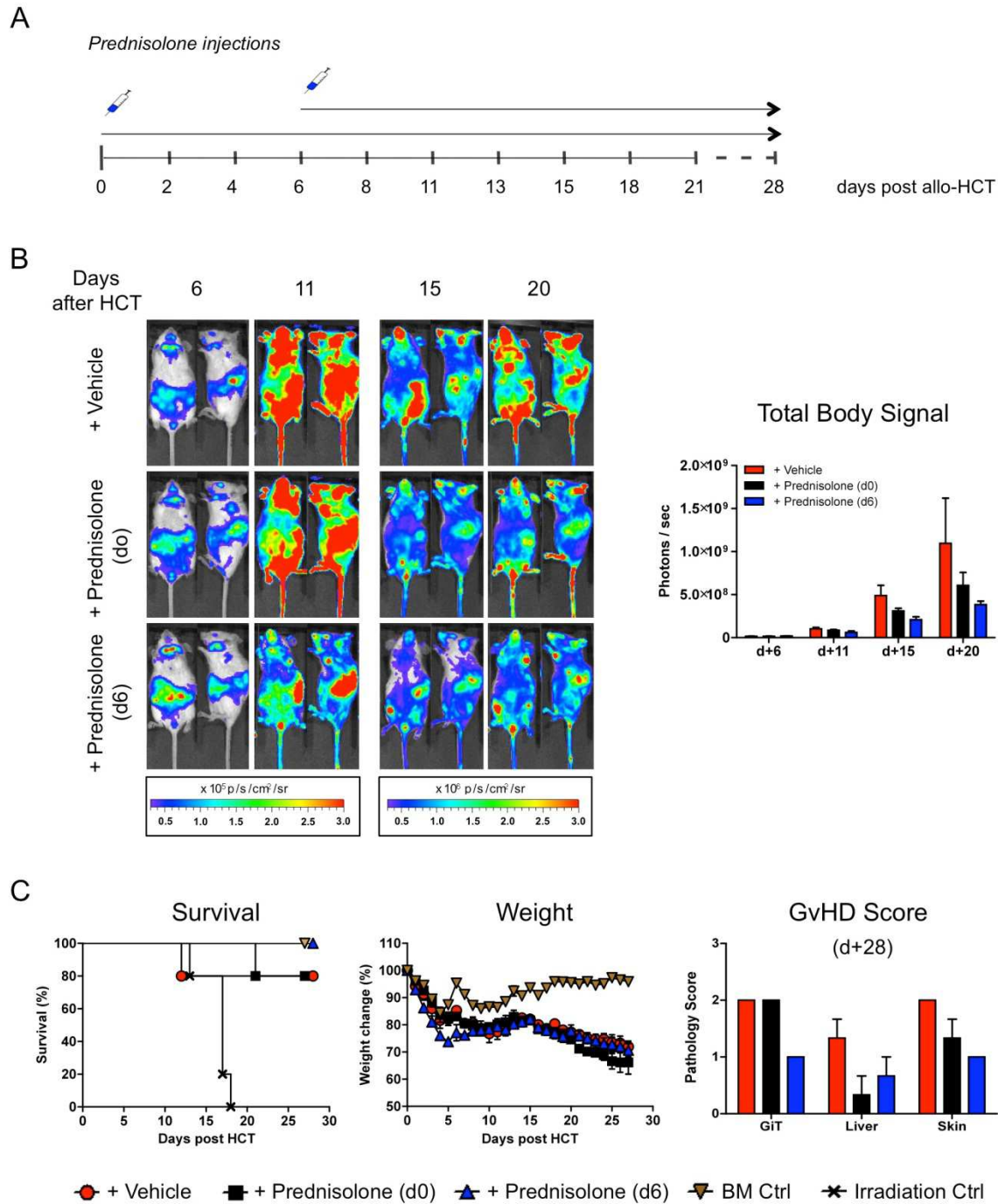


Figure 28: Prednisolone treatment after miHAg mismatch allo-HCT

(A) Timeline of Prednisolone injections (5 mg / kg BW): mice were treated daily starting on d0 and d6 after miHAg mismatch allo-HCT, respectively. On day+28, mice were sacrificed for histopathological analyses. (B) Ventral and lateral BLI images of one representative mouse per group ($n = 5$) at indicated time points. To better resolve organ distribution of donor T cells the threshold had to be adjusted between day+11 and day+15 (see color bars underneath the pictures). (C) Quantification of ventral and lateral whole body signals are shown in the graphs. (D) Survival, weight change and histopathological aGvHD score of different groups are shown. Error bars display plus or minus SEM.

5.3.2 Pentostatin treatment

In the next experiment, we treated the mice with pentostatin. Due to its known cytotoxic side effects, we administered single doses of pentostatin at donor T cell migration peaks (days+6, +11, +15) and days+18 and +21 (Figure 29A). Treated mice showed the same donor T cell distribution patterns and BLI signal intensities as untreated control mice from day+6 to day+15 (Figure 29B and Figure 14). However, some mice showed reduced signal intensities from abdominal regions and the skin. BLI on day+21, after four pentostatin injections, revealed very inhomogeneous signal intensities within the group. Two out of five mice displayed a very weak signal only, signal intensity of two mice was intermediate and one mouse gave a very strong total body signal which was comparable to the control mice. Pentostatin treatment did not influence the overall homing pattern of donor T cells. Quantification of BLI data showed no difference between treated mice and vehicle controls until day+15. However, average signal intensity on day+21 was 1.6-fold lower in drug recipients than in vehicle controls (Figure 29B).

Until day+30, clinical aGvHD scores and weight changes did not differ between both groups. However, from day+30 on, pentostatin treated mice performed worse and had to be sacrificed on day+38 due to severe aGvHD symptoms (Figure 29C).

5 Results

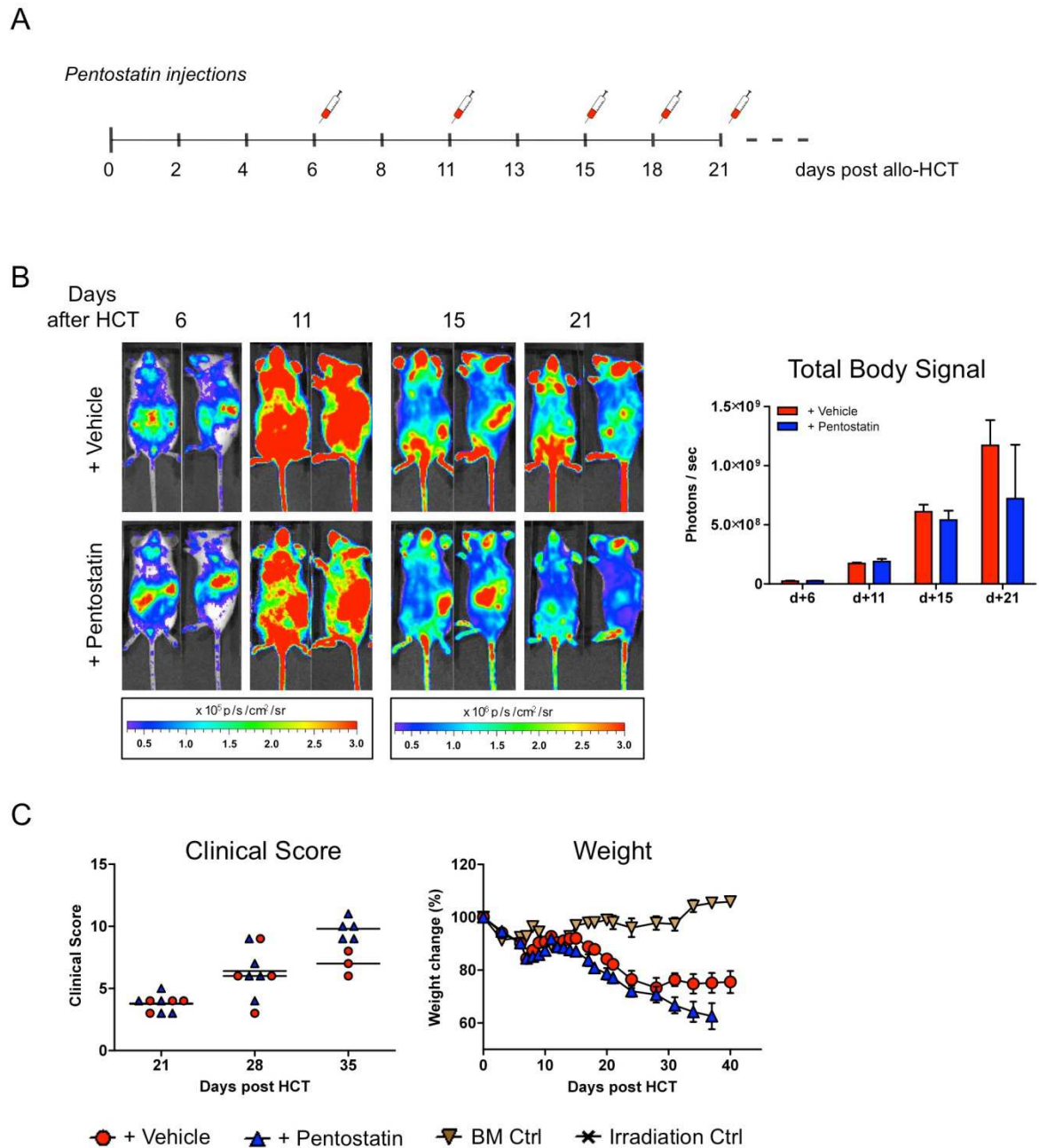


Figure 29: Pentostatin treatment after miHAg mismatch allo-HCT

(A) Timeline of Pentostatin injections (0.75 mg / kg BW): mice were treated at indicated time points after allo-HCT. (B) Ventral and lateral BLI images of one representative mouse per group (n = 5) at indicated time points. To better resolve organ distribution of donor T cells the threshold had to be adjusted between day+11 and day+15 (see color bars underneath the pictures). (C) Quantification of ventral and lateral whole body signals are shown in the graphs. (D) Clinical GvHD scores and weight change of different groups are shown. All treated mice had to be sacrificed on day+38 due to severe signs of GvHD. Error bars display plus or minus SEM.

5.3.3 Rapamycin treatment

In the last set of experiments we treated the mice with rapamycin which is established for aGvHD prevention and therapy in humans.

5.3.3.1 10 days of rapamycin treatment prolong survival

We administered the drug for 10 consecutive days starting on day+6 after miHAg mismatch allo-HCT (Figure 30A). BLI at selected time points revealed that by day+11, treated mice already showed reduced overall body signal intensities compared to vehicle controls with the strongest signal coming from the spleen, the skin, and the BM compartment (Figure 30B). In contrast, signals from the gastrointestinal region were low indicating that rapamycin treatment also influenced the homing pattern of donor T cells. On day+15, signal intensities of treated mice stayed low in comparison to constantly increasing whole body BLI signals of vehicle controls. On day+21, after the treatment was stopped, BLI signals of treated mice slightly increased but still remained below signal intensities of mice receiving the vehicle only. Quantification of ventral total body images confirmed a constantly low signal of rapamycin recipients during the treatment period compared to steadily increasing signal intensities in the control group (Figure 30B). Treated mice showed significantly lower signal intensities than vehicle controls (7-fold lower by day+11 and 13-fold lower by day+15). After the treatment was stopped (day+15) signal intensity of rapamycin recipients slightly increased but BLI still revealed a 4.5-fold difference between both groups on day+21. In addition, rapamycin treated mice also recovered from first aGvHD symptoms they showed by day+21 (Figure 30C). Over time, the clinical score of the treated group decreased in comparison to a constant increase of the controls. All treated mice survived until the end of the experiment (day+100) whereas some of the vehicle controls succumbed due to aGvHD.

Due to the dramatically reduced signal intensity in rapamycin treated animals by *in vivo* BLI we investigated lymphoid organs and aGvHD target tissues in more detail. To analyze whether rapamycin effects T cell proliferation and expansion locally or systemically we performed *ex vivo* BLI imaging of representative animals per group. In addition to vehicle controls we included completely untreated aGvHD control mice to this set of experiments to exclude inhibitory effects of the vehicle alone.

5 Results

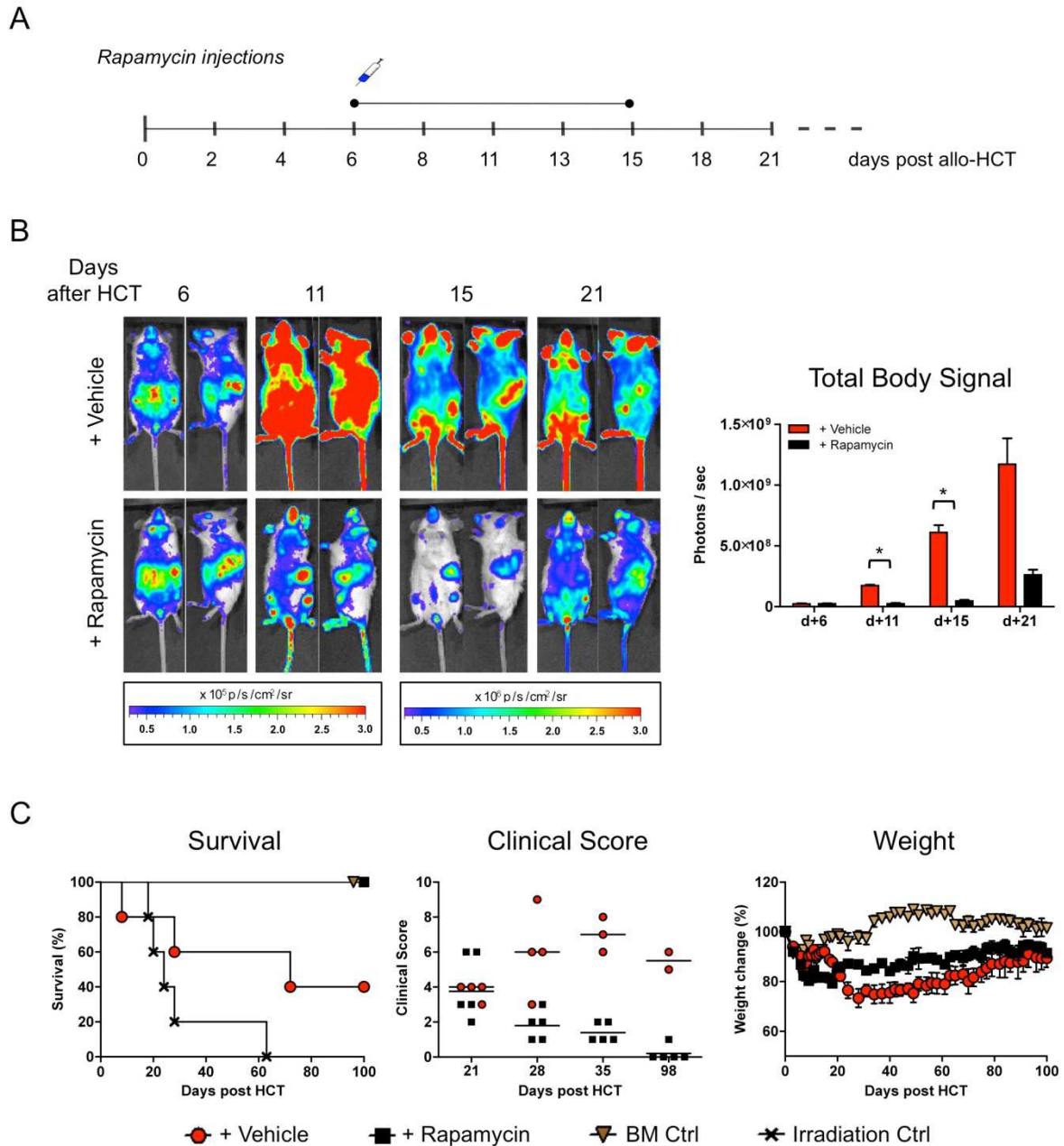


Figure 30: Rapamycin treatment after miHAg mismatch allo-HCT

(A) Timeline of rapamycin treatment (1.5 mg / kg BW): mice were treated daily for 11 days starting on day+6 after miHAg mismatch allo-HCT. (B) Ventral and lateral BLI images of one representative mouse per group ($n = 5$) at indicated time points. To better resolve organ distribution of donor T cells the threshold had to be adjusted between day+11 and day+15 (see color bars underneath the pictures). (C) Quantification of ventral and lateral whole body signals are shown in the graphs. * $p < 0.05$ (D) Survival, clinical aGvHD score, and weight change of different groups are shown. Error bars display plus or minus SEM.

Ex vivo BLI on day+11 after miHAg mismatch allo-HCT of untreated control mice revealed a similar donor T cell distribution pattern as observed in the previous experiment (see Figure 18). We detected signals from the gastrointestinal tract and first liver signals in addition to strong signals from SLOs as well as lung and thymus (Figure 31A). Vehicle treated mice showed the same cell distribution pattern with slightly reduced gastrointestinal signal intensities. Due to the very strong splenic signal in both control groups indicating an extremely high cell turn over, we removed the spleens before taking the pictures. In contrast, organs from rapamycin treated mice showed reduced signal intensities from all organs. In this group, gastrointestinal BLI signals were confined to mLNs and PPs and only discretely the large bowel. Quantification of the data confirmed a significant reduction of signal intensities in all lymphoid organs as well as in all target tissues of rapamycin treated mice compared to untreated controls (Figure 31B) indicating a systemic rather than a local effect of the drug.

5.3.3.2 Rapamycin treatment influences regulatory T cell expansion

The enormous reduction in BLI signal intensity prompted us to further investigate possible mechanisms leading to the observed effects. Since it is known that rapamycin influences T_{reg} expansion we performed immunofluorescence stainings for the transcription factor and Treg marker FoxP3 in mLNs and iLNs on day+11 after miHAg mismatch allo-HCT (Figure 32A, B). As in the previous experiments, rapamycin treatment started with first alloreactive donor T cell detection, on day+6 after allo-HCT

Quantification of FoxP3 expressing cells in both lymph nodes revealed significantly higher cell numbers in rapamycin treated mice compared to both control groups. In mLNs of rapamycin treated mice we found 2.5-fold more Tregs than in mLNs of untreated control mice. iLNs of treated mice showed 3-fold more FoxP3 expressing cells than the controls. These results confirm the influence of rapamycin treatment on the expansion of T_{reg} cells after allo-HCT.

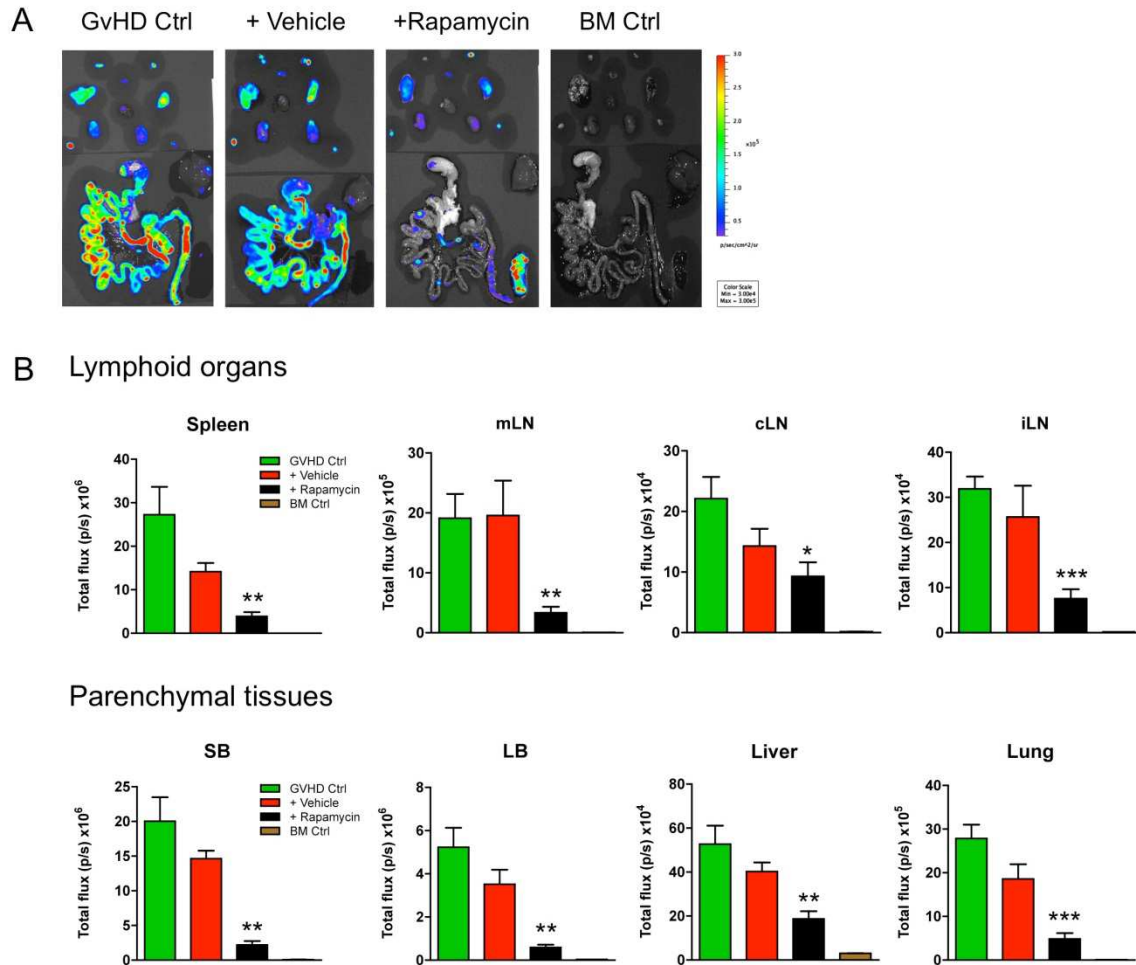


Figure 31: ex vivo BLI of lymphoid and target organs after rapamycin treatment

Donor T cell infiltration of lymphoid organs and parenchymal tissues on day+11 after miHAg mismatch allo-HCT of rapamycin treated and control mice. (A) Organs of one representative mouse per group (n = 3). (B) Quantification of the measured photons per second per organ. Error bars indicate plus or minus SEM. One out of two independent experiments is shown. mLN = mesenteric lymph node; cLN = cervical lymph node; iLN = inguinal lymph node; SB = small bowel; LB = large bowel.

5.3.3.3 Single shots of rapamycin insufficient for survival benefit

The daily rapamycin treatment appeared stressful for the mice as they displayed ruffled fur and weight loss during the treatment period. Furthermore, most of the rapamycin treated mice developed periorbital alopecia which likely is a drug dose-related side effect as reported by Blazar and colleagues.⁸⁵ Therefore, we changed the treatment schedule such that we administered single rapamycin injections only at the time points of donor T cell migration peaks (days+6, +11, +15 or days+11, +15 after miHAg mismatch allo-HCT; Figure 33A)

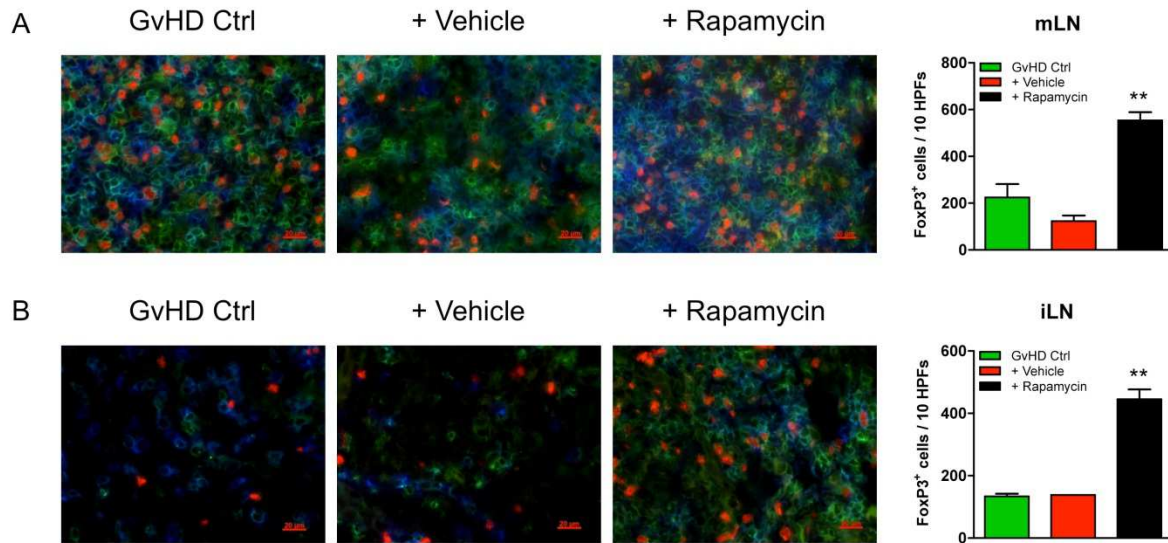


Figure 32: FoxP3 expression in lymph nodes after rapamycin treatment

Immunofluorescence staining of donor (CD90.1⁺, blue) CD4⁺ (green) FoxP3 (red) expressing cells in mLNs (A) and iLNs (B) on day+11 after miHAg mismatch allo-HCT. Shown is one representative image per group (n = 3-5 mice), 40x magnification. Error bars display plus or minus SEM. HPF = High Power Field; mLN = mesenteric lymph node; iLN = inguinal lymph node.

On day+11, BLI signal intensity did not differ between groups. On day+15, treated mice of both groups showed a slightly reduced whole body signal compared to vehicle controls. We observed a more pronounced difference in mice that already got two rapamycin injections (day+6 and +11; Figure 33B). However, by day+21, signal intensities of both treated groups almost reached the values of control mice. Furthermore, treated mice of either group did not have a survival benefit compared to control mice (Figure 33C). However, two mice per treated group survived until the end of the experiment (day+70). They completely recovered from all signs of aGvHD that remained apparent until day+34. In contrast, the one survivor of the control group was severely affected by aGvHD (Figure 33C, middle panel).

These experiments proved that starting a preemptive immunosuppressive treatment at the time point of first alloreactive cell detection in the PB protects mice from developing aGvHD after miHAg mismatch allo-HCT. A consecutive treatment with rapamycin for 10 days markedly reduced BLI signal intensity and prolonged survival in contrast to only mild effects of prednisolone or pentostatin administration.

5 Results

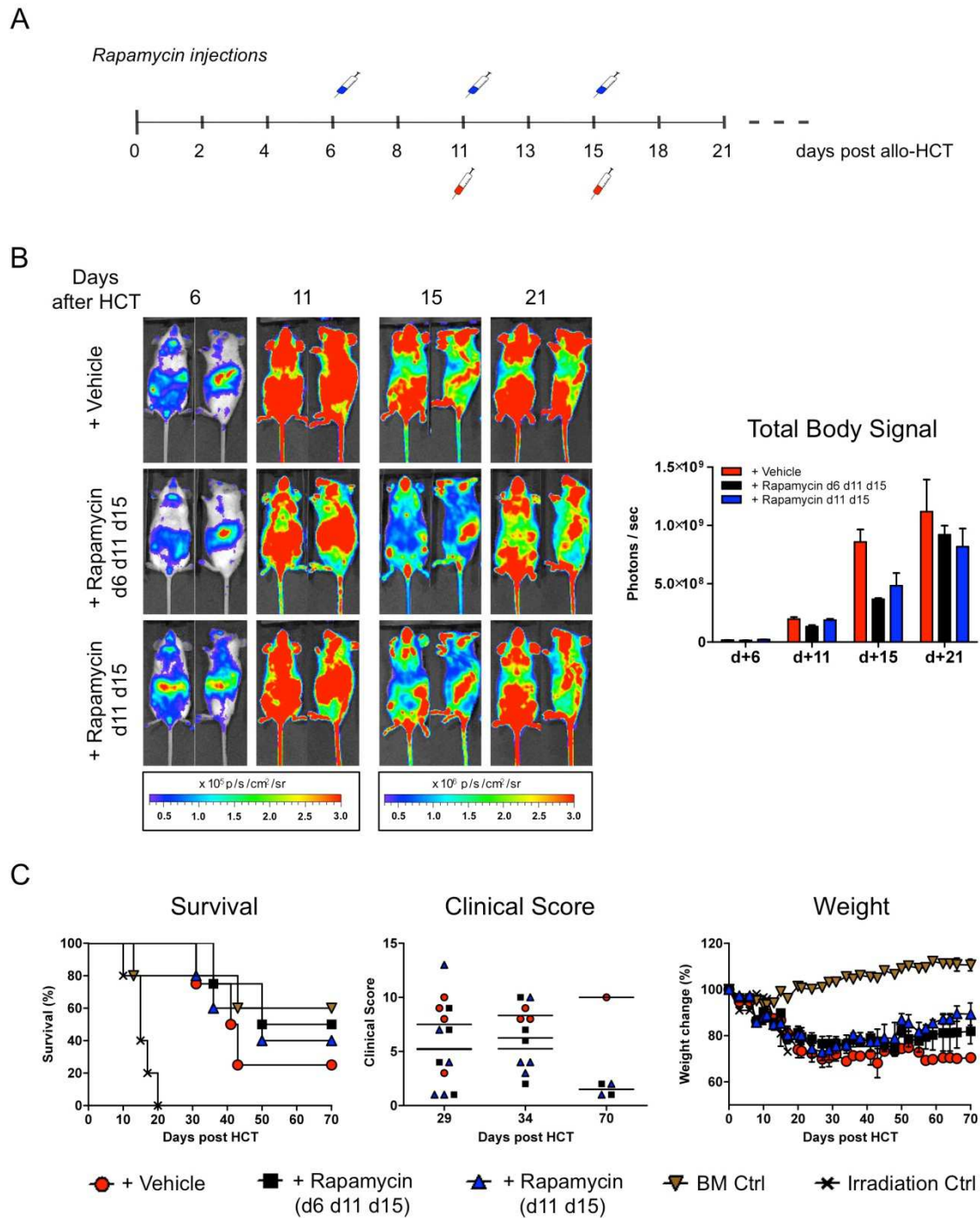


Figure 33: Single shots of rapamycin after miHAg mismatch allo-HCT

(A) Timeline of single rapamycin injections (1.5 mg / kg BW): mice were given 2 and 3 shots after allo-HCT, respectively. (B) Ventral and lateral BLI images of one representative mouse per group ($n = 4-5$) at indicated time points. To better resolve organ distribution of donor T cells the threshold had to be adjusted between day+11 and day+15 (see color bars underneath the pictures). (C) Quantification of ventral and lateral whole body signals are shown in the graphs. Error bars display plus or minus SEM. (D) Survival graph.

6. Discussion

This study addressed whether it is possible to detect migrating alloreactive donor T cells in the peripheral blood before aGvHD manifestation in a clinical relevant murine model across minor histocompatibility antigen barriers. We identified a phase of two weeks of massive alloreactive cell migration in the blood of transplanted mice before clinical aGvHD symptoms appeared. The precise analysis of the homing receptor expression profile suggested a strong association of the up-regulation of $\alpha 4\beta 7$ integrin, and P- and E-selectin ligand on highly activated alloreactive donor T cells during this migration phase with aGvHD induction. Treatment with the immunosuppressive drug rapamycin from the earliest detection time of alloreactive donor T cells (day+6) onwards significantly prolonged the survival of mice after miHAg mismatch allo-HCT. Thus, we propose that the T cell migration phase after allo-HCT opens a potential diagnostic window to identify alloreactive T cells based on their receptor expression profile for a timely therapeutic intervention prior to clinical disease manifestation.

6.1 aGvHD pathophysiology after miHAg mismatch allo-HCT

The first part of this study focused on donor T cell migration kinetics in an aGvHD mouse model across miAHg mismatch barriers (B6 \rightarrow Balb/B).¹²⁶ This genetic scenario corresponds to matched unrelated allo-HCT in patients and therefore is of high clinical relevance.¹²⁷ A complete HLA match between unrelated donor and recipient improves the chance of a successful engraftment after HCT. However, for most patients even completely matched donors harbour differences in miHAgs which can cause aGvHD.¹²⁸

Early detection of alloreactive donor T cells appears attractive to make a timely therapeutic intervention before clinical aGvHD onset feasible. Therefore, a detailed understanding of pathophysiological processes including the biology of engraftment and immune reconstitution as well as the kinetics of alloreactive T cell priming, migration, and effector mechanisms early after allo-HCT is necessary to provide important prognostic information. Recently, several groups investigated the correlation between lymphocyte recovery, T cell frequencies, and long-term survival

in allo-HCT patients: The assessment of cytotoxic and T-helper cell precursors by limiting dilution analyses showed a trend towards a better overall survival with low precursor frequencies.^{129,130} Other groups reported that the absolute lymphocyte count on day+30 after allo-HCT as well as after cord blood transplantation might serve as a surrogate to identify patients at risk for the development of aGvHD.¹³¹⁻¹³³ Therefore, a precise timing of T cell engraftment and a closer investigation of the cell migration patterns appear necessary for further investigations on phenotypic and functional changes within the lymphocyte populations during life-threatening immune syndromes such as aGvHD.

Ferrara and colleagues proposed that aGvHD pathophysiology proceeds in three steps: tissue damage and inflammation due to host conditioning result in the activation of APCs which leads to donor T cell activation, proliferation, differentiation, and migration followed by target tissue destruction.¹⁴ Until now it remained elusive whether alloreactive T cell extravasation would steadily increase after activation in SLOs or whether alloreactive T cell proliferation and migration would rather occur in self-amplifying loops. In accordance with the Ferrara model, *in vivo* and *ex vivo* BLI showed that donor T cells first home to SLOs in both the MHC major mismatched and the miHAg mismatched allogeneic models. From day+4 on, alloreactive donor T cells started to leave their priming sites and migrated towards their target organs which allowed the detection of an increasing number of T cells in the peripheral blood after allo-HCT (Figure 14, Figure 16). Daily *in vivo* BLI revealed the same spatio-temporal shift from aGvHD initiation to effector phase in both allo-HCT models but a slower increase in signal intensity in miHAg mismatch recipients compared to MHC major mismatch recipients. This observation can be explained by the high precursor frequency of T cells directed against MHC molecules of the host in the complete mismatched situation leading to the rapid development of a hyperacute form of GvHD.^{126,134} In contrast, after miHAg mismatch allo-HCT only few, immunodominant miHAgs are responsible for inducing aGvHD in donor/recipient pairs differing in numerous miHAg loci.¹³⁵⁻¹³⁷ Therefore, the development of an immune response is delayed.

In the presented miHAg mismatch allo-HCT model, first histopathological signs of tissue damage appeared by day+11 but mice did not show severe clinical aGvHD symptoms before day+21 (Figure 9C). Interestingly, the characterization of alloreactive T cell kinetics early after miHAg mismatch allo-HCT revealed two weeks

of massive donor T cell migration that fluctuated in cell numbers and peaked at defined time points (Figure 16). A possible explanation for these kinetics may be that host tissue damage results in an increasing release of host antigens and subsequent engagement of an increasing pool of donor T cell clones in the alloreactive immune response preceding each peak of T cell migration. Lehmann and colleagues first described this phenomenon of epitope spreading in experimental allergic encephalomyelitis (EAE).¹³⁸ They showed that the autoimmune response of CD4⁺ T cells is not fixed and the involved pool of T cell clones evolves over time. Epitope spreading is very well investigated in the context of chronic tissue damage in autoimmunity¹³⁹⁻¹⁴¹ but it might also play an active role in the ongoing pathology of other inflammatory diseases where tissue damage – regardless of the initiating event – can lead to epitope spreading.

Unexpectedly and not predicted by the three-step Ferrara model of aGvHD pathophysiology, we found that migrating peripheral blood donor T cell numbers decreased after allo-HCT in both models for several days before clinical symptoms appeared. This decrease in cell numbers inversely correlated with an increasing whole body BLI signal intensity indicating an accumulation of donor T cells in the respective target organs. There are several possible scenarios that may explain the observed decrease in detectable cells:

The decline in peripheral T cell numbers might be due to activation-induced cell death (AICD) as a control mechanism to regain homeostasis triggered by the inflammatory response after allo-HCT. In AICD, activation through the T cell receptor results in cell death caused by apoptosis.¹⁴² There are several signals that can lead to AICD. One important signaling pathway is mediated by Fas-FasL interaction in peripheral tissues.¹⁴³ FasL expression is important in HCT recipients as a negative regulator of the donor T cell allo-response in GvHD and FasL deficient mice showed more intestinal GvHD compared to WT recipients.¹⁴⁴

Alternatively, immunosuppressive modulators may mediate the reduction in detectable cells by counteracting the prolonged expansion of alloreactive T cells. These may involve T_{reg} cells, myeloid-derived suppressor cells (MDSC), and biological mediators such as arginase or indoleamine 2,3-dioxygenase (IDO).

CD4⁺ CD25⁺ FoxP3⁺ T_{reg} cells adopt important regulatory functions in *in vivo* homeostasis and prevention of autoimmunity. T_{reg} cells exert suppressive functions in aGvHD by limiting effector T cell proliferation and thereby preventing immune

responses to allo-antigens.^{145,146} *In vitro* activated and expanded, or naturally occurring T_{reg} cells offer substantial aGvHD protection.^{147,148}

MDSCs are a well-defined cell population with inhibitory effects on immune responses.¹⁴⁹ Their role in cancer as an escape mechanism for immune surveillance has been studied intensively in different mouse models.^{150,151} Recently, one group reported a potential beneficial role of MDSCs in regulating allo-reactivity after HCT.¹⁵² The administration of *in vitro* generated MDSCs together with the donor cell inoculum inhibited murine aGvHD in an arginase-1 dependent manner while the GvL effect was preserved.¹⁵³

IDO is another critical regulator of intestinal GvHD. It is induced in the colon and regulates T cell proliferation and survival.¹⁵⁴ With its suppressive effects it efficiently diminishes gastrointestinal inflammation and reduces murine aGvHD severity.^{155,156} The assessment of IDO expression in patients after allo-HCT was consistent with the results from mouse models.¹⁵⁷

Therefore, it is likely that a combination of different inhibitory mechanisms leads to the observed decrease in detectable alloreactive donor T cells in our model even if they may not sufficiently prevent the onset of aGvHD symptoms.

6.2 Donor T cell receptor profile after miHAg mismatch allo-HCT

Adhesion molecules as well as chemokines and their respective receptors play an important role for T cell homing into tissues. Therefore, in the context of this study we investigated the dynamic changes of the expression levels of different homing receptors and activation markers in order to identify suitable markers for alloreactive donor T cell detection in the peripheral blood early after miHAg mismatch allo-HCT.

6.2.1 $\alpha 4\beta 7$ integrin is highly up-regulated on donor T cells

Daily flow cytometric measurements revealed $\alpha 4\beta 7$ integrin to be highly up-regulated on alloreactive, peripheral blood donor T cells after miHAg mismatch allo-HCT compared to syngeneic controls (Figure 22). Several previously published, independent murine studies are consistent with these results. They showed an important role of $\alpha 4\beta 7$ integrin in intestinal aGvHD development. For example, mice lacking PPs – the main priming site for $\alpha 4\beta 7$ integrin expressing T cells – did not

develop aGvHD after allo-HCT and blocking access to PPs by administering a monoclonal antibody protected mice from aGvHD.²⁴ Using $\alpha 4\beta 7$ negative donor T cells caused less aGvHD morbidity and mortality compared to WT donor T cells mainly due to reduced homing to the intestinal tract. The GvTE was still preserved in this model.¹⁰⁸ However, results of donor T cells lacking the $\beta 7$ subunit alone are contradictory. Waldman and colleagues reported that a selective knockout of $\beta 7$ integrin resulted in less intestinal aGvHD due to decreased homing of alloreactive T cells to the intestine⁹⁹ whereas another group showed that the lack of $\beta 7$ was insufficient to modify intestinal aGvHD.¹⁵⁸ A general conclusion from these studies is difficult due to the different mouse models used. Nevertheless, all studies point towards an important, but perhaps redundant, role of $\alpha 4\beta 7$ integrin in lymphocyte trafficking and the infiltration of mucosa-associated tissues, subsequently leading to intestinal aGvHD development which is in accordance with the results presented here.

Furthermore, the up-regulation of $\alpha 4\beta 7$ integrin on peripheral blood T cells observed in this work is in line with three recently published patient studies suggesting a role of this molecule in the development of acute intestinal aGvHD after allo-HCT. Chen and colleagues found an at least 10-fold up-regulation of $\alpha 4\beta 7$ integrin on naïve and memory T cell subsets in the peripheral blood before the onset of clinically apparent intestinal aGvHD compared to cutaneous or no aGvHD in a retrospective case-controlled study including 59 patients.¹⁵⁹ However, in this study the timing of sample collection was heterogeneous and samples were frozen prior to analysis. Therefore, they confirmed these results in a follow-up publication using fresh blood samples collected at the time point of first aGvHD symptom appearance and before any treatment. They again showed that $\alpha 4\beta 7$ integrin was significantly higher expressed on CD8⁺ memory T cells of patients with intestinal aGvHD compared to patients with skin or no aGvHD in relative as well as absolute values. Interestingly, patients successfully treated against intestinal aGvHD showed a lower $\alpha 4\beta 7$ expression level several months after diagnosis.¹⁶⁰ A different study including 33 patients investigated the $\alpha 4\beta 7$ integrin expression on suppressive T_{reg} cells. They found a correlation between a decreased expression level with a subsequent intestinal aGvHD development.¹⁶¹ These clinical results indicate an important role for $\alpha 4\beta 7$ integrin up-regulation at the time point of aGvHD onset but further studies with larger patient

cohorts are needed to validate the use of $\alpha 4\beta 7$ integrin as a predictive marker or potential therapeutic target.

6.2.2 Alloreactive donor T cells up-regulate selectin ligands

Migrating allogeneic donor T cells highly up-regulated P- and E-selectin ligands compared to peripheral blood T cells after syngeneic HCT (Figure 23, Figure 24). The interaction between P-selectin and its ligands plays an important role for T cell trafficking in aGvHD as P-selectin deficient host mice demonstrated ameliorated aGvHD after miHA_g mismatch allo-HCT.¹¹¹ However, donor T cells deficient for P-selectin glycoprotein ligand-1, which represents the major ligand for P-selectin, caused similar aGvHD severity as WT T cells in this study indicating that donor T cells may use multiple ligands apart from PSGL-1 to interact with P-selectin and to enter their target tissues. Another group also observed normal aGvHD induction when using donor T cells which completely lack functional P- and E-selectin ligands concluding that donor T cells can traffic to aGvHD target organs independently of P- and E-selectin ligands after MHC major mismatch allo-HCT.¹⁶² Nevertheless, the elevated expression levels of P- and E-selectin ligand on peripheral blood donor T cells measured in this study are consistent with the previously mentioned reports. Independently of the fact that donor T cells can infiltrate target tissues lacking selectins the upregulation of selectin ligands on circulating T cells could serve as possible predictive markers to identify them. Expression levels measured after allo-HCT significantly exceeded expression levels detected after syngeneic HCT. Asaduzzaman and colleagues confirmed the pivotal role of the interaction of PSGL-1 on CD8⁺ donor T cells and P-selectin on the endothelium for entering the large intestine. In addition, they also investigated L-selectin expression and found a down-regulation on activated CD8⁺ T cells of aGvHD mice compared to controls¹⁶³ which is consistent with the results presented here: L-selectin expression differed significantly on peripheral blood donor T cells of allogeneic and of syngeneic HCT recipients. Several groups demonstrated the importance of L-selectin for aGvHD initiation: Transfer of purified memory T cells lacking L-selectin did not induce aGvHD after allo-HCT most likely due to inefficient trafficking to SLOs in the MHC major mismatch^{20,164} as well as in the miHA_g mismatch allo-HCT scenario.¹⁶⁵ Another

group observed a pronounced decrease in donor-derived peripheral blood L-selectin⁺ T cells in rats suffering from aGvHD compared to controls after miHA_g mismatch allo-HCT. These results suggest the potential use of L-selectin-expressing frequencies as disease-associated biomarker for aGvHD.¹⁶⁶

Taken together, the significant higher expression of P- and E-selectin ligand as well as the down-regulation of L-selectin on detected peripheral blood donor T cells early after allo-HCT underline the potential use as predictive markers in combination with other receptors.

6.2.3 Chemokine receptors do not define alloreactive donor T cells

In contrast to the integrin and the selectin family of analyzed homing receptors, none of the tested chemokine receptors seemed suitable as predictive marker for aGvHD. Especially on day+6 after allo-HCT, peripheral blood donor T cells highly up-regulated all CCRs in both allogeneic models compared to untreated WT controls. However, also syngeneic HCT recipients showed elevated levels of CCRs on peripheral blood donor T cells and comparable MFI values to allo-HCT recipients at all tested time points (Figure 26).

Within the first week after HCT syngeneic recipients also show increased cytokine levels in combination with minor changes in weight, fur texture, and mobility. These effects are due to irradiation toxicity-related tissue damage and mice continuously recover from them over time in contrast to allo-HCT recipients.⁷³ In line with this, Eyrich and colleagues reported the up-regulation of different cell adhesion molecules on the epithelium of allogeneic as well as syngeneic HCT recipients by day+3. However, following syngeneic HCT these effects are only transient in contrast to a further up-regulation after allo-HCT until day+22.²⁷ Since all recipients receive the same irradiation conditioning before HCT the transiently caused inflammatory scenario could explain the similar CCR expression level of peripheral blood donor T cells found in all three models at early time points in this study. Inflammation induced by conditioning plays an important role in the initial recruitment of T cells which induces an inflammatory cascade promoting further recruitment of T cells to aGvHD target organs.²⁶ In the work presented here, CCR expression on peripheral blood donor T cells of allogeneic as well as of syngeneic HCT recipients declined at later

time points compared to day+6. This indicates that after the initial recruitment of T cells to inflamed tissues other mechanisms and receptor – ligand interactions than CCRs may be involved in further cell recruitment to target organs. In line with this, one group reported that activated effector and memory T cells undergo a switch in surface receptor expression within 6 hours of TCR stimulation down-regulating CCRs1, 2, 3, 5, 6 and CXCR3.¹⁶⁷ Because of endothelial cell recovery from the initial conditioning damage together with reduced cytokine production in syngeneic HCT recipients CCRs and further cell recruitment are no longer needed.

Another group demonstrated a marked but transient increase in chemokine expression in the colon after syngeneic HCT.¹⁶⁸ In particular, they found the ligands for the general inflammation marker CXCR3 up-regulated which is consistent with the results presented here. We also found CXCR3 highly up-regulated on peripheral blood donor T cells after miHA_g mismatch allo-HCT but also syngeneic HCT recipients showed high expression levels compared to steady-state conditions in untreated mice. From day+6 on, CXCR3 expression of CTLs of syngeneic HCT recipients even exceeded the expression levels of allogeneic donor T cells (Figure 25). The transfer of CXCR3 knock out donor T cells did not significantly reduce aGvHD severity after MHC major mismatch allo-HCT¹⁶⁸ diminishing its role in aGvHD development and as possible predictive marker. However, another study reported an involvement of CXCR3 in aGvHD development after miHA_g mismatch allo-HCT but not across MHC major mismatch barriers.¹¹⁸ Furthermore, Chen and colleagues demonstrated a complex pattern of CXCR3 up- and down-regulation on inflammatory T cells during migration, proliferation, and activation in a murine, ocular inflammation model¹⁶⁹ confirming the results presented here for CXCR3 in the context of aGvHD.

In general, the partly conflicting results for the importance of different chemokine – receptor interactions in aGvHD initiation and development might be dependent to some extent on the mouse model used and the conditioning regimen applied.^{25,168} Furthermore, CCR expression is a dynamically regulated process. One cell can express multiple receptors and the presence of a specific chemokine for one receptor can affect other receptors as well.¹⁷⁰ In addition, interactions of inflammatory chemokines and their respective receptors are highly redundant, limiting the hopes for aGvHD prevention by blocking a specific receptor.¹⁰¹ Despite this, different studies recently targeted single CCRs using monoclonal antibodies with some promising results: The administration of an anti-CXCR3 neutralizing antibody for 21 days after

miHg mismatch allo-HCT significantly reduced alloreactive donor T cell infiltration in aGvHD target organs and inhibited disease onset.¹⁷¹

Another group presented preliminary results in a clinical trial adding an oral antagonist of CCR5 to conventional aGvHD prophylaxis. In their study including 38 patients they observed a decreased incidence of intestinal and liver aGvHD at day+180 after HCT compared to a control group¹⁷² which was consistent with previously published results in murine models.^{24,114} This is the first study showing that aGvHD can potentially be influenced by inhibiting lymphocyte trafficking. However, considering the small sample size further studies will be needed to confirm these results.

6.2.4 Alloreactive donor T cells are highly activated

The analysis of the activation status of alloreactive T cells revealed them to be highly positive for CD44 (Figure 27, upper panel). Triggering of the TCR induces CD44 up-regulation on lymphocytes and leads to an activation-dependent interaction with its major ligand hyaluronate, an extracellular matrix component, directing activated lymphocytes to inflammatory sites.^{110,173} In the context of aGvHD, a subset of CD8⁺ CD44⁺ memory T cells mediated potent GvL activity while causing minimal aGvHD only after murine MHC major mismatch allo-HCT.¹⁷⁴ However, in the experiments presented here peripheral blood donor T cells of syngeneic HCT recipients also showed highly elevated levels of CD44 expression, possibly caused by irradiation-induced temporary inflammation, lowering its value as useful predictive marker.

In contrast, from day+6 on, donor T cells expressed significantly more CD69 after miHAg mismatch than after syngeneic HCT (Figure 27, middle panel). Generally regarded as an early activation marker, CD69 is known as an immunomodulatory molecule induced early on leukocytes upon activation¹⁷⁵ which is consistent with the results of this study showing CD69 to be highly up-regulated on peripheral blood CD8⁺ T cells of all groups as early as day+4 after HCT. However, its actual role in immune responses remains unclear. Several studies suggest a pro-inflammatory role of CD69 but recent observations have been contradictory pointing more towards a role as a negative regulator of T cell responses by especially inhibiting Th17 cell differentiation.^{176,177} In addition, CD69 might be involved in T_{reg} generation and

activity.¹⁷⁸ Other groups suggest a potential role of transiently expressed CD69 in the regulation of thymocyte and T cell trafficking.^{179,180} In spite of partially contradictory reports about the role of CD69 on leukocytes in immune responses the significant higher expression observed on peripheral blood CD8⁺ donor T cells after miHAg mismatch allo-HCT compared to syngeneic HCT recipients from day+6 on underlines its potential value as predictive marker in combination with others.

Similarly, on days+6, +15 and +21 after HCT the frequency of CD8⁺ CD25⁺ donor T cells in the peripheral blood of miHAg mismatch allo-HCT recipients exceeded the frequency of this cell populations after syngeneic HCT significantly (Figure 27, lower panel). Lymphocytes constitutively express low levels of CD25, the IL-2R α chain. IL-2 stimulation is the main T cell growth factor and is essential for the accumulation of effector CD8⁺ T cells during immune responses.¹⁸¹ Inflammation enables the IL-2 responsiveness of T lymphocytes by inducing IL-2R up-regulation.¹⁸² This could explain the elevated CD8⁺ CD25⁺ donor T cell frequency as well after syngeneic HCT (day+4) compared to untreated WT controls. However, at later time points, the increasing inflammatory scenario due to tissue injury in allo-HCT recipients may sustain CD25 expression and IL-2 sensitivity whereas after syngeneic HCT irradiation-induced tissue injury declined and the cells became less sensitive for IL-2. Though commonly used as an activation marker for CD8⁺ T cells, CD25 also represents an important marker for CD4⁺ FoxP3⁺ T_{reg} cells and plays a central role in the generation, maintenance, and function of this regulatory T cell subset.¹⁸³ A recent publication reported the identification of a highly suppressive CD8⁺ FoxP3⁺ regulatory T cell subpopulation which converts from conventional CD8⁺ donor T cells after allogeneic but not syngeneic HCT.¹⁸⁴ Further investigations are needed to test whether the CD8⁺ CD25⁺ donor T cell population detected in the peripheral blood of miHAg mismatch allo-HCT recipients in this study belongs to this newly identified suppressive subset. Nevertheless, the significant higher expression on donor T cells after allogeneic compared to syngeneic HCT suggests a possible use of this marker for alloreactive T cell definition in the peripheral blood.

Taken together, the combination of the expression levels of α 4 β 7 integrin as well as P- and E-selectin ligand, and L-selectin together with the activation markers CD69 and CD25 seems promising as a predictive marker panel for alloreactive cell detection early after allo-HCT.

6.3 Directed preemptive treatment with rapamycin significantly prolongs survival

In this study, we tested three different drugs for a directed preemptive treatment of aGvHD before disease onset. Based on the results presented above, we started treatments within the identified potential diagnostic window at the time point of first alloreactive cell detection in the peripheral blood (day+6 after miHAg mismatch allo-HCT).

The administration of the glucocorticoid prednisolone at a dose of 5 mg / kg BW, commonly used in patients,¹⁸⁵ did not result in a significant reduction in BLI signal intensity in this mouse model. However, lower BLI signals indicated some therapeutic effect in treated mice. Histopathological analyses on day+28 after allo-HCT confirmed that less donor T cells accumulated in aGvHD target organs in treated mice than in untreated controls (Figure 28C). Bouazzaoui and colleagues reported that prednisolone treatment can reduce clinical aGvHD, improve survival, and reduce GIT injury when given in a concentration of 2 mg / kg BW in a murine haploidentical aGvHD model. They started the treatment shortly after aGvHD onset, on day+10 after HCT in their model.⁷³ Different murine and human studies indicate that the administration of steroids as aGvHD prophylaxis or within a few days after HCT is associated with increased morbidity and significant higher acute and chronic GvHD incidences implying the administration of steroids before GvHD onset as not beneficial.¹⁸⁶⁻¹⁸⁸ Day+6 after allo-HCT in the B6 → Balb/B miHAg mismatch model in this study marked an early time point before aGvHD onset which could explain the lack of a significant benefit for the treated mice.

The cytotoxic drug pentostatin impairs effector T cell expansion and reduces proinflammatory cytokine production while preserving regulatory T cell populations and functions in a murine model for inflammatory bowel disease. In this study, the authors administered pentostatin daily at a concentration of 0.75 mg / kg BW for 7 days.¹⁸⁹ However, in the miHAg mismatch allo-HCT model used in our study pentostatin did not reduce donor T cell expansion or ameliorate aGvHD symptoms indicating that at this dose five injections were not sufficient to significantly prolong survival.

In contrast, treatment of miHAg mismatch allo-HCT recipients with rapamycin for 10 consecutive days significantly reduced BLI signal intensity and prolonged survival.

The dose of 1.5 mg / kg BW has been proven to be optimal for aGvHD protection starting the treatment on day+0 followed by daily injections. Higher doses led to a survival decrease and toxic side effects whereas lower doses could not protect from lethal aGvHD.^{85,120} There are several different scenarios that could explain the reduced BLI signal intensity observed in the current study: one group showed that at a dose of 1.5 mg / kg BW rapamycin inhibited splenic expansion of CD4⁺ (by day+7) and CD8⁺ (by day+14) T cells.⁸⁵ Chen and colleagues identified an antigen independent regulatory cell population in aGvHD target organs which was generated in a dose-dependent manner in rapamycin treated animals and may contribute to aGvHD-free long-term survival.¹⁹⁰ Furthermore, rapamycin influences T_{reg} expansion¹²⁰ which we confirmed by microscopy of FoxP3⁺ T cells in this study (Figure 32). We found elevated numbers of this cell population in mLN and iLN of miHAg mismatch allo-HCT recipients after rapamycin treatment which likely exerted a suppressive effect on expanding effector T cells. Possibly, a combination of the above mentioned effects of rapamycin contributed to the substantial inhibition of donor T cell expansion leading to the observed significantly lower BLI signal intensity of treated mice.

Rapamycin treatment not only inhibited alloreactive donor T cell expansion but also influenced their homing pattern after miHAg mismatch allo-HCT. In contrast to vehicle treated control mice, BLI of Rapamycin treated recipients revealed a strong signal from the BM compartment from day+11 on indicating an accumulation of donor T cells in this area. In contrast, the gastrointestinal tract showed reduced signal intensities. The different homing pattern might be explained by the effect of rapamycin on dendritic cells (DCs). Rapamycin treatment interferes with DC functions by affecting maturation¹⁹¹, antigen uptake capacity,¹⁹² and cytokine production.¹⁹³ Moreover, mature DCs exert immunosuppressive effects on allogeneic T cells after rapamycin treatment.¹⁹⁴ Host-derived DCs are important but not crucial for the induction of homing receptor expression on alloreactive donor T cells during proliferation in SLOs in aGvHD development.^{195,196} DCs of the mLN and the PPs imprint the gut-homing specificity of T cells by vitamin A production. Under steady-state conditions, vitamin A-deficient mice showed reduced numbers of $\alpha 4\beta 7^+$ T cells in SLOs and in the intestinal lamina propria indicating its important role in $\alpha 4\beta 7$ integrin up-regulation.¹⁹⁷ However, in the context of aGvHD, a vitamin A-deficient diet did not protect from disease onset. These mice showed reduced T cell numbers in

the intestine but increased numbers and tissue damage in other organs and succumbed to aGvHD.¹⁹⁸ Therefore, the observed changes in the homing pattern of donor T cells in rapamycin treated mice could be due to the effect of rapamycin on DCs or other host APC populations but most likely other mechanisms are involved as well.

Daily rapamycin application appeared stressful for treated mice as we observed ruffled fur and weight loss during the treatment period. Furthermore, most of the rapamycin treated mice developed periocular alopecia which likely is a drug dose-related side effect.⁸⁵ Therefore, we changed the treatment schedule and administered single rapamycin injections only at donor T cell migration peaks (days+11 and +15 or days+6, +11 and +15; Figure 33). In this setting, we detected slight reductions in BLI signal intensities compared to vehicle controls but these differences did not reach statistical significance most likely due to the half-life time of rapamycin of approximately 62 hours.¹⁹⁹ Apparently, the intervals between the single injections were too long and additional injections between the migration peaks are necessary for inducing the protective effect.

In summary, in my thesis project, I demonstrated that it is possible to detect migrating alloreactive donor T cells in the peripheral blood in a clinical relevant mouse model across miHAg mismatch barriers early after allo-HCT. Thus, we propose that a phase of two weeks of massive donor T cell migration in the peripheral blood may open a potential diagnostic window. The homing receptors $\alpha 4\beta 7$ integrin, P- and E-selectin ligand, and L-selectin in combination with the activation markers CD69 and CD25 helped to identify alloreactive donor T cells in the peripheral blood of mice before aGvHD manifestation after allogeneic but not syngeneic HCT. The consecutive, preemptive rapamycin treatment starting at the time point of first cell detection after miHAg mismatch allo-HCT prolonged survival of treated mice.

One advantage of first using animal models to investigate donor T cell kinetics is the possibility of dynamically tracing donor T cell migration patterns by daily *in vivo* imaging applications. Mice in our study did not receive preemptive immunosuppressive treatment before homing receptor analysis as is done in patients. For this reason, experimental aGvHD is not influenced by such medication thus better reflecting the native disease. Since the prediction of aGvHD is highly relevant for the clinical outcome it appears valuable to closely monitor the kinetics of

T cell engraftment, expansion, and homing receptor expression in patients undergoing allo-HCT and interfere with immunosuppressive treatment if biomarker patterns indicate an increased risk of aGvHD.

We already performed a follow-up study to analyze the receptor expression profile in patients after allo-HCT. The data is currently statistically analyzed. A predictive blood test based on a certain receptor combination is highly desirable and would allow a timely, preemptive, therapeutic intervention before the onset of clinical aGvHD.

7. Zusammenfassung

Die allogene hämatopoetische Stammzelltransplantation ist oft die einzig mögliche Behandlungsmethode für maligne und nicht-maligne hämatologische Erkrankungen. Die Graft-versus-Host Disease stellt den größten, limitierenden Faktor dieser Therapie dar. Bei diesem Immunsyndrom greifen alloreaktive Spender-T-Zellen gezielt Organe des Empfängers an, insbesondere den Gastrointestinaltrakt, die Leber und die Haut. Die frühe Diagnose einer bevorstehenden, akuten GvHD gestaltet sich nach wie vor schwierig und basiert heutzutage hauptsächlich auf dem Auftreten klinischer Symptome und histopathologischen Befunden. Die Entwicklung eines prädiktiven Tests zur Früherkennung gefährdeter Patienten hat daher hohe Priorität. Verschiedene Gruppen zeigten kürzlich, dass Spender-T-Zellen spezifische Rezeptoren, sogenannte Homing-Rezeptoren, exprimieren müssen, um in die Zielorgane einwandern zu können. Deshalb scheint die Entwicklung eines auf dem spezifischen Homing-Rezeptor-Expressionsmuster der T-Zellen im peripheren Blut basierenden Tests vielversprechend, um gezielt Patienten zu identifizieren, die möglicherweise eine aGvHD entwickeln werden.

Das Ziel dieser Arbeit war die genaue Analyse der Migrationskinetik alloreaktiver Spender-T-Zellen im peripheren Blut in einem klinisch relevanten Mausmodell mit Unterschieden in minor Histokompatibilitätsantigenen. Es folgte eine präzise Charakterisierung des Homing-Rezeptor-Expressionsprofils der migrierenden Spenderlymphozyten zu ausgewählten Zeitpunkten nach Transplantation, um mögliche, geeignete Rezeptoren für einen prädiktiven Test zu identifizieren.

Die Kombination von täglicher *in vivo* Bildgebung der transplantierten Mäuse mit durchflusszytometrischen Analysen des peripheren Blutes ermöglichte es, eine zweiwöchige Phase massiver Spenderzellmigration vor dem Auftreten klinischer aGvHD Symptome zu definieren. Die detektierten Spenderlymphozyten zeigten eine stark erhöhte Expression des für die Migration in den Gastrointestinaltrakt wichtigen Moleküls $\alpha 4\beta 7$ Integrin sowie der Liganden für P- und E-Selektin, die in das Haut-Homing involviert sind. Die Kombination dieser Marker mit der stark reduzierten Expression von L-Selektin, einem Marker für naive T-Zellen, sowie der signifikant höheren Expression der Aktivierungsmarker CD25 und CD69 im Vergleich zu syngen transplantierten Kontrolltieren ermöglichte die Definition von alloreaktiven Spender-T-Zellen. Eine gezielte, vorbeugende Behandlung mit Rapamycin, beginnend am Tag

der Detektion erster alloreaktiver T-Zellen (Tag+6), erhöhte die Überlebensrate der behandelten Mäuse.

Aufgrund dieser Daten schlagen wir ein potentiell, diagnostisches Fenster zur Anwendung prädiktiver Tests vor, um Patienten, mit erhöhtem aGvHD-Risiko rechtzeitig zu identifizieren und vorbeugend behandeln zu können.

8. Reference list

1. Horowitz MM. Uses and Growth of Hematopoietic Cell Transplantation. Thomas' Hematopoietic Cell Transplantation: Wiley-Blackwell; 2009:15-21.
2. Appelbaum FR. Haematopoietic cell transplantation as immunotherapy. *Nature*. 2001;411(6835):385-389.
3. Barnes DW, Corp MJ, Loutit JF, Neal FE. Treatment of murine leukaemia with X rays and homologous bone marrow; preliminary communication. *British Medical Journal*. 1956;2(4993):626-627.
4. Lorenz E, Congdon C, Uphoff D. Modification of Acute Irradiation Injury in Mice and Guinea-Pigs by Bone Marrow Injections. *Radiology*. 1952;58(6):863-877.
5. Bach F, Albertini R, Joo P, Anderson J, Bortin M. Bone-marrow transplantation in a patient with the wiskott-aldrich syndrome. *The Lancet*. 1968;292(7583):1364-1366.
6. De Koning J, Van Bekkum DW, Dicke KA, Dooren LJ, Van Rood JJ, Rádl J. Transplantation of bone-marrow cells and fetal thymus in an infant with lymphopenic immunological deficiency. *The Lancet*. 1969;293(7608):1223-1227.
7. Gatti R, Meuwissen H, Allen H, Hong R, Good R. Immunological reconstitution of sex-linked lymphopenic immunological deficiency. *The Lancet*. 1968;292(7583):1366-1369.
8. Kondo M, Wagers AJ, Manz MG, et al. Biology of hematopoietic stem cells and progenitors: Implications for Clinical Application. *Annual Review of Immunology*. 2003;21(1):759-806.
9. Welniak LA, Blazar BR, Murphy WJ. Immunobiology of Allogeneic Hematopoietic Stem Cell Transplantation. *Annual Review of Immunology*. 2007;25(1):139-170.
10. Wagner J, Steinbuch M, Kernan N, Broxmayer H, Gluckman E. Allogeneic sibling umbilical-cord-blood transplantation in children with malignant and non-malignant disease. *The Lancet*. 1995;346(8969):214-219.
11. Barker JN, Weisdorf DJ, DeFor TE, et al. Transplantation of 2 partially HLA-matched umbilical cord blood units to enhance engraftment in adults with hematologic malignancy. *Blood*. 2005;105(3):1343-1347.
12. Schmitz N, Dreger P, Suttorp M, et al. Primary transplantation of allogeneic peripheral blood progenitor cells mobilized by filgrastim (granulocyte colony-stimulating factor) [see comments]. *Blood*. 1995;85(6):1666-1672.
13. Ferrara JLM, Deeg HJ. Graft-versus-Host Disease. *New England Journal of Medicine*. 1991;324(10):667-674.

14. Ferrara JL, Levine JE, Reddy P, Holler E. Graft-versus-host disease. *Lancet*. 2009;373(9674):1550-1561.
15. Billingham RE. The biology of graft-versus-host reactions. *Harvey Lectures*. 1966;62:21-78.
16. Klein J, Sato A. The HLA System. *New England Journal of Medicine*. 2000;343(10):702-709.
17. Shlomchik WD. Graft-versus-host disease. *Nature Reviews Immunology*. 2007;7(5):340-352.
18. Sullivan KM. Graft-vs.-Host Disease. Thomas' Hematopoietic Cell Transplantation: Blackwell Publishing Ltd; 2007:633-664.
19. Filipovich AH, Weisdorf D, Pavletic S, et al. National Institutes of Health Consensus Development Project on Criteria for Clinical Trials in Chronic Graft-versus-Host Disease: I. Diagnosis and Staging Working Group Report. *Biology of Blood and Marrow Transplantation*. 2005;11(12):945-956.
20. Beilhack A, Schulz S, Baker J, et al. In vivo analyses of early events in acute graft-versus-host disease reveal sequential infiltration of T-cell subsets. *Blood*. 2005;106(3):1113-1122.
21. Panoskaltsis-Mortari A, Price A, Hermanson JR, et al. In vivo imaging of graft-versus-host-disease in mice. *Blood*. 2004;103(9):3590-3598.
22. Miller MJ, Wei SH, Parker I, Cahalan MD. Two-photon imaging of lymphocyte motility and antigen response in intact lymph node. *Science*. 2002;296(5574):1869-1873.
23. Stoll S, Delon J, Brotz TM, Germain RN. Dynamic imaging of T cell-dendritic cell interactions in lymph nodes. *Science*. 2002;296(5574):1873-1876.
24. Murai M, Yoneyama H, Ezaki T, et al. Peyer's patch is the essential site in initiating murine acute and lethal graft-versus-host reaction. *Nature Immunology*. 2003;4(2):154-160.
25. Wysocki CA, Panoskaltsis-Mortari A, Blazar BR, Serody JS. Leukocyte migration and graft-versus-host disease. *Blood*. 2005;105(11):4191-4199.
26. Chakraverty R, Cote D, Buchli J, et al. An inflammatory checkpoint regulates recruitment of graft-versus-host reactive T cells to peripheral tissues. *The Journal of Experimental Medicine*. 2006;203(8):2021-2031.
27. Eyrich M, Burger G, Marquardt K, et al. Sequential expression of adhesion and costimulatory molecules in graft-versus-host disease target organs after murine bone marrow transplantation across minor histocompatibility antigen barriers. *Biology of Blood and Marrow Transplantation*. 2005;11(5):371-382.

28. Hallahan D, Kuchibhotla J, Wyble C. Cell adhesion molecules mediate radiation-induced leukocyte adhesion to the vascular endothelium. *Cancer Research*. 1996;56(22):5150-5155.
29. Charron DJ. Obituary: Jean Dausset (1916-2009). *Nature*. 2009;460(7253):338-338.
30. Dutton RW, Panfili PR, Swain SL. Alloreactivity, the development of the T cell repertoire and the understanding of T cell function. *Immunological Reviews*. 1978;42:20-59.
31. Vallera DA, Soderling CC, Carlson GJ, Kersey JH. Bone marrow transplantation across major histocompatibility barriers in mice. II. T cell requirement for engraftment in total lymphoid irradiation-conditioned recipients. *Transplantation*. 1982;33(3):243-248.
32. Korngold R, Sprent J. Lethal graft-versus-host disease after bone marrow transplantation across minor histocompatibility barriers in mice. Prevention by removing mature T cells from marrow. *The Journal of Experimental Medicine*. 1978;148(6):1687-1698.
33. Miyamoto T, Akashi K, Hayashi S, et al. Serum concentration of the soluble interleukin-2 receptor for monitoring acute graft-versus-host disease. *Bone Marrow Transplantation*. 1996;17(2):185-190.
34. Nakamura H, Komatsu K, Ayaki M, et al. Serum levels of soluble IL-2 receptor, IL-12, IL-18, and IFN- γ in patients with acute graft-versus-host disease after allogeneic bone marrow transplantation. *Journal of Allergy and Clinical Immunology*. 2000;106(1, Supplement):S45-S50.
35. Foley R, Couban S, Walker I, et al. Monitoring soluble interleukin-2 receptor levels in related and unrelated donor allogeneic bone marrow transplantation. *Bone Marrow Transplantation*. 1998;21(8):769-773.
36. Liem LM, van Houwelingen HC, Goulmy E. Serum cytokine levels after HLA-identical bone marrow transplantation. *Transplantation*. 1998;66(7):863-871.
37. Visentainer JEL, Lieber SR, Persoli LBL, et al. Serum cytokine levels and acute graft-versus-host disease after HLA-identical hematopoietic stem cell transplantation. *Experimental Hematology*. 2003;31(11):1044-1050.
38. Luft T, Conzelmann M, Benner A, et al. Serum cytokeratin-18 fragments as quantitative markers of epithelial apoptosis in liver and intestinal graft-versus-host disease. *Blood*. 2007;110(13):4535-4542.
39. Seidel C, Ringdén O, Remberger M. Increased levels of syndecan-1 in serum during acute graft-versus-host disease. *Transplantation*. 2003;76(2):423-426.
40. Paczesny S, Krijanovski OI, Braun TM, et al. A biomarker panel for acute graft-versus-host disease. *Blood*. 2009;113(2):273-278.

41. Paczesny S, Braun TM, Levine JE, et al. Elafin Is a Biomarker of Graft-Versus-Host Disease of the Skin. *Science Translational Medicine*. 2010;2(13):13ra12.
42. Ferrara JLM, Harris AC, Greenson JK, et al. Regenerating islet-derived 3-alpha is a biomarker of gastrointestinal graft-versus-host disease. *Blood*. 2011;118(25):6702-6708.
43. Levine JE, Logan BR, Wu J, et al. Acute graft-versus-host disease biomarkers measured during therapy can predict treatment outcomes: a Blood and Marrow Transplant Clinical Trials Network study. *Blood*. 2012.
44. Harris AC, Ferrara JLM, Braun TM, et al. Plasma biomarkers of lower gastrointestinal and liver acute GVHD. *Blood*. 2012;119(12):2960-2963.
45. Kaiser T, Kamal H, Rank A, et al. Proteomics applied to the clinical follow-up of patients after allogeneic hematopoietic stem cell transplantation. *Blood*. 2004;104(2):340-349.
46. Glucksberg H, Storb R, Fefer A, et al. Clinical manifestations of graft-versus-host disease in human recipients of marrow from HL-A-matched sibling donors. *Transplantation*. 1974;18(4):295-304.
47. Przepiorka D, Weisdorf D, Martin P, et al. 1994 Consensus Conference on Acute GVHD Grading. *Bone Marrow Transplantation*. 1995;15(6):825-828.
48. Rowlings PA, Przepiorka D, Klein JP, et al. IBMTR Severity Index for grading acute graft-versus-host disease: retrospective comparison with Glucksberg grade. *British Journal of Haematology*. 1997;97(4):855-864.
49. Storb R, Antin JH, Cutler C. Should Methotrexate plus Calcineurin Inhibitors Be Considered Standard of Care for Prophylaxis of acute Graft-versus-Host Disease? *Biology of Blood and Marrow Transplantation*. 2010;16(1, Supplement):S18-S27.
50. Liu J, Farmer Jr JD, Lane WS, Friedman J, Weissman I, Schreiber SL. Calcineurin is a common target of cyclophilin-cyclosporin A and FKBP-FK506 complexes. *Cell*. 1991;66(4):807-815.
51. MacMillan ML, Weisdorf DJ, Wagner JE, et al. Response of 443 patients to steroids as primary therapy for acute graft-versus-host disease: Comparison of grading systems. *Biology of Blood and Marrow Transplantation*. 2002;8(7):387-394.
52. Pidala J, Anasetti C. Glucocorticoid-Refractory Acute Graft-versus-Host Disease. *Biology of Blood and Marrow Transplantation*. 2010;16(11):1504-1518.
53. Arai S, Margolis J, Zahurak M, Anders V, Vogelsang GB. Poor outcome in steroid-refractory graft-versus-host disease with antithymocyte globulin treatment. *Biology of Blood and Marrow Transplantation*. 2002;8(3):155-160.

54. Dugan MJ, DeFor TE, Steinbuch M, Filipovich AH, Weisdorf DJ. ATG plus corticosteroid therapy for acute graft-versus-host disease: predictors of response and survival. *Annals of Hematology*. 1997;75(1-2):41-46.
55. Khoury H, Kashyap A, Adkins DR, et al. Treatment of steroid-resistant acute graft-versus-host disease with anti-thymocyte globulin. *Bone Marrow Transplantation*. 2001;27(10):1059-1064.
56. Deeg HJ, Blazar BR, Bolwell BJ, et al. Treatment of steroid-refractory acute graft-versus-host disease with anti-CD147 monoclonal antibody ABX-CBL. *Blood*. 2001;98(7):2052-2058.
57. Hebart H, Ehninger G, Schmidt H, et al. Treatment of steroid-resistant graft-versus-host disease after allogeneic bone marrow transplantation with anti-CD3/TCR monoclonal antibodies. *Bone Marrow Transplantation*. 1995;15(6):891-894.
58. Byers V, Henslee P, Kernan N, et al. Use of an anti-pan T-lymphocyte ricin A chain immunotoxin in steroid-resistant acute graft-versus-host disease. *Blood*. 1990;75(7):1426-1432.
59. Przepiora D, Kernan NA, Ippoliti C, et al. Daclizumab, a humanized anti-interleukin-2 receptor alpha chain antibody, for treatment of acute graft-versus-host disease. *Blood*. 2000;95(1):83-89.
60. Pidala J, Kim J, Field T, et al. Infliximab for Managing Steroid-Refractory Acute Graft-versus-Host Disease. *Biology of Blood and Marrow Transplantation*. 2009;15(9):1116-1121.
61. Busca A, Locatelli F, Marmont F, Ceretto C, Falda M. Recombinant human soluble tumor necrosis factor receptor fusion protein as treatment for steroid refractory graft-versus-host disease following allogeneic hematopoietic stem cell transplantation. *American Journal of Hematology*. 2007;82(1):45-52.
62. Ho VT, Zahrieh D, Hochberg E, et al. Safety and efficacy of denileukin diftitox in patients with steroid-refractory acute graft-versus-host disease after allogeneic hematopoietic stem cell transplantation. *Blood*. 2004;104(4):1224-1226.
63. Pidala J, Kim J, Perkins J, et al. Mycophenolate mofetil for the management of steroid-refractory acute graft vs host disease. *Bone Marrow Transplant*. 2010;45(5):919-924.
64. Ghez D, Rubio MT, Maillard N, et al. Rapamycin for Refractory Acute Graft-Versus-Host Disease. *Transplantation*. 2009;88(9):1081-1087
10.1097/TP.1080b1013e3181ba1080a1013.
65. Hoda D, Pidala J, Salgado-Vila N, et al. Sirolimus for treatment of steroid-refractory acute graft-versus-host disease. *Bone Marrow Transplant*. 2010;45(8):1347-1351.

66. Bolaños-Meade J, Jacobsohn DA, Margolis J, et al. Pentostatin in Steroid-Refractory Acute Graft-Versus-Host Disease. *Journal of Clinical Oncology*. 2005;23(12):2661-2668.
67. Greinix HT, Volc-Platzer B, Kalhs P, et al. Extracorporeal photochemotherapy in the treatment of severe steroid-refractory acute graft-versus-host disease: a pilot study. *Blood*. 2000;96(7):2426-2431.
68. Perfetti P, Carlier P, Strada P, et al. Extracorporeal photopheresis for the treatment of steroid refractory acute GVHD. *Bone Marrow Transplant*. 2008;42(9):609-617.
69. Meyers JD. Infection in Bone-Marrow Transplant Recipients. *American Journal of Medicine*. 1986;81(1A):27-38.
70. Liberman AC, Druker J, Garcia FA, Holsboer F, Arzt E. Intracellular Molecular Signaling. *Annals of the New York Academy of Sciences*. 2009;1153(1):6-13.
71. Amsterdam A, Sasson R. The anti-inflammatory action of glucocorticoids is mediated by cell type specific regulation of apoptosis. *Molecular and Cellular Endocrinology*. 2002;189(1-2):1-9.
72. Groth CG, Gahrton G, Lundgren G, et al. Successful treatment with prednisone and graft-versus-host disease in an allogeneic bone-marrow transplant recipient. *Scandinavian Journal of Haematology*. 1979;22(4):333-338.
73. Bouazzaoui A, Spacenko E, Mueller G, et al. Steroid treatment alters adhesion molecule and chemokine expression in experimental acute graft-vs.-host disease of the intestinal tract. *Experimental Hematology*. 2011;39(2):238-249 e231.
74. Showalter HD, Bunge RH, French JC, et al. Improved production of pentostatin and identification of fermentation cometabolites. *The Journal of Antibiotics (Tokyo)*. 1992;45(12):1914-1918.
75. Saven A, Piro L. Newer Purine Analogues for the Treatment of Hairy-Cell Leukemia. *New England Journal of Medicine*. 1994;330(10):691-697.
76. Epstein J, Bealmear PM, Kennedy DW, Herrmann MJ, Islam A, Wiedl SC. Prevention of graft-versus-host disease in allogeneic bone marrow transplantation by pretreatment with 2'-deoxycoformycin. *Experimental Hematology*. 1986;14(9):845-849.
77. Klein S, Mousset S, Bug G, Wassmann B, Martin H. Long-term follow-up of a phase II study of pentostatin in patients with steroid refractory acute intestinal graft-versus-host disease. *Bone Marrow Transplantation*. 2008;41:S223-S223.
78. Schmitt T, Luft T, Hegenbart U, Tran TH, Ho AD, Dreger P. Pentostatin for treatment of steroid-refractory acute GVHD: a retrospective single-center analysis. *Bone Marrow Transplantation*. 2011;46(4):580-585.

79. Vezina C, Kudelski A, Sehgal SN. Rapamycin (AY-22,989), a new antifungal antibiotic. I. Taxonomy of the producing streptomycete and isolation of the active principle. *The Journal of Antibiotics (Tokyo)*. 1975;28(10):721-726.
80. Sehgal SN, Baker H, Vezina C. Rapamycin (AY-22,989), a new antifungal antibiotic. II. Fermentation, isolation and characterization. *J Antibiot (Tokyo)*. 1975;28(10):727-732.
81. Calne RY, Collier DS, Lim S, et al. Rapamycin for immunosuppression in organ allografting. *Lancet*. 1989;2(8656):227.
82. Terada N, Takase K, Papst P, Nairn AC, Gelfand EW. Rapamycin inhibits ribosomal protein synthesis and induces G1 prolongation in mitogen-activated T lymphocytes. *Journal of Immunology*. 1995;155(7):3418-3426.
83. Sehgal SN. Rapamune (RAPA, rapamycin, sirolimus): mechanism of action immunosuppressive effect results from blockade of signal transduction and inhibition of cell cycle progression. *Clinical Biochemistry*. 1998;31(5):335-340.
84. Bjornsti MA, Houghton PJ. The TOR pathway: a target for cancer therapy. *Nature Review Cancer*. 2004;4(5):335-348.
85. Blazar BR, Taylor PA, Snover DC, Sehgal SN, Valleria DA. Murine recipients of fully mismatched donor marrow are protected from lethal graft-versus-host disease by the in vivo administration of rapamycin but develop an autoimmune-like syndrome. *Journal of Immunology*. 1993;151(10):5726-5741.
86. Antin JH, Kim HT, Cutler C, et al. Sirolimus, tacrolimus, and low-dose methotrexate for graft-versus-host disease prophylaxis in mismatched related donor or unrelated donor transplantation. *Blood*. 2003;102(5):1601-1605.
87. Cutler C, Kim HT, Hochberg E, et al. Sirolimus and tacrolimus without methotrexate as graft-versus-host disease prophylaxis after matched related donor peripheral blood stem cell transplantation. *Biology of Blood and Marrow Transplantation*. 2004;10(5):328-336.
88. Benito AI, Furlong T, Martin PJ, et al. Sirolimus (rapamycin) for the treatment of steroid-refractory acute graft-versus-host disease. *Transplantation*. 2001;72(12):1924-1929.
89. Khan SA, Moreb JS. Reversal of severe graft-versus-host disease after nonmyeloablative matched unrelated donor stem cell transplant by infusion of backup autologous peripheral blood stem cells. *Bone Marrow Transplant*. 2005;36(3):267-268.
90. Butcher EC, Picker LJ. Lymphocyte homing and homeostasis. *Science*. 1996;272(5258):60-66.
91. Springer TA. Traffic signals for lymphocyte recirculation and leukocyte emigration: The multistep paradigm. *Cell*. 1994;76(2):301-314.

92. Johnson-Léger C, Imhof B. Forging the endothelium during inflammation: pushing at a half-open door? *Cell and Tissue Research*. 2003;314(1):93-105.
93. Campbell JJ, Hedrick J, Zlotnik A, Siani MA, Thompson DA, Butcher EC. Chemokines and the Arrest of Lymphocytes Rolling Under Flow Conditions. *Science*. 1998;279(5349):381-384.
94. Kansas G. Selectins and their ligands: current concepts and controversies. *Blood*. 1996;88(9):3259-3287.
95. Jung TM, Gallatin WM, Weissman IL, Dailey MO. Down-regulation of homing receptors after T cell activation. *The Journal of Immunology*. 1988;141(12):4110-4117.
96. Muller G, Reiterer P, Hopken UE, Golfier S, Lipp M. Role of homeostatic chemokine and sphingosine-1-phosphate receptors in the organization of lymphoid tissue. *Annals of the New York Academy of Science*. 2003;987:107-116.
97. Pribila JT, Quale AC, Mueller KL, Shimizu Y. Integrins and T Cell-Mediated Immunity. *Annual Review of Immunology*. 2004;22(1):157-180.
98. Plow EF, Haas TA, Zhang L, Loftus J, Smith JW. Ligand Binding to Integrins. *Journal of Biological Chemistry*. 2000;275(29):21785-21788.
99. Waldman E, Lu SX, Hubbard VM, et al. Absence of $\beta 7$ integrin results in less graft-versus-host disease because of decreased homing of alloreactive T cells to intestine. *Blood*. 2006;107(4):1703-1711.
100. Rollins BJ. Chemokines. *Blood*. 1997;90(3):909-928.
101. Moser B, Wolf M, Walz A, Loetscher P. Chemokines: multiple levels of leukocyte migration control. *Trends in Immunology*. 2004;25(2):75-84.
102. Ley K, Kansas GS. Selectins in T-cell recruitment to non-lymphoid tissues and sites of inflammation. *Nature Reviews Immunology*. 2004;4(5):325-336.
103. Beilhack A, Schulz S, Baker J, et al. Prevention of acute graft-versus-host disease by blocking T-cell entry to secondary lymphoid organs. *Blood*. 2008;111(5):2919-2928.
104. Campbell DJ, Butcher EC. Rapid Acquisition of Tissue-specific Homing Phenotypes by CD4+ T Cells Activated in Cutaneous or Mucosal Lymphoid Tissues. *The Journal of Experimental Medicine*. 2002;195(1):135-141.
105. El-Asady R, Yuan R, Liu K, et al. TGF- β -dependent CD103 expression by CD8+ T cells promotes selective destruction of the host intestinal epithelium during graft-versus-host disease. *The Journal of Experimental Medicine*. 2005;201(10):1647-1657.

106. Kunkel EJ, Campbell JJ, Haraldsen G, et al. Lymphocyte Cc Chemokine Receptor 9 and Epithelial Thymus-Expressed Chemokine (Teck) Expression Distinguish the Small Intestinal Immune Compartment. *The Journal of Experimental Medicine*. 2000;192(5):761-768.
107. Agace WW. T-cell recruitment to the intestinal mucosa. *Trends in Immunology*. 2008;29(11):514-522.
108. Petrovic A, Alpdogan O, Willis LM, et al. LPAM (alpha 4 beta 7 integrin) is an important homing integrin on alloreactive T cells in the development of intestinal graft-versus-host disease. *Blood*. 2004;103(4):1542-1547.
109. Lesley J, Hyman R, Kincade PW. CD44 and its interaction with extracellular matrix. *Advances in Immunology*. 1993;54:271-335.
110. DeGrendele HC, Estess P, Siegelman MH. Requirement for CD44 in Activated T Cell Extravasation into an Inflammatory Site. *Science*. 1997;278(5338):672-675.
111. Lu SX, Holland AM, Na I-K, et al. Absence of P-Selectin in Recipients of Allogeneic Bone Marrow Transplantation Ameliorates Experimental Graft-versus-Host Disease. *The Journal of Immunology*. 2010;185(3):1912-1919.
112. Terwey TH, Kim TD, Kochman AA, et al. CCR2 is required for CD8-induced graft-versus-host disease. *Blood*. 2005;106(9):3322-3330.
113. Charo IF, Peters W. Chemokine Receptor 2 (CCR2) in Atherosclerosis, Infectious Diseases, and Regulation of T-Cell Polarization. *Microcirculation*. 2003;10(3-4):259-264.
114. Murai M, Yoneyama H, Harada A, et al. Active participation of CCR5(+)CD8(+) T lymphocytes in the pathogenesis of liver injury in graft-versus-host disease. *The Journal of Clinical Investigation*. 1999;104(1):49-57.
115. Kunkel EJ, Boisvert J, Murphy K, et al. Expression of the Chemokine Receptors CCR4, CCR5, and CXCR3 by Human Tissue-Infiltrating Lymphocytes. *The American Journal of Pathology*. 2002;160(1):347-355.
116. Coghill JM, Carlson MJ, Panoskaltsis-Mortari A, et al. Separation of graft-versus-host disease from graft-versus-leukemia responses by targeting CC-chemokine receptor 7 on donor T cells. *Blood*. 2010;115(23):4914-4922.
117. Förster R, Schubel A, Breitfeld D, et al. CCR7 Coordinates the Primary Immune Response by Establishing Functional Microenvironments in Secondary Lymphoid Organs. *Cell*. 1999;99(1):23-33.
118. Duffner U, Lu B, Hildebrandt GC, et al. Role of CXCR3-induced donor T-cell migration in acute GVHD. *Experimental Hematology*. 2003;31(10):897-902.

119. Cao Y-A, Wagers AJ, Beilhack A, et al. Shifting foci of hematopoiesis during reconstitution from single stem cells. *Proceedings of the National Academy of Sciences of the United States of America*. 2004;101(1):221-226.
120. Zeiser R, Leveson-Gower DB, Zambricki EA, et al. Differential impact of mammalian target of rapamycin inhibition on CD4+CD25+Foxp3+ regulatory T cells compared with conventional CD4+ T cells. *Blood*. 2008;111(1):453-462.
121. Herzenberg LA, Tung J, Moore WA, Herzenberg LA, Parks DR. Interpreting flow cytometry data: a guide for the perplexed. *Nature Immunology*. 2006;7(7):681-685.
122. Tung JW, Heydari K, Tirouvanziam R, et al. Modern Flow Cytometry: A Practical Approach. *Clinics in Laboratory Medicine*. 2007;27(3):453-468.
123. Betts MR, Koup RA. Detection of T-cell degranulation: CD107a and b. *Methods in Cell Biology*. 2004;75:497-512.
124. Betts MR, Brenchley JM, Price DA, et al. Sensitive and viable identification of antigen-specific CD8+ T cells by a flow cytometric assay for degranulation. *Journal of Immunological Methods*. 2003;281(1-2):65-78.
125. Lerner KG, Kao GF, Storb R, Buckner CD, Clift RA, Thomas ED. Histopathology of graft-vs.-host reaction (GvHR) in human recipients of marrow from HL-A-matched sibling donors. *Transplantation proceedings*. 1974;6(4):367-371.
126. Korngold R. Biology of Graft-vs.-Host Disease. *Journal of Pediatric Hematology/Oncology*. 1993;15(1):18-27.
127. Morishima Y, Sasazuki T, Inoko H, et al. The clinical significance of human leukocyte antigen (HLA) allele compatibility in patients receiving a marrow transplant from serologically HLA-A, HLA-B, and HLA-DR matched unrelated donors. *Blood*. 2002;99(11):4200-4206.
128. Warren EH, Zhang XC, Li S, et al. Effect of MHC and non-MHC donor/recipient genetic disparity on the outcome of allogeneic HCT. *Blood*. 2012;120(14):2796-2806.
129. Schwarer AP, Jiang YZ, Deacock S, et al. Comparison of helper and cytotoxic antirecipient T cell frequencies in unrelated bone marrow transplantation. *Transplantation*. 1994;58(11):1198-1203.
130. Kircher B, Niederwieser D, GÄChter A, et al. T-cell precursor frequencies and long-term outcome following unrelated hematopoietic stem cell transplantation. *International Journal of Laboratory Hematology*. 2008;30(6):499-507.
131. Saliba RM, Komanduri K, Giralt S, et al. 269: Correlates and outcome of absolute lymphocyte count (ALC) on day 30 post allogeneic stem cell transplantation (SCT) for treatment of AML. *Biology of Blood and Marrow Transplantation*. 2007;13(2):98.

132. Savani BN, Mielke S, Rezvani K, et al. Absolute Lymphocyte Count on Day 30 Is a Surrogate for Robust Hematopoietic Recovery and Strongly Predicts Outcome after T Cell-Depleted Allogeneic Stem Cell Transplantation. *Biology of Blood and Marrow Transplantation*. 2007;13(10):1216-1223.
133. Tedeschi SK, Jagasia M, Engelhardt BG, et al. Early lymphocyte reconstitution is associated with improved transplant outcome after cord blood transplantation. *Cytherapy*. 2011;13(1):78-82.
134. Sprent J, Korngold R. T cell subsets controlling graft-v-host disease in mice. *Transplantation Proceedings*. 1987;19(6 Suppl 7):41-47.
135. Korngold R, Leighton C, Mobraaten LE, Berger MA. Inter-strain graft-vs.-host disease T-cell responses to immunodominant minor histocompatibility antigens. *Biology of Blood and Marrow Transplantation*. 1997;3(2):57-64.
136. Brochu S, Baron C, Héту F, Roy DC, Perreault C. Oligoclonal expansion of CTLs directed against a restricted number of dominant minor histocompatibility antigens in hemopoietic chimeras. *The Journal of Immunology*. 1995;155(11):5104-5114.
137. Perreault C, Roy DC, Fortin C. Immunodominant minor histocompatibility antigens: the major ones. *Immunology Today*. 1998;19(2):69-74.
138. Lehmann PV, Sercarz EE, Forsthuber T, Dayan CM, Gammon G. Determinant spreading and the dynamics of the autoimmune T-cell repertoire. *Immunology Today*. 1993;14(5):203-208.
139. Vincent A, Willcox N, Hill M, Curnow J, MacLennan C, Beeson D. Determinant spreading and immune responses to acetylcholine receptors in myasthenia gravis. *Immunological Reviews*. 1998;164:157-168.
140. Moudgil KD, Chang TT, Eradat H, et al. Diversification of T Cell Responses to Carboxy-terminal Determinants within the 65-kD Heat-shock Protein Is Involved in Regulation of Autoimmune Arthritis. *The Journal of Experimental Medicine*. 1997;185(7):1307-1316.
141. Vanderlugt CL, Neville KL, Nikceovich KM, Eagar TN, Bluestone JA, Miller SD. Pathologic Role and Temporal Appearance of Newly Emerging Autoepitopes in Relapsing Experimental Autoimmune Encephalomyelitis. *The Journal of Immunology*. 2000;164(2):670-678.
142. Russell JH. Activation-induced death of mature T cells in the regulation of immune responses. *Current Opinion in Immunology*. 1995;7(3):382-388.
143. van Parijs L, Abbas AK. Role of Fas-mediated cell death in the regulation of immune responses. *Current Opinion in Immunology*. 1996;8(3):355-361.

144. van den Brink MR, Moore E, Horndasch KJ, Crawford JM, Murphy GF, Burakoff SJ. Fas ligand-deficient gld mice are more susceptible to graft-versus-host-disease. *Transplantation*. 2000;70(1):184-191.
145. Cohen JL, Boyer O. The role of CD4+CD25hi regulatory T cells in the physiopathogeny of graft-versus-host disease. *Current Opinion in Immunology*. 2006;18(5):580-585.
146. Nguyen VH, Zeiser R, Dasilva DL, et al. In vivo dynamics of regulatory T-cell trafficking and survival predict effective strategies to control graft-versus-host disease following allogeneic transplantation. *Blood*. 2007;109(6):2649-2656.
147. Taylor PA, Lees CJ, Blazar BR. The infusion of ex vivo activated and expanded CD4(+)CD25(+) immune regulatory cells inhibits graft-versus-host disease lethality. *Blood*. 2002;99(10):3493-3499.
148. Hoffmann P, Ermann J, Edinger M, Fathman CG, Strober S. Donor-type CD4(+)CD25(+) regulatory T cells suppress lethal acute graft-versus-host disease after allogeneic bone marrow transplantation. *The Journal of Experimental Medicine*. 2002;196(3):389-399.
149. Serafini P, Borrello I, Bronte V. Myeloid suppressor cells in cancer: Recruitment, phenotype, properties, and mechanisms of immune suppression. *Seminars in Cancer Biology*. 2006;16(1):53-65.
150. Movahedi K, Guillems M, Van den Bossche J, et al. Identification of discrete tumor-induced myeloid-derived suppressor cell subpopulations with distinct T cell-suppressive activity. *Blood*. 2008;111(8):4233-4244.
151. Youn J-I, Nagaraj S, Collazo M, Gajilovich DI. Subsets of Myeloid-Derived Suppressor Cells in Tumor-Bearing Mice. *The Journal of Immunology*. 2008;181(8):5791-5802.
152. Luyckx A, Schoupe E, Rutgeerts O, et al. Subset characterization of myeloid-derived suppressor cells arising during induction of BM chimerism in mice. *Bone Marrow Transplant*. 2012;47(7):985-992.
153. Highfill SL, Rodriguez PC, Zhou Q, et al. Bone marrow myeloid-derived suppressor cells (MDSCs) inhibit graft-versus-host disease (GVHD) via an arginase-1-dependent mechanism that is up-regulated by interleukin-13. *Blood*. 2010;116(25):5738-5747.
154. Fallarino F, Grohmann U, Vacca C, et al. T cell apoptosis by tryptophan catabolism. *Cell Death and Differentiation*. 2002;9(10):1069-1077.
155. Jaspersen LK, Bucher C, Panoskaltsis-Mortari A, et al. Indoleamine 2,3-dioxygenase is a critical regulator of acute graft-versus-host disease lethality. *Blood*. 2008;111(6):3257-3265.

156. Reddy P, Sun Y, Toubai T, et al. Histone deacetylase inhibition modulates indoleamine 2,3-dioxygenase-dependent DC functions and regulates experimental graft-versus-host disease in mice. *The Journal of Clinical Investigation*. 2008;118(7):2562-2573.
157. Ratajczak P, Janin A, Peffault de Larour R, et al. IDO in human gut graft-versus-host disease. *Biology of Blood and Marrow Transplantation*. 2012;18(1):150-155.
158. Dutt S, Ermann J, Tseng D, et al. L-selectin and beta7 integrin on donor CD4 T cells are required for the early migration to host mesenteric lymph nodes and acute colitis of graft-versus-host disease. *Blood*. 2005;106(12):4009-4015.
159. Chen YB, Kim HT, McDonough S, et al. Up-Regulation of alpha4beta7 integrin on peripheral T cell subsets correlates with the development of acute intestinal graft-versus-host disease following allogeneic stem cell transplantation. *Biology of Blood and Marrow Transplantation*. 2009;15(9):1066-1076.
160. Chen YB, McDonough S, Chen H, et al. Expression of alpha4beta7 integrin on memory CD8(+) T cells at the presentation of acute intestinal GVHD. *Bone Marrow Transplantation*. 2012.
161. Engelhardt BG, Jagasia M, Savani BN, et al. Regulatory T cell expression of CLA or alpha(4)beta(7) and skin or gut acute GVHD outcomes. *Bone Marrow Transplantation*. 2011;46(3):436-442.
162. Eom H-S, Rubio M-T, Means TK, Luster AD, Sykes M. T-cell P/E-selectin ligand $\alpha(1,3)$ fucosylation is not required for graft-vs-host disease induction. *Experimental Hematology*. 2005;33(12):1564-1573.
163. Asaduzzaman M, Mihaescu A, Wang Y, Sato T, Thorlacius H. P-Selectin and P-Selectin Glycoprotein Ligand 1 Mediate Rolling of Activated CD8+ T Cells in Inflamed Colonic Venules. *Journal of Investigative Medicine*. 2009;57(7):765-768 710.231/JIM.760b013e3181b3918fb.
164. Chen BJ, Cui X, Sempowski GD, Liu C, Chao NJ. Transfer of allogeneic CD62L- memory T cells without graft-versus-host disease. *Blood*. 2004;103(4):1534-1541.
165. Anderson BE, McNiff J, Yan J, et al. Memory CD4+ T cells do not induce graft-versus-host disease. *The Journal of Clinical Investigation*. 2003;112(1):101-108.
166. Zinocker S, Sviland L, Dressel R, Rolstad B. Kinetics of lymphocyte reconstitution after allogeneic bone marrow transplantation: markers of graft-versus-host disease. *Journal of Leukocyte Biology*. 2011;90(1):177-187.
167. Sallusto F, Kremmer E, Palermo B, et al. Switch in chemokine receptor expression upon TCR stimulation reveals novel homing potential for recently activated T cells. *European Journal of Immunology*. 1999;29(6):2037-2045.

168. Mapara MY, Leng C, Kim Y-M, et al. Expression of Chemokines in GVHD Target Organs Is Influenced by Conditioning and Genetic Factors and Amplified by GVHR. *Biology of Blood and Marrow Transplantation*. 2006;12(6):623-634.
169. Chen J, Vistica BP, Takase H, et al. A unique pattern of up- and down-regulation of chemokine receptor CXCR3 on inflammation-inducing Th1 cells. *European Journal of Immunology*. 2004;34(10):2885-2894.
170. Munoz LM, Holgado BL, Martinez AC, Rodriguez-Frade JM, Mellado M. Chemokine receptor oligomerization: a further step toward chemokine function. *Immunology Letters Journal*. 2012;145(1-2):23-29.
171. He S, Cao Q, Qiu Y, et al. A New Approach to the Blocking of Alloreactive T Cell-Mediated Graft-versus-Host Disease by In Vivo Administration of Anti-CXCR3 Neutralizing Antibody. *The Journal of Immunology*. 2008;181(11):7581-7592.
172. Reshef R, Luger SM, Hexner EO, et al. Blockade of Lymphocyte Chemotaxis in Visceral Graft-versus-Host Disease. *New England Journal of Medicine*. 2012;367(2):135-145.
173. Siegelman MH, DeGrendele HC, Estess P. Activation and interaction of CD44 and hyaluronan in immunological systems. *Journal of Leukocyte Biology*. 1999;66(2):315-321.
174. Dutt S, Baker J, Kohrt HE, et al. CD8+CD44(hi) but not CD4+CD44(hi) memory T cells mediate potent graft antilymphoma activity without GVHD. *Blood*. 2011;117(11):3230-3239.
175. Sancho D, Gomez M, Sanchez-Madrid F. CD69 is an immunoregulatory molecule induced following activation. *Trends in Immunology*. 2005;26(3):136-140.
176. Martin P, Gomez M, Lamana A, et al. CD69 association with Jak3/Stat5 proteins regulates Th17 cell differentiation. *Molecular and Cellular Biology*. 2010;30(20):4877-4889.
177. Martin P, Sanchez-Madrid F. CD69: an unexpected regulator of TH17 cell-driven inflammatory responses. *Science Signaling*. 2011;4(165):pe14.
178. Han Y, Guo Q, Zhang M, Chen Z, Cao X. CD69+ CD4+ CD25- T cells, a new subset of regulatory T cells, suppress T cell proliferation through membrane-bound TGF-beta 1. *Journal of Immunology*. 2009;182(1):111-120.
179. Feng C, Woodside KJ, Vance BA, et al. A potential role for CD69 in thymocyte emigration. *International Immunology*. 2002;14(6):535-544.
180. Shioh LR, Rosen DB, Brdickova N, et al. CD69 acts downstream of interferon-alpha/beta to inhibit S1P1 and lymphocyte egress from lymphoid organs. *Nature*. 2006;440(7083):540-544.

181. D'Souza WN, Schluns KS, Masopust D, Lefrançois L. Essential Role for IL-2 in the Regulation of Antiviral Extralymphoid CD8 T Cell Responses. *The Journal of Immunology*. 2002;168(11):5566-5572.
182. Pipkin ME, Sacks JA, Cruz-Guilloty F, Lichtenheld MG, Bevan MJ, Rao A. Interleukin-2 and inflammation induce distinct transcriptional programs that promote the differentiation of effector cytolytic T cells. *Immunity*. 2010;32(1):79-90.
183. Fontenot JD, Rasmussen JP, Gavin MA, Rudensky AY. A function for interleukin 2 in Foxp3-expressing regulatory T cells. *Nature Immunology*. 2005;6(11):1142-1151.
184. Robb RJ, Lineburg KE, Kuns RD, et al. Identification and expansion of highly suppressive CD8(+)FoxP3(+) regulatory T cells after experimental allogeneic bone marrow transplantation. *Blood*. 2012;119(24):5898-5908.
185. Ruutu T, Hermans J, van Biezen A, Niederwieser D, Gratwohl A, Apperley JF. How should corticosteroids be used in the treatment of acute GVHD? EBMT Chronic Leukemia Working Party. European Group for Blood and Marrow Transplantation. *Bone Marrow Transplant*. 1998;22(6):614-615.
186. Ancin I, Ferra C, Gallardo D, et al. Do corticosteroids add any benefit to standard GVHD prophylaxis in allogeneic BMT? *Bone Marrow Transplant*. 2001;28(1):39-45.
187. Storb R, Pepe M, Anasetti C, et al. What role for prednisone in prevention of acute graft-versus-host disease in patients undergoing marrow transplants? *Blood*. 1990;76(5):1037-1045.
188. D'Costa S, Hurwitz JL. Antibody and pre- plus post-transplant prednisone treatments support T cell-depleted stem cell engraftment without drug-induced morbidity. *Bone Marrow Transplant*. 2002;29(7):553-556.
189. Brown JB, Lee G, Grimm GR, Barrett TA. Therapeutic benefit of pentostatin in severe IL-10^{-/-} colitis. *Inflammatory Bowel Disease*. 2008;14(7):880-887.
190. Chen BJ, Morris RE, Chao NJ. Graft-versus-host disease prevention by rapamycin: Cellular mechanisms. *Biology of Blood and Marrow Transplantation*. 2000;6(5A):529-536.
191. Hackstein H, Taner T, Zahorchak AF, et al. Rapamycin inhibits IL-4--induced dendritic cell maturation in vitro and dendritic cell mobilization and function in vivo. *Blood*. 2003;101(11):4457-4463.
192. Monti P, Mercurio A, Leone BE, Valerio DC, Allavena P, Piemonti L. Rapamycin impairs antigen uptake of human dendritic cells. *Transplantation*. 2003;75(1):137-145.

193. Chiang PH, Wang L, Liang Y, et al. Inhibition of IL-12 signaling Stat4/IFN-gamma pathway by rapamycin is associated with impaired dendritic cell function. *Transplantation Proceedings*. 2002;34(5):1394-1395.
194. Wang GY, Chen GH, Li H, et al. Rapamycin-treated mature dendritic cells have a unique cytokine secretion profile and impaired allostimulatory capacity. *Transplant International*. 2009;22(10):1005-1016.
195. Koyama M, Kuns RD, Olver SD, et al. Recipient nonhematopoietic antigen-presenting cells are sufficient to induce lethal acute graft-versus-host disease. *Nature Medicine*. 2012;18(1):135-142.
196. Markey KA, Banovic T, Kuns RD, et al. Conventional dendritic cells are the critical donor APC presenting alloantigen after experimental bone marrow transplantation. *Blood*. 2009;113(22):5644-5649.
197. Iwata M, Hirakiyama A, Eshima Y, Kagechika H, Kato C, Song SY. Retinoic acid imprints gut-homing specificity on T cells. *Immunity*. 2004;21(4):527-538.
198. Koenecke C, Prinz I, Bubke A, et al. Shift of graft-versus-host-disease target organ tropism by dietary vitamin A. *PLoS One*. 2012;7(5):e38252.
199. Zimmerman J, Kahan B. Pharmacokinetics of sirolimus in stable renal transplant patients after multiple oral dose administration. *The Journal of Clinical Pharmacology*. 1997;37(5):405-415.

9. Appendix

9.1 List of figures

FIGURE 1: PATHOPHYSIOLOGY OF AGVHD	5
FIGURE 2: T CELL HOMING TO THE LAMINA PROPRIA	11
FIGURE 3: PRIOR AND POST ENRICHMENT FACS ANALYSIS.....	15
FIGURE 4: PRIOR AND POST DEPLETION FACS ANALYSIS.....	16
FIGURE 5: TITRATION ROW FOR AN ANTI-A4B7 INTEGRIN ANTIBODY	20
FIGURE 6: COMPENSATION ROW FOR A 6 COLOR FACS ANALYSIS USING COMPBEADS.....	22
FIGURE 7: FMO GATING EXAMPLE.....	23
FIGURE 8: PHENOTYPING GATING EXAMPLE	24
FIGURE 9: SURVIVAL, WEIGHT CHANGE AND CLINICAL AGVHD SCORING OF REPRESENTATIVE EXPERIMENTS .	28
FIGURE 10: AGVHD SCORING ON DAYS+6 AND +21 AFTER HCT	29
FIGURE 11: DONOR T CELL INFILTRATION OF THE SMALL BOWEL.....	30
FIGURE 12: DONOR T CELL INFILTRATION OF THE LARGE BOWEL	31
FIGURE 13: QUANTIFICATION OF TARGET ORGAN INFILTRATING DONOR T CELLS.....	32
FIGURE 14: DAILY IN VIVO BLI.....	35
FIGURE 15: VENTRAL AND LATERAL VIEWS OF REPRESENTATIVE MICE	36
FIGURE 16: DAILY MEASUREMENT OF DONOR T CELLS IN THE PB.....	38
FIGURE 17: CD107 DEGRANULATION ASSAY TO PROOF ALLOREACTIVITY OF PB DONOR T CELLS	40
FIGURE 18: EX VIVO BLI OF TARGET ORGANS AND PARENCHYMAL TISSUES	42
FIGURE 19: QUANTIFICATION OF EX VIVO BLI SIGNALS AT INDICATED TIME POINTS AFTER HCT	43

9 Appendix

FIGURE 20: PROPOSAL OF A POTENTIAL DIAGNOSTIC WINDOW BASED ON DONOR T CELL MIGRATION KINETICS	44
FIGURE 21: REPRESENTATIVE FACS BLOTS OF HOMING RECEPTOR ANALYSES AT IMPORTANT TIME POINTS ...	45
FIGURE 22: A4B7 INTEGRIN EXPRESSION ON PB DONOR T CELLS DAILY AFTER HCT	47
FIGURE 23: P-SELECTIN LIGAND EXPRESSION ON PB DONOR T CELLS DAILY AFTER HCT	48
FIGURE 24: L-SELECTIN AND E-SELECTIN LIGAND EXPRESSION ON PB CD8 ⁺ T CELLS.....	49
FIGURE 25: CXCR3 EXPRESSION ON PB DONOR T CELLS DAILY AFTER HCT	51
FIGURE 26: CHEMOKINE RECEPTOR EXPRESSION ON PB CD8 ⁺ DONOR T CELLS DAILY AFTER HCT	52
FIGURE 27: ACTIVATION MARKER EXPRESSION ON PB CD8 ⁺ DONOR T CELLS.....	53
FIGURE 28: PREDNISOLONE TREATMENT AFTER MIHAG MISMATCH ALLO-HCT	56
FIGURE 29: PENTOSTATIN TREATMENT AFTER MIHAG MISMATCH ALLO-HCT	58
FIGURE 30: RAPAMYCIN TREATMENT AFTER MIHAG MISMATCH ALLO-HCT	60
FIGURE 31: EX VIVO BLI OF LYMPHOID AND TARGET ORGANS AFTER RAPAMYCIN TREATMENT	62
FIGURE 32: FOXP3 EXPRESSION IN LYMPH NODES AFTER RAPAMYCIN TREATMENT.....	63
FIGURE 33: SINGLE SHOTS OF RAPAMYCIN AFTER MIHAG MISMATCH ALLO-HCT	64

9.2 List of tables

TABLE 1: ANTIBODIES USED FOR FC AND IFM	20
TABLE 2: SYNTHETIC PROTEINS	21
TABLE 3: SECONDARY REAGENTS	21

9.3 Acknowledgement

First of all I would like to thank Dr. Andreas Beilhack for giving me the opportunity to perform my PhD thesis under his supervision. I am very grateful for his support, his encouragement, all the stimulating discussions, and the freedom he gave me for performing my experiments. All this was fundamental for overcoming the challenges which appeared during the course of this work.

I am very thankful to all the members of the Beilhack laboratory for providing a very nice working atmosphere throughout the last four and a half years, for helpful and constructive discussions and for helping me with time consuming experiments. I especially appreciate the friendships that developed and the good times we had, also outside of the lab.

In addition, I would like to thank Dr. Martin Chopra for proof-reading my thesis and all the helpful corrections and suggestions.

Thanks to the members of my Supervisory Committee Prof. Hermann Einsele, Prof. Harald Wajant and Prof. Tor Stuge for inspiring contributions and discussions to my work.

Special thanks goes to Prof. Tor Stuge for giving me the opportunity to spend two interesting weeks in his laboratory in Tromsø and for introducing me to the method of single cell sorting.

I also would like to thank the organizers of the Graduate College Immunomodulation, especially Prof. Thomas Hünig and Eliza Monzón Casanova, for the possibility to exchange knowledge between graduate students and project leaders. The meetings and retreats were very constructive and joyful.

Thanks to the Wilhelm-Sander-Stiftung and the Deutsche José Carreras Leukämie-Stiftung for financially supporting my research.

Finally, I want to thank my family and friends for their love and support throughout the years. Without the encouragement and support of my parents and sister this would not have been possible to achieve.

9.4 Curriculum Vitae

Carina Annette Bäuerlein

University Hospital Würzburg
Medical Clinic II
Experimental Stem Cell Transplantation
Zinklesweg 10, ZEMM
97078 Würzburg
Phone: +49 (0)931 201 27637
email: Baeuerlein_C@medizin.uni-wuerzburg.de

Personal Information:

Date of birth:
Place of birth: Würzburg
Nationality: German

Education:

Since Apr 2008	PhD in experimental stem cell transplantation at the Medical Clinic II, Würzburg University Hospital, Würzburg, Germany Supervisor: Dr. Andreas Beilhack <u>Thesis title:</u> Identification of new predictive markers for an imminent acute Graft-versus-Host Disease
Jan 2008 – Mar 2008	Research assistant at the Medical Clinic II, Würzburg University Hospital, Würzburg, Germany Supervisor: PD Dr. rer. nat. Jürgen Löffler
Mar 2007 – Dec 2007	Diploma thesis in molecular hematology at the Medical Clinic II, Würzburg University Hospital, Würzburg, Germany Supervisor: PD Dr. rer. nat. Jürgen Löffler <u>Thesis title:</u> Analysis of the interaction of recombinant proteins and peptides of <i>Aspergillus fumigatus</i> with human antigen presenting cells.
Oct 2002 – Mar 2007	Graduate in Biology, specialized in Microbiology, Genetics and Biochemistry at the University of Würzburg, Germany

Publications:

C.A. Bäuerlein, S.S. Riedel, J. Baker, C. Brede, A.L. Jordán Garrote, M. Chopra, M. Ritz, G.F. Beilhack, S. Schulz, R. Zeiser, P.G. Schlegel, H. Einsele, R.S. Negrin, and A. Beilhack, *A diagnostic window for the treatment of acute GVHD prior to visible symptoms in a murine model*. Under Review.

S.S. Riedel, A. Mottok, C. Brede, **C.A. Bäuerlein**, A.L. Jordán Garrote, M. Ritz, K. Mattenheimer, A. Rosenwald, H. Einsele, B. Bogen, and A. Beilhack, *Non-invasive imaging provides spatiotemporal information on disease progression and response to therapy in a murine model of multiple myeloma*. PLOSOne, in press.

C. Brede, M. Friedrich, A.L. Jordán Garrote, S.S. Riedel, **C.A. Bäuerlein**, K.G. Heinze, T. Bopp, S. Schulz, A. Mottok, C. Kiesel, K. Mattenheimer, M. Ritz, V. von Krosigk, A. Rosenwald, H. Einsele, R.S. Negrin, G.S. Harms, and A. Beilhack, *Mapping Immune Processes in Intact Tissues at cellular Resolution*. *Journal of Clinical Investigation*, 2012. 122(12): 4439-46.

M. Ok, J.P. Latge, **C.A. Bäuerlein**, F. Ebel, M. Mezger, M. Topp, O. Kurzai, D. Killian, M. Kapp, G.U. Grigoleit, H. Sennefelder, J. Arroyo, H. Einsele, and J. Loeffler, *Immune Responses of Human Immature Dendritic Cells Can Be Modulated by the Recombinant Aspergillus fumigatus Antigen Asp1*. *Clinical and Vaccine Immunology*, 2009. **16**(10): p. 1485-1492.

Stipends and Grants:

Apr 2012 – Mar 2013	Stipend of the Deutsche José Carreras Leukämie-Stiftung
Dec 2010	Travel Award of the American Society of Hematology to attend their annual meeting in Orlando, FL, USA

Participation in Scientific Conferences:

14 – 17 Jun 2012:	17 th Congress of the European Hematology Association (EHA), Amsterdam, Netherlands <u>Talk:</u> Distinct receptor profile defines alloreactive T cells before GVHD onset
14 – 15 Mar 2011:	6 th International Symposium on Cellular Therapy, Erlangen, Germany <u>Talk:</u> Peripheral blood analysis defines a diagnostic window prior to the onset of clinical apparent murine acute GVHD

- 04 – 07 Dec 2010: 52nd Annual Meeting of the American Society of Hematology (ASH), Orlando, FL, USA
Poster: Definition of a diagnostic window prior to the onset of clinically apparent acute graft-versus-host disease
- 01 – 05 Oct 2010: Deutsche, österreichische und schweizer Gesellschaft für Hämatologie und Onkologie (DGHO), Jahrestagung 2010, Berlin, Germany
Talk: Monitoring of amplifying proliferation loops in donor T cell expansion establishes critical time points in acute graft-versus-host disease
- 10 – 13 Jun 2010: 15th Congress of the European Hematology Association (EHA), Barcelona, Spain
Talk: Differences in alloreactive proliferation loops in donor T cell expansion establishes critical time points in acute graft-versus-host disease
- 21 – 24 Mar 2010: European Group for Blood and Marrow Transplantation (EBMT), Vienna, Austria
Poster: CD107 surface mobilization of peripheral blood T-cells to predict acute graft-versus-host disease

Additional Activities:

- Jun 2005 – Nov 2005: and
Jun 2006 – Nov 2006: Research assistant at the Institute for Molecular Infections at the University of Würzburg
Supervisor: Dr. rer. nat. Ulrich Dobrindt
Project: Pathogenic variability and host reactions in infectious diseases

Research Retreats and Workshops of the Beilhack Laboratory:

- 3 – 4 Mar 2009: Immunofluorescence Microscopy – IFM Workshop I
Würzburg (München-Würzburg)
- 10 – 12 Aug 2009: Immunofluorescence Microscopy – IFM Workshop II
Würzburg (München-Würzburg)
- 13 – 14 Nov 2009: 1st eBMT (Experimental Blood and Marrow Transplantation) Retreat Schauinsland (Freiburg-Erlangen-Würzburg)

- 15 – 16 Jul 2010: 2nd eBMT Retreat Schwanberg (Freiburg-Erlangen-Würzburg),
- 16 – 17 Jun 2011: 3rd eBMT Retreat Feuerstein (Freiburg-Erlangen-Würzburg)
- 12 – 13 Jul 2012: 4th eBMT Retreat Schauinsland (Freiburg-Erlangen-Würzburg)

Transferable Skills Courses and Lectures at the University of Würzburg:

- Sep 2010 How does Statistics work? (20-hrs Workshop)
- Feb 2010 Poster Design and Presentation (7-hrs Workshop)
- Apr 2009 Writing for Publication (15-hrs Workshop)
- Apr – Jun 2009 Clinical Medicine Lecture (2 hrs per week)

Flow Cytometric Courses offered by Becton Dickinson, Heidelberg, Germany:

- 06/2010 Intracellular Proteins/Bead Technology (1-day Seminar)
- 04/2009 Basic Course in Flow Cytometry (3-day Intensive Course)

Working Stays:

- Aug 2011 – Sept 2011 Department of Medical Biology, University of Tromsø, Norway
Supervisor: Prof. Tor B. Stuge
- Jul 2001 – Aug 2002 AuPair in Potomac, MD, USA
Course at the University of Maryland: English as a foreign language
TOEFL-Test: 283 of 300 points – 94%

Würzburg.....
Date Signature

9.5 Avidavit (Eidesstattliche Erklärung)

I hereby declare that my thesis entitled 'Identification of new predictive markers for an imminent acute Graft-versus-Host Disease' is the result of my own work. I did not receive any help or support from commercial consultants. All sources and / or materials applied are listed and specified in the thesis.

Furthermore, I verify that this thesis has not yet been submitted as part of another examination process neither in identical nor in similar form.

Würzburg.....
Date Signature